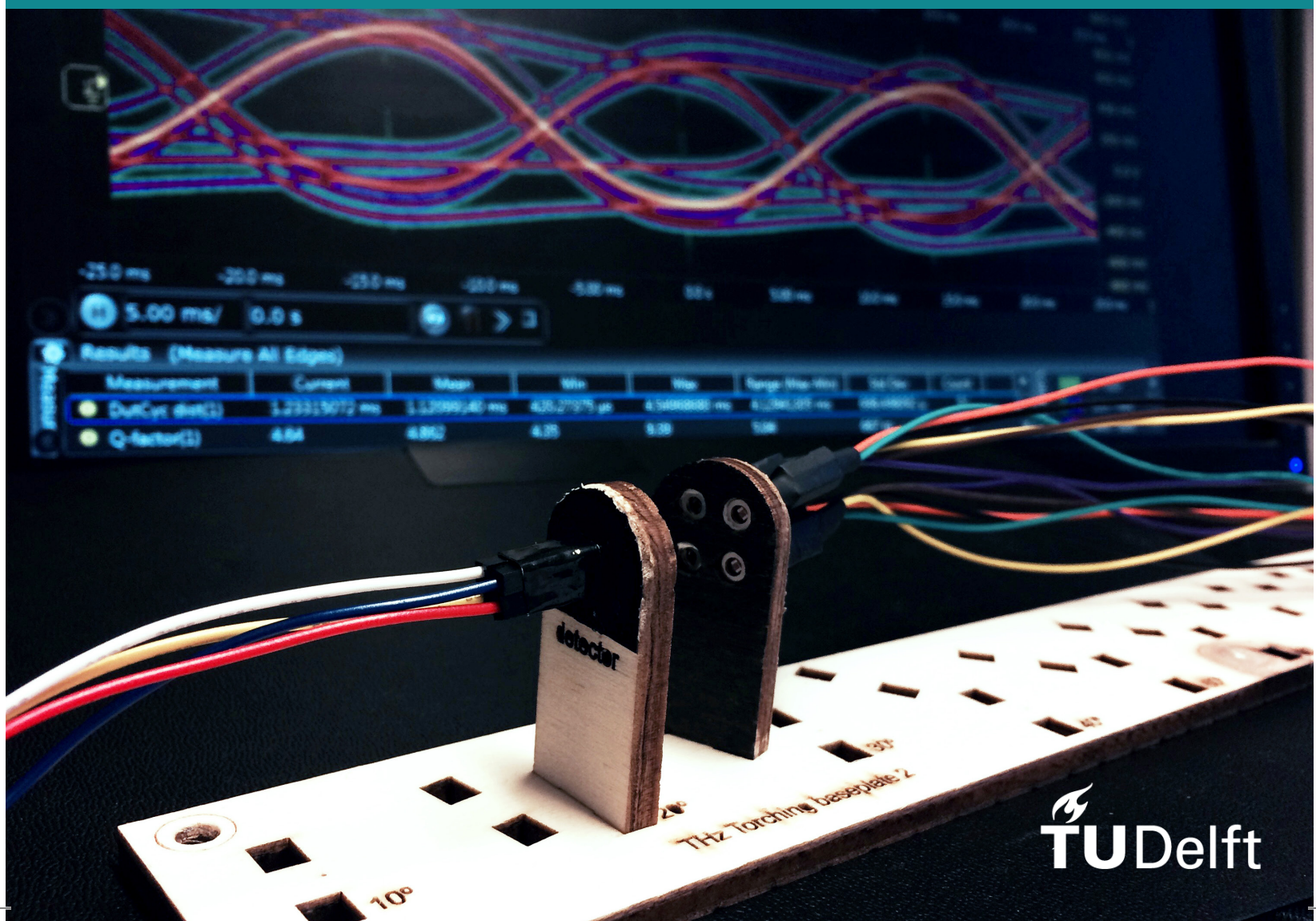


# Terahertz Torching

Towards closed-loop neurostimulation of group-housed freely moving rodents

Master Thesis by Jinne E. Geelen



# Terahertz Torching

Towards closed-loop neurostimulation of group-housed  
freely moving rodents

by

**Jinne E. Geelen**

in partial fulfillment of the requirements for the degree of

**Master of Science**

in Biomedical Engineering

at the Delft University of Technology

to be defended publicly on Friday September 15, 2017 at 10:00 AM.

Graduation Committee: Prof. dr. ir. Wouter A. Serdijn, TU Delft, Bioelectronics  
Dr. Freek E. Hoebeek, Erasmus MC, Neuroscience  
Dr. ir. Alfred C. Schouten, TU Delft, Neuro Muscular Control  
Dr. Vasiliki Giagka, TU Delft, Bioelectronics



*Det har jag aldrig provat förut, så det klarar jag helt säkert!*<sup>1</sup>  
- Astrid Lindgren, Pippi Långstrump

---

<sup>1</sup>I have never tried this before, so I should definitely be able to do it!



# Abstract

Close collaboration between the Bioelectronics department at Delft University of Technology and the Neuroscience department at the Erasmus Medical Centre has resulted in a successful tethered design for a real-time epileptic seizure detection and suppression method for mice. The goal of the Neuromate project is to develop this method into a wireless setup containing group-housed freely moving and interacting mice for use in behavioural studies. The system will include continuous monitoring and stimulation at set points in time. The Neuromate project comprises three links, two of which have previously been established.

The main goal of this study was to find and evaluate a technique to complement the current Neuromate project with a wireless downlink, channelling the communication from the researchers towards the mice.

This new downlink should fit in the ongoing project and meet particular specifications. The most critical requirements are that it should be lightweight and small-scale and should allow simultaneous multi-user communication. Also crucial are the prevention of interference with the two other links, reliability and low power consumption. The three most promising techniques, power source keying, optical wireless transmission and terahertz torching are elaborated.

Terahertz (THz) torching, covering the high thermal part of the THz band (10 to 100 THz), was chosen as the technique to be developed in this thesis. This decision was based on the fundamental limitations of power source keying and optical wireless transmission, which appear in the weighted criteria evaluation of the requirements. The challenges of THz torching are mainly practical, while fundamentally it provides the opportunity to form a reliable non-interfering wireless link. The feasibility of THz torching for our specific application was tested by creating a proof-of-principle and conducting five different experiments.

The prototype includes two components. The first is a thermal source, which in the final design will be placed above the cage, and the second is a pyroelectric detector, which will later be positioned on top of the head module of each of the mice. During the experiments, communication with the recently developed THz torch was proven to be feasible. Experiment 1 resulted in an optimum data rate of 35.71 bps, allowing for the simultaneous stimulation of the mice. And the divergence of the source was sufficient to cover the entire cage, as it was found in experiment 3 that an angle of 50° was the maximum misalignment still allowing reliable transfer of the data. However, the prototype did fail to reach the required distance. In experiment 2 only 8 cm could reliably be bridged. The source was not strong enough to overcome the attenuation in the air. A more powerful source will allow an increased reachable distance, making sure the entire cage is covered.

In this work an innovative and promising proof-of-concept has been realized for the wireless downlink of the Neuromate project.



# Preface

I started my studies at Industrial Design Engineering, including a minor in Medicine for Technical Students and an elective course about software. It made me realize my interest has never been regular consumer products but instead the interaction between medical applications and challenging technical questions and solutions. Thus I followed bridging courses from Mechanical Engineering to switch to the Master Biomedical Engineering with a specialisation in Biomechatronics. This specialisation focusses on prosthetics, orthotics, diagnostic devices for neurological disorders, neurorehabilitation robots, and haptic interfaces. Even though my interests have always been broad, I finally found a direction that integrated my fascination for the brain together with my analytical strength. After this journey, I ended up doing my internship at the Neuroscience department and my graduation project in the Bioelectronics group. A unique project that combined the skills I gained during this unusual journey. And a great opportunity to learn even more about different disciplines and to get out of my comfort zone.

I was very fortunate to be able to join the interdisciplinary Neuromate team and to be guided and supported by three supervisors with completely different backgrounds but who are all experts in their field and motivated to share their knowledge.

*Jinne E. Geelen  
Delft, September 2017*





# Contents

|          |                                                     |           |
|----------|-----------------------------------------------------|-----------|
| <b>1</b> | <b>Introduction</b>                                 | <b>1</b>  |
| 1.1      | Neuromate . . . . .                                 | 1         |
| 1.2      | Closed-Loop Optogenetic Stimulation . . . . .       | 3         |
| 1.3      | Problem statement . . . . .                         | 3         |
| 1.4      | Goal . . . . .                                      | 4         |
| 1.5      | Approach . . . . .                                  | 5         |
| <b>2</b> | <b>Background</b>                                   | <b>7</b>  |
| 2.1      | Previous Master Projects. . . . .                   | 7         |
| 2.1.1    | Wireless Power Harvesting . . . . .                 | 7         |
| 2.1.2    | Wireless Communication Uplink . . . . .             | 8         |
| 2.2      | Downlink Requirements . . . . .                     | 8         |
| 2.3      | Wishes . . . . .                                    | 10        |
| 2.4      | Other wireless projects in literature . . . . .     | 11        |
| <b>3</b> | <b>Communication and Modulation</b>                 | <b>15</b> |
| 3.1      | Modulation . . . . .                                | 16        |
| 3.1.1    | Amplitude Modulation . . . . .                      | 16        |
| 3.1.2    | Frequency Modulation . . . . .                      | 16        |
| 3.1.3    | Phase Modulation . . . . .                          | 17        |
| 3.2      | Multiple access . . . . .                           | 17        |
| 3.2.1    | Time division multiple access (TDMA). . . . .       | 18        |
| 3.2.2    | Frequency division multiple access (FDMA) . . . . . | 18        |
| 3.2.3    | Code division multiple access (CDMA) . . . . .      | 19        |
| 3.2.4    | Space division multiple access (SDMA). . . . .      | 19        |
| <b>4</b> | <b>Concepts</b>                                     | <b>21</b> |
| 4.1      | Power Source Keying . . . . .                       | 21        |
| 4.1.1    | Carrier. . . . .                                    | 21        |
| 4.1.2    | Modulation . . . . .                                | 21        |
| 4.1.3    | Multiple access . . . . .                           | 22        |
| 4.1.4    | Drawbacks . . . . .                                 | 23        |
| 4.2      | Visual Light Communication . . . . .                | 23        |
| 4.2.1    | Carrier. . . . .                                    | 23        |
| 4.2.2    | Modulation . . . . .                                | 24        |
| 4.2.3    | Multiple access . . . . .                           | 24        |
| 4.2.4    | Drawbacks . . . . .                                 | 24        |
| 4.3      | Terahertz Torching . . . . .                        | 25        |
| 4.3.1    | Carrier. . . . .                                    | 25        |
| 4.3.2    | Modulation . . . . .                                | 26        |
| 4.3.3    | Multiple access . . . . .                           | 26        |
| 4.3.4    | Drawbacks . . . . .                                 | 26        |
| 4.4      | Multi-criteria analysis. . . . .                    | 27        |
| <b>5</b> | <b>Components</b>                                   | <b>29</b> |
| 5.1      | THz Sources . . . . .                               | 29        |
| 5.1.1    | Thermal sources . . . . .                           | 30        |
| 5.1.2    | Electrical sources. . . . .                         | 30        |
| 5.1.3    | Optical sources . . . . .                           | 31        |
| 5.2      | THz Detectors . . . . .                             | 32        |
| 5.2.1    | Thermal Detectors . . . . .                         | 32        |

|          |                                         |           |
|----------|-----------------------------------------|-----------|
| 5.2.2    | Photoconductive Detectors . . . . .     | 32        |
| 5.2.3    | Heterodyne Detection . . . . .          | 33        |
| 5.3      | Component Selection . . . . .           | 34        |
| <b>6</b> | <b>Experiment</b>                       | <b>35</b> |
| 6.1      | Materials . . . . .                     | 36        |
| 6.1.1    | Source . . . . .                        | 36        |
| 6.1.2    | Detector . . . . .                      | 37        |
| 6.1.3    | Cases and Baseplate. . . . .            | 37        |
| 6.1.4    | Oscilloscope . . . . .                  | 38        |
| 6.2      | Measurement Method . . . . .            | 38        |
| 6.2.1    | Experiment 1 - Data rate . . . . .      | 38        |
| 6.2.2    | Experiment 2 - Distance . . . . .       | 39        |
| 6.2.3    | Experiment 3 - Misalignment. . . . .    | 39        |
| 6.2.4    | Experiment 4 - Power . . . . .          | 40        |
| 6.2.5    | Experiment 5 - Medium . . . . .         | 40        |
| 6.3      | Analysis Method . . . . .               | 40        |
| 6.3.1    | Eyediagram . . . . .                    | 40        |
| <b>7</b> | <b>Results</b>                          | <b>43</b> |
| 7.1      | Data rate . . . . .                     | 43        |
| 7.2      | Distance. . . . .                       | 44        |
| 7.3      | Misalignment . . . . .                  | 45        |
| 7.4      | Power . . . . .                         | 45        |
| 7.5      | Medium . . . . .                        | 46        |
| <b>8</b> | <b>Concluding remarks</b>               | <b>47</b> |
| 8.1      | Conclusion . . . . .                    | 47        |
| 8.2      | Contribution. . . . .                   | 49        |
| 8.3      | Discussion and recommendations. . . . . | 49        |
|          | <b>Bibliography</b>                     | <b>57</b> |
|          | <b>Appendices</b>                       | <b>65</b> |
|          | <b>A - Multiple Criteria Analysis</b>   | <b>67</b> |
|          | <b>B - Pilot</b>                        | <b>69</b> |
|          | <b>C - CDMA</b>                         | <b>71</b> |
|          | <b>D - Arduino</b>                      | <b>73</b> |
|          | <b>E - Matlab</b>                       | <b>77</b> |
|          | <b>F - Eyediagrams</b>                  | <b>81</b> |
|          | <b>G - Lunteren</b>                     | <b>95</b> |

# Introduction

## 1.1. Neuromate

Close collaboration between the Bioelectronics department of the Delft University of Technology and the Neuroscience department at the Erasmus Medical Centre has resulted in a successful tethered design for a real-time epileptic seizure detection and suppression method for mice [56] [96]. Figure 1.1.A shows the system overview of this closed-loop project. The electrocorticography (ECoG) signals of the mouse are recorded, and once a seizure is detected the optogenetic<sup>1</sup> stimulator provides a pulse of light (represented by the blue bar in 1.1.B). Untreated brain tissue would not react to such a light pulse but in this case, specific cell types within a particular area of the brain are modified by a virus that transports the DNA coding for the light sensitive proteins called channelrhodopsin-2 (ChR2) to the cells. The cells that express these proteins in the cerebellar nuclei (CN), and their projections are shown in Figure 1.1.C [55][56].

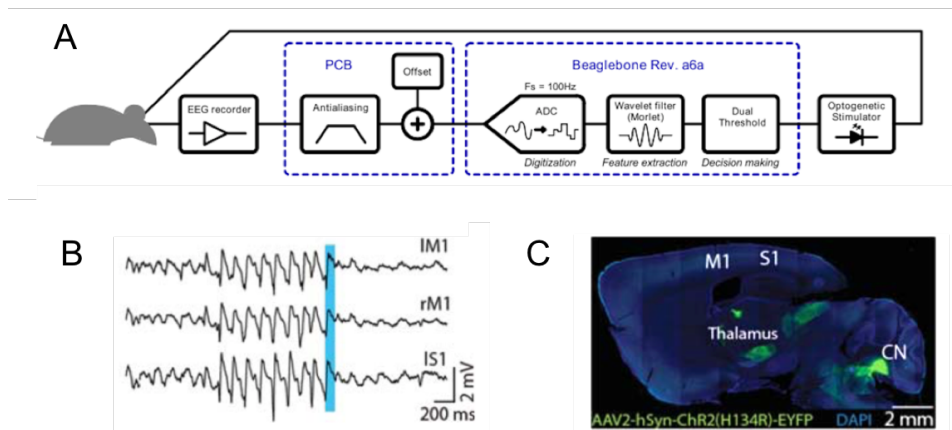


Figure 1.1: A. System overview of the closed-loop project [96] B. Representative electrocorticograms (ECoG) which exemplify how optogenetic stimulation stops a seizure. [56] C. Confocal image of sagittal brain section showing ChR2 expression in the CN with projections to the thalamus (M1, S1 represent primary motor and sensory cortex, respectively) [56]

The closed-loop project is successful in ending seizures. However, it still has one significant drawback namely that it is a tethered solution. The wires prohibit free movement of the mouse and thus restricts the experimental setup [39] [68] [9]. Even if the mouse could walk around with attached cables, the interaction with the researcher at the beginning of the experiment could result in behavioural changes of the mouse [68] [101]. Furthermore, the wires will induce 50Hz mains noise and movement artefacts [77] [22]. The risk of entanglement and cable damage is another significant constraint of tethered project for head-fixed mice, as the number of observed animals becomes limited [101]. Therefore, the next

<sup>1</sup>the technique optogenetics is discussed in more detail in section 1.2

step will be to develop the closed-loop tethered project for head-fixed mice into a wireless closed-loop project for group-housed animals, which will from now on be called the Neuromate project.

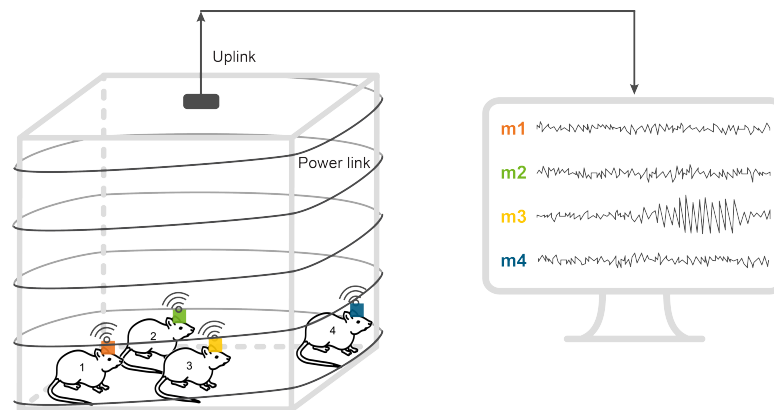


Figure 1.2: Current project overview: the power link, indicated by the metal coil and explained in more detail in section 2.1.1, and the uplink, indicated by the radiowaves and the connection with the computer and explained in more detail in section 2.1.2 (does not represent a realistic scale)

In Figure 1.2 the already established parts of the Neuromate project are schematically represented. The coil around the cage represents the wireless power link. The WiFi symbol represents the communication link from the mice to the researcher (uplink). Chapter 2 briefly explains these two projects.

The Neuromate project will provide a technique which is applicable in many behavioural studies. As an example of the new possibilities, the previously mentioned epilepsy study will be presented. At Hoebeeks lab the mechanisms behind epilepsy are studied which recently resulted in solid evidence for the therapeutic benefit of cerebellar stimulation, namely the stimulation of the CN, as was shown in Figure 1.1 [55] [56]. Considering the success rates in mice it is their intention to bring the technique to the clinic to help patients. However, before the transit from mice to human can securely be made one important factor should be studied, the side effects. Patients will only consider undergoing an invasive treatment like deep brain stimulation (DBS) when the benefits outweigh the costs. Note that DBS in humans will not include optogenetics due to ethical concerns only electrical stimulation is used in human patients. Reducing the number of epileptic seizures is favourable, but it should also be clear that the treatment does not induce anxiety, aggression, nor depression. For testing such social behaviour a group-housed mice experiment is required.

Epilepsy is one of the most common neurological disorders, with more than 50 million people affected worldwide [91] [57] [94] [55]. The recurring seizures that patients suffer from differ in terms of their cause and appearance depending on the type of epilepsy [57] [55]. Current treatment options often consist of medication, and for the more severe cases might even include surgery. Although most patients benefit from these interventions, approximately 20 to 30 percent of all patients are treatment-resistant and experience monthly seizures. Half of the resistant patients have a seizure every week and one-third experience daily seizures [94] [32] [74] [92] [107].

As engineering students, we learn to describe phenomena on the basis of models, systems and simulations. Therefore, the description of Epilepsy by Wang et al. (2016) is a helpful translation of a medical phenomenon into engineering principles:

*“Epilepsy is thought to be a dynamical disorder of the brain at the systems level, which makes it particularly suitable to be studied from the perspectives of computational modelling and system theory”* [99]

When a system does not operate as desired, applying distortions can create a better state. Likewise, when a brain does not function as desired, applying distortions, such as light or electric pulses, might change it to a healthier state. Enhancing our understanding of the systems or subsystems involved in epilepsy and our understanding of their response to different artificial inputs will optimise the implementation of perturbations as a new treatment method. Current assumptions can be connected in models and verified by neuroscientific experiments [33].

## 1.2. Closed-Loop Optogenetic Stimulation

The results of circuit-based models will become more valuable once verified by closed-loop (CL) control experiments [65]. By adding a feedback link to the control scheme, perturbations could guide the circuit toward a targeted activity pattern. Figure 1.3 shows an example provided by Grosenick et al. (2015) of a possible closed-loop system based on a neural microcircuit. The observed output is estimated by the modelled micro-circuit and fed back to the controller. The controller compares the target pattern with the predicted outcome and tries to decrease the error while minimising the cost function [33]. Such a closed-loop circuit also requires both an uplink and a downlink to be responsive.

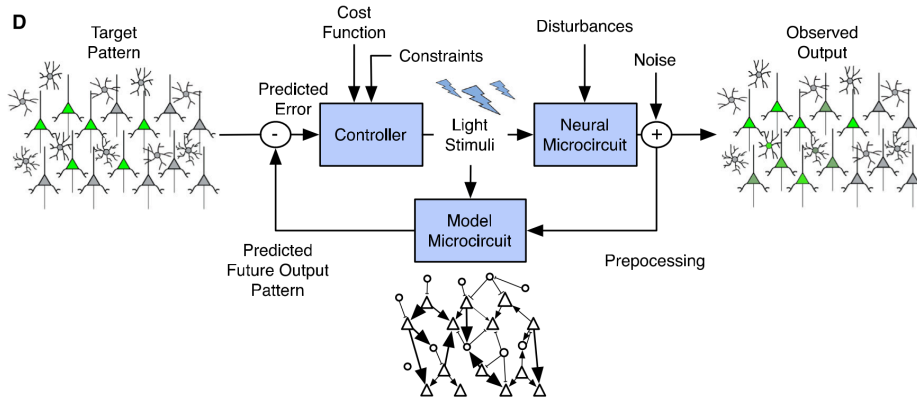


Figure 1.3: Example of a closed-loop control system applied to Neuroscience by Grosenick et al. 2015. The green neurons indicate the cell-specific control of cell types [33]

In this model the perturbation given to the system is a light stimulus. This light stimulus refers to the use of optogenetics, due to its high temporal and cellular precision a widely used technique for research [107] [24] [19] [104]. However, it is not yet applicable to clinical use due to various technical and ethical limitations. The main concern with optogenetics is the fact that it requires modification of the targeted neuronal cells to make them light sensitive. Inserting different types of opsins into the cell membranes facilitates different control strategies. For example, Channelrhodopsins can be used to depolarise the neurons after a blue light stimulation, and Halorhodopsins can be used to hyperpolarize the neurons with yellow light [107] [24] [19] [104]. The high cellular and temporal specificity together with the freedom of control make optogenetics an extremely helpful tool for closed-loop experiments.

## 1.3. Problem statement

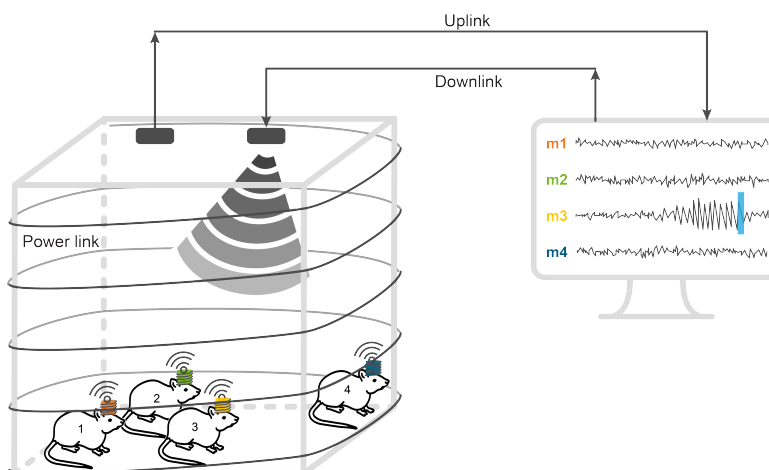


Figure 1.4: The missing downlink, is added to the schematic overview of the Neuromate project

The goal of the Neuromate project is to transform the successful closed-loop project into a wireless

setup. Creating a setup for long-term studies of group-housed mice, which enables continuous monitoring and interaction with each animal. Two previous master projects have established an uplink and a power link. Both projects are successful wireless solutions. However, there is still a link missing that would make the Neuromate a closed-loop system, the downlink. In Figure 1.4 the future downlink is visualized.

The challenges that the Neuromate should address are (1) individual and simultaneous monitoring of four mice that stay in one cage, and (2) the system should be wireless and battery-free, plus (3) the mice should receive individual stimulation controlled by the neuroscientist.

There is limited power available over the wireless power link. Thus the two communication links have a tight power budget. The backscattering method is an energy efficient uplink that enables individual monitoring of the mice (1). However, the technique only allows for a one-way communication link. Both solutions are wireless and, once the miniaturisation steps are completed, will allow for freely moving group-housed animals (2). But there is still one function missing: the individual control of the stimulation paradigms (3). This function can be added by creating a downlink from the researcher towards the mice. The requirements for such a link are elaborated in more detail in Chapter 2.

## 1.4. Goal

The overall goal of the Neuromate project is to build a setup for long-term studies of group-housed mice, which enables continuous monitoring and interaction with each animal.

In Figure 1.5 four different stimulation paradigms are shown. The most simple one is continuous stimulation, the microLED will turn on with a regular interval. The microLED might blink at, for example, 20Hz or 50Hz. In the figure all mice receive the same continuous stimulation pattern, but it should also be possible to give a mouse individual continuous stimulation. Another parameter that should be controllable is the colour of the stimulation. The implanted optrode might include up to three microLEDs with varying colours. As explained in section 1.2 these colours will activate different opsins. Besides individual stimulation patterns asynchronous individual stimulation with irregular intervals should also be supported, allowing for the final option of responsive stimulation. Once the researcher detects an event in the ECoG data or in the behaviour a stimulation pulse should be applied. In the future this responsive stimulation will also allow for closing the loop by detecting events without the intervention of a neuroscientist. An algorithm could determine the most optimal stimulation onsets. Until now the downlink was missing and it should support all four stimulation options to work towards this closed-loop goal.

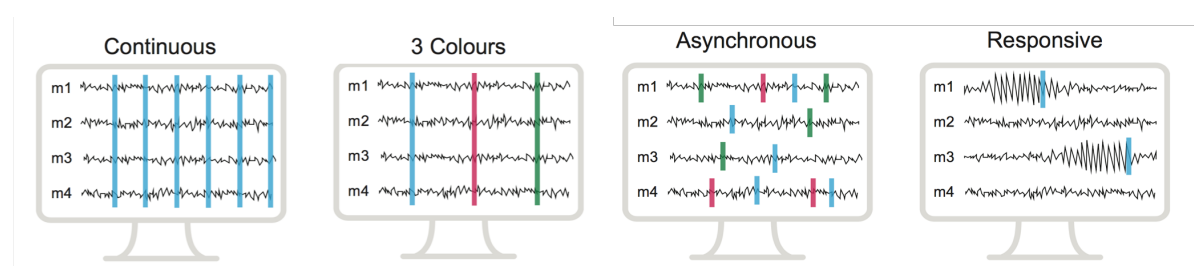


Figure 1.5: Example of stimulation paradigms of the Neuromate: Continuous, 3 Colours, Asynchronous, Responsive

**The first goal of this study is to determine and test what the most optimal technique is for establishing the downlink of the Neuromate project.** This should be achieved without interfering with the wireless power link and the wireless ECoG uplink. The technique should be power efficient and suitable to individually and simultaneously address four mice.

**After choosing the best technology for the Neuromate application, the second goal is to build a prototype and to test the principle of the chosen technique.**

## 1.5. Approach

First the requirements have to be determined to ensure that the chosen technique will suit the current project and will lead to the most optimal solution. These needs will rely on the outcome of both the power link project and the uplink project. Chapter 2 will present a brief introduction to both projects, followed by the determined requirements and lastly, it will provide an overview of other wireless projects described in the relevant literature. This overview enables us to learn from the different approaches of other research groups and at the same time it is a comparison of their and our results.

In Chapter 3 the basic variables of communication and modulation will be elucidated and four different multiple access techniques are explained. Based on the specified variables the next chapter, Chapter 4 will describe the three most promising techniques: power source keying, optical wireless transmission (Li-Fi), and terahertz torching including their most suitable multiple access methods. Followed by a choice between these three methods based on a weighted multi-criteria analysis, including the most critical requirements.

After the most optimal technique has been determined, the focus will shift to the prototype. In Chapter 5 the essential components and a range of widely used options will be discussed. The prototype and the experiments performed will be discussed in more depth in Chapter 6. And the results of the experiments are presented in Chapter 7. Finally, Chapter 8 will return to the initial goals of this study and evaluate the chosen technique. This final chapter will give a brief review of the decisions and the outcomes throughout this research and discusses the results and concludes with some recommendations including suggestions for further study.





# 2

## Background

### 2.1. Previous Master Projects

Other students have laid a foundation for the project by working on the uplink and powerlink components. Integrating these can help to create a complete solution. The first master thesis is written by ir.Farnaz Nassiri Nia. Her main goal was to harvest power at the head module of the mouse [72].The other master thesis is written by ir. Ide S. Swager. He focused mainly on the data transmission from the mice towards the receiver outside the cage [93].

When combining these two projects, a critical component is still missing. With the addition of communication from the neuroscientist towards the head module, a downlink, more complex experimental design become available. Adding this missing link would make closed-loop, real-time interaction with the mouse brain possible.

The requirements for the downlink rely on the outcome of both the power link project and the uplink project. Thus, a brief introduction to both projects is given. However, the interested reader is referred to both master thesis reports for more details.

#### 2.1.1. Wireless Power Harvesting

Batteries are bulky, result in waste products and require intervention from the neuroscientist for timely replacements [3] [53]. Therefore, a wireless power link consisting of two resonating coils was created to harvest power at the mouse's head module [66]. The first coil is a large coil wound around the walls of the entire cage. The second smaller coil surrounds the head module on the mouse. The large coil induces a magnetic field through the cage and thus through the smaller coil [58]. The amount of harvested power depends on the efficiency of the link between the transmitting coil and the receiving coil [66]. It also depends on the maximum allowable exposure for mice to radiofrequency electromagnetic fields [1]. The Fourier transform of the Maxwell–Faraday equation leads to this relationship between induced voltage and the magnetic field [38].

$$V = j \omega \mu_0 \int H dS \quad (2.1)$$

With

- $j$  =  $\sqrt{-1}$
- $\omega$  = Frequency
- $\mu_0$  = Constant magnetic permeability [Henry/m]
- $H$  = Magnetic field [A/m]
- $dS$  = Vector element of surface area, S, normal to surface

Power transmission in the short range, the small coil is located inside the large coil, via magnetic induction has advantages such as the efficiency and small coil size. However, it also has some disadvantages such as the restricted position [86].

From now on the project performed by Nassiri Nia (2016) will be called the power link project.

### 2.1.2. Wireless Communication Uplink

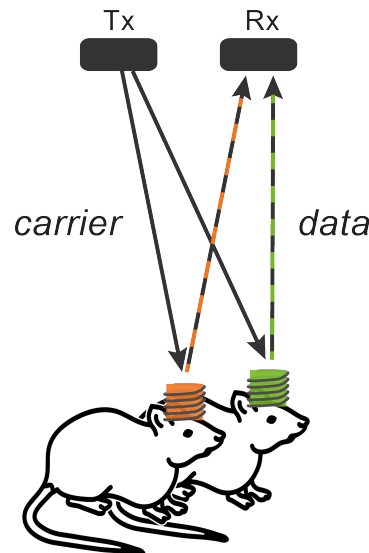


Figure 2.1: Simplified principle of backscattering, with Tx transmitter and Rx receiver [93]

Back-scattering is a passive technique that can achieve low power consumption at the head module. With a power consumption of only 0.25mW Swagers solution is much more efficient than conventional transmitters are. However, the total power consumption of the prototype is 20.3 mW for one channel 20kHz recording. Swager (2016) established a high bitrate backscattering link that uses digitally generated sub-carriers and frequency division multiple access (FDMA) to support multiple concurrent measurements, as is illustrated in figure 2.1. The main carrier frequency is chosen to be the 915 MHz ISM band. A prototype of the system is built and tested. [93]

## 2.2. Downlink Requirements

To achieve the goal of creating a wireless and wearable design, strict requirements apply to this project. The size and weight of the end product will determine if the mice can successfully carry the device and thus enable interesting experiments. However, next to the great demand for miniaturisation more requirements can be derived based on the goals for this project. At the start of the two previous thesis projects, bioelectronics students and the neuroscientist already determined some requirements in close collaboration. More specific requirements complement the list based on the life-cycle of the prototype.

### I Production/Purchase

- i Off the shelf components
- ii The prototype should be a low-cost solution
- iii Reproducibility with similar components, thus components should be easily available

### II Assembly

- i PCB techniques, no cleanroom or IC design
- ii A prototype should be assembled at the bioelectronics or neuroscience lab

- iii The production steps should be reproducible

### III Testing

- i Chosen technique should be safe for mice and for humans
- ii Verification should be possible before implantation

### IV Storage

- i Regulations should be met
- ii Product should be stored at room temperature

### V Attachment

- i The final product should consist of two parts: 1. Implantable part, including  $\mu$ LEDs and the electrodes. 2. External part, including the antenna's and the coil
  - a Part 1 should be attached to the mouse during surgery
  - b Part 2 should be attached to the mouse right before the experiment starts
- ii After implantation of the first part the mouse should be able to live group housed. With either an optional cover part or with a finished connector
- iii Safety
  - a A warning should indicate an incorrect attachment and/or a wrong settings
  - b Clear instructions and optional training should be available when the prototype is in use at the Neuroscience department

### VI Experiment

- i A laboratory mice (C57BL/6 weighing around 10g [93]) should be able to carry the device
  - a max. volume of 1 cm<sup>2</sup> [93] [72]
  - b max. weight of 1 g [93] [72]
- ii Operating time should be minimal three days without the need for intervention by the neuroscientist
  - a The new downlink may not be lost during monitoring
  - b The new downlink should use a low power receiver that consumes max. 0.3mW (explained in 2.4)
- iii Safety
  - a The prototype should not induce unnecessary damage to the mouse
  - b The prototype should not induce damage to the researcher
  - c The prototype should not have negative influence on the environment
- iv Multiple mouse should be able to each carry the product without disrupting the natural behaviour
- v The new technique should not interfere with the two prior developed links, the uplink and the powerlink
- vi the new downlink should wirelessly reach the mice from outside the cage
- vii the setup should be build in an existing measurement setup at the Erasmus MC
- viii All four mice should receive a unique control signal to change their stimulation within one second

### VII Detachment

- i After the experiment the external part should be detachable from the implanted part without damage
- ii It should be possible to place the mouse back into the group housing after the experiment (Requirement V.ii.)

#### VIII Further development

- i When better (in term of performance, size or weight) components become available parts of the product should be replaceable OR the product should be reproducible within the bio-electronics or the neuroscience lab.

### 2.3. Wishes

- I Water resistant, so it can be used in a watermaze, and withstand drinking bottles, urine and other excrements.
- II Multiple setups next to each other without interference
- III Low power consumption of both the transmitter and the receiver
- IV Prototype should be 'fool-proof' so that students can use the device without help of engineers
- V Device enables continuous monitoring of multiple mice for months
- VI Could also be worn by mice with a bodyweight lower than 10g

Changes in requirements since Swagers project: he determined a maximum weight of the product to be one gram based on a body weight of 10 grams. However, adult mice (C57BL/6) can grow up to 20 to 30g and therefore together with the neuroscientist this requirement is stretched up to 2 grams maximal weight for the total product [64][93]. The volume requirement remains 1 cm<sup>2</sup>.

To determine a new power requirement solely for the downlink technique the assumption about the uplink being optimized later on was made. A rough estimation was made to divide the total available power over the future functionalities. When a total of 20mW would be available via the powerlink, a division over the four main power consuming functional blocks can be assigned. The four main blocks are: the stimulation (enlight the LEDs), the microcontroller (early data processing, controlling all other functionalities), the uplink (changing impedance and encoding the ECoG signals into transferable bits), the downlink (receiving and demodulation of the control signal). An equal amount of power is chosen to send the data from or to the mice. This is a rough estimation to provide boundaries for the project. In a later phase of integration of the Neuromate project these ratios might change.

|                 |   |        |      |
|-----------------|---|--------|------|
| Harvested power | = | 20mW   |      |
| Microcontroller | = | 10.9mW | [93] |
| Stimulation     | = | 8.5mW  | [72] |
| Uplink          | = | 0.3mW  | [93] |
| Downlink        | = | 0.3mW  |      |

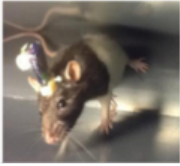
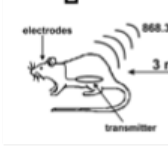
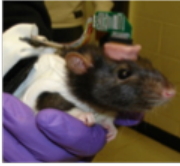


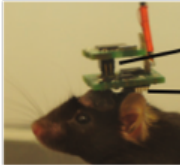
## 2.4. Other wireless projects in literature

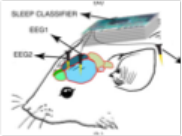
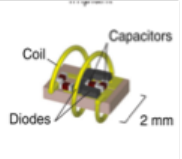
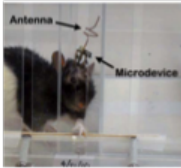
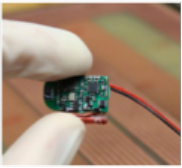
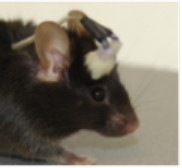
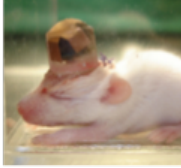
Establishing a wireless monitoring setup for small rodents is of high demand in many neuroscience departments worldwide. This interest is due to the increasing possible experimental designs with such a configuration. For example, behavioural studies can investigate mice within a (water) maze or a group without the burden of wires. Currently long-term studies are conducted in single-housed settings and thus include social isolation of the rodents which by nature live in colonies. This social isolation has impact on their behaviour and neuronal activity. Therefore, studying rodents in group-housed setting is preferred. Especially the relation between the neuronal activity and social behaviour are of interest.

An overview of the most relevant examples from this research field is given in Figure 2.2. The following summary elaborates on the focus and achievements of other groups. The first observation concerns the small number of projects available for mice [82][101][22][106][83] [54][35][39]. Rats are larger, heavier and can carry more weight than mice can. Most projects still include a heavy battery backpack attached to a Velcro jacket that can be worn by the animal [37][102][4][15][7][103]. One of the projects set up by Lapray et al. 2008 chose to implant the batteries within the abdomen [59]. Some groups used power harvesting instead of bulky batteries, which considerably decreased the size of the total product [51][101][39]. Another project focused on long-term monitoring and succeeded in implantation on postnatal day 12 (P12) in mice and P7 in rats [106]. Moreover, the way of stimulating varied between electrical stimulation and optical stimulation. Some projects did not have a stimulation function and were focused only on data harvesting [59][36][22][9][106][83]. Other projects solely focused on optical stimulation [79][39][101]. One group created a purely wireless deep brain stimulation (DBS) system [35]. Other techniques were also integrated into wireless setups, such as a microfluidic system to deliver droplets of drugs [50]. Most projects tried to stack the layers of PCB to create a more compact model [108][101][9]. One project even used partially flexible PCB but failed to make their prototype wearable [29]. None of the groups created an integrated product, and most are still in the prototyping phase. Pinnell et al. 2016 did succeed in creating a waterproof shell to cover their prototype, which enabled them to perform experiments within a water maze [78].


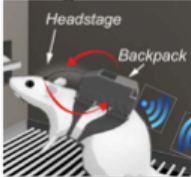

All figures and values included in the table in Figure 2.2 are taken from the reviewed paper mentioned by author and year, references can be found in the caption below. Note: Care should be taken when comparing projects with a different application. For example, various stimulation techniques and paradigms will influence the battery life.

Figure 2.2: Table - Overview other wireless projects [78] [59] [36] [22] [108] [101] [54] [39] [79] [8] [83] [35] [106] [9] [4]

|                       | <b>Pinnell2015</b>                                                                 | <b>Lapray2008</b>                                                                   | <b>Hampson2009</b>                                                                   |
|-----------------------|------------------------------------------------------------------------------------|-------------------------------------------------------------------------------------|--------------------------------------------------------------------------------------|
|                       |   |   |   |
| Animal                | Rat                                                                                | Rat                                                                                 | Rat                                                                                  |
| Housing               | Pair                                                                               | Single                                                                              | Single                                                                               |
| Size                  | 28x17x7 mm                                                                         | 40x8x5 mm                                                                           | (backpack)                                                                           |
| Weight                | 8.5 g                                                                              | 4 g                                                                                 | 60.3 g                                                                               |
| Battery life          | 30 min                                                                             | 14 h                                                                                | 5 h                                                                                  |
| Transmitter frequency | 2.4 GHz                                                                            | 868.35 MHz                                                                          | 2.4 GHz                                                                              |
| Transmission range    | 4 m                                                                                | 3 m                                                                                 | 10 m                                                                                 |
| <b>EEG</b>            | ✓                                                                                  | ✓                                                                                   | ✓                                                                                    |
| # of channels         | 4                                                                                  | 1                                                                                   | 16                                                                                   |
| Bandwidth             | 1.5 - 100 Hz                                                                       | 1 - 80 Hz                                                                           | 250Hz - 6 kHz                                                                        |
| Sample rate           | 500 Hz                                                                             | 500 Hz                                                                              | 25 kHz                                                                               |
| Data rate             | 115.2 kbps*                                                                        | 115.2 kbps                                                                          | 115.2 kbps                                                                           |
| <b>DBS</b>            | ✓                                                                                  | ✗                                                                                   | ✗                                                                                    |
| # of channels         | 2                                                                                  | -                                                                                   | -                                                                                    |
| <b>Optogenetics</b>   | ✗                                                                                  | ✗                                                                                   | ✗                                                                                    |
| # of channels         | -                                                                                  | -                                                                                   | -                                                                                    |
| Colour                | -                                                                                  | -                                                                                   | -                                                                                    |
|                       | <b>Fan2011</b>                                                                     | <b>Zuo2012</b>                                                                      | <b>Wentz2011</b>                                                                     |
|                       |  |  |  |
| Animal                | Mouse&Rat                                                                          | Rat                                                                                 | Mouse                                                                                |
| Housing               | Single                                                                             | Single                                                                              | Single                                                                               |
| Size                  | 2.2 cm <sup>3</sup>                                                                | 27x12 mm                                                                            | <1cm <sup>3</sup>                                                                    |
| Weight                | 4.5 g                                                                              | 15 g                                                                                | 3 g                                                                                  |
| Battery life          | 6 h                                                                                | 39 h                                                                                | continuous (2W)                                                                      |
| Transmitter frequency | 3.05 GHz                                                                           | 2.4 GHz                                                                             | 2.4 GHz                                                                              |
| Transmission range    | 4 m                                                                                | -                                                                                   | 20 cm                                                                                |
| <b>EEG</b>            | ✓                                                                                  | ✓                                                                                   | ✗                                                                                    |
| # of channels         | 16                                                                                 | 1                                                                                   | -                                                                                    |
| Bandwidth             | 0.8 Hz - 7 kHz                                                                     | 60 Hz - 10 kHz                                                                      | -                                                                                    |
| Sample rate           | 50 kHz                                                                             | 100 kHz                                                                             | -                                                                                    |
| Data rate             | -                                                                                  | 10 kbps                                                                             | -                                                                                    |
| <b>DBS</b>            | ✗                                                                                  | ✓                                                                                   | ✗                                                                                    |
| # of channels         | -                                                                                  | 1                                                                                   | -                                                                                    |
| <b>Optogenetics</b>   | ✗                                                                                  | ✗                                                                                   | ✓                                                                                    |
| # of channels         | -                                                                                  | -                                                                                   | 8                                                                                    |
| Colour                | -                                                                                  | -                                                                                   | Blue***                                                                              |

|                       | <b>Kassiri2016</b><br>  | <b>Ho2015</b><br>    | <b>Azin2011</b><br>         |
|-----------------------|----------------------------------------------------------------------------------------------------------|-------------------------------------------------------------------------------------------------------|----------------------------------------------------------------------------------------------------------------|
| Animal Housing        | Mouse<br>Single                                                                                          | Mouse<br>Group                                                                                        | Rat<br>Single                                                                                                  |
| Size                  | 30 mm × 22 mm                                                                                            | 10 mm <sup>3</sup>                                                                                    | 3.6 × 1.3 × 0.6 cm <sup>3</sup>                                                                                |
| Weight                | > 12g                                                                                                    | 20 mg                                                                                                 | 1.7 g                                                                                                          |
| Battery life          | 10 h <sup>*****</sup>                                                                                    | continuous (15 mW)                                                                                    | 24 h                                                                                                           |
| Transmitter frequency | 2.4 GHz <sup>*****</sup>                                                                                 | 1.5 GHz                                                                                               | 433 MHz                                                                                                        |
| Transmission range    | -                                                                                                        | 21 cm                                                                                                 | 1-2 m                                                                                                          |
| <b>EEG</b>            | ✓                                                                                                        | ✗                                                                                                     | ✓                                                                                                              |
| # of channels         | 2 (+1 EMG)                                                                                               | -                                                                                                     | 4                                                                                                              |
| Bandwidth             | 0.5 Hz –5 kHz                                                                                            | -                                                                                                     | 525 - 5.1 kHz                                                                                                  |
| Sample rate           | 9600 kbps <sup>**</sup>                                                                                  | -                                                                                                     | 357 kHz                                                                                                        |
| Data rate             | 12 bits                                                                                                  | -                                                                                                     | 500 kbps                                                                                                       |
| <b>DBS</b>            | ✗                                                                                                        | ✗                                                                                                     | ✗                                                                                                              |
| # of channels         | -                                                                                                        | -                                                                                                     | -                                                                                                              |
| <b>Optogenetics</b>   | ✗                                                                                                        | ✓                                                                                                     | ✗                                                                                                              |
| # of channels         | -                                                                                                        | 1                                                                                                     | -                                                                                                              |
| Colour                | -                                                                                                        | Red <sup>****</sup>                                                                                   | -                                                                                                              |
|                       | <b>Russell2011</b><br> | <b>Haas2012</b><br> | <b>Zavachkiykv2015</b><br> |
| Animal Housing        | Mouse<br>Single                                                                                          | Mouse<br>Single                                                                                       | Mouse&Rat<br>Single                                                                                            |
| Size                  | -                                                                                                        | 8 × 30 mm                                                                                             | <1.4 cm <sup>3</sup>   7 × 12 mm                                                                               |
| Weight                | 2.4 g                                                                                                    | 2.1 g                                                                                                 | 4 g                                                                                                            |
| Battery life          | continuous (20mW)                                                                                        | 10 h                                                                                                  | continuous                                                                                                     |
| Transmitter frequency | 2.4 GHz                                                                                                  | -                                                                                                     | -                                                                                                              |
| Transmission range    | -                                                                                                        | -                                                                                                     | -                                                                                                              |
| <b>EEG</b>            | ✓ (ECG)                                                                                                  | ✗                                                                                                     | ✓                                                                                                              |
| # of channels         | 2                                                                                                        | -                                                                                                     | 4                                                                                                              |
| Bandwidth             | -                                                                                                        | -                                                                                                     | 0.1-100 Hz                                                                                                     |
| Sample rate           | 2 kHz                                                                                                    | -                                                                                                     | 500 Hz                                                                                                         |
| Data rate             | -                                                                                                        | -                                                                                                     | -                                                                                                              |
| <b>DBS</b>            | ✗                                                                                                        | ✓                                                                                                     | ✗                                                                                                              |
| # of channels         | -                                                                                                        | 2                                                                                                     | -                                                                                                              |
| <b>Optogenetics</b>   | ✗                                                                                                        | ✗                                                                                                     | ✗                                                                                                              |
| # of channels         | -                                                                                                        | -                                                                                                     | -                                                                                                              |
| Colour                | -                                                                                                        | -                                                                                                     | -                                                                                                              |



|                       | <b>Ball2014</b>                                                                   | <b>Angotzi2014</b>                                                                 | <b>Future prototype</b>                                                             |
|-----------------------|-----------------------------------------------------------------------------------|------------------------------------------------------------------------------------|-------------------------------------------------------------------------------------|
|                       |  |  |  |
| Animal Housing        | Rat<br>Single                                                                     | Rat<br>Single                                                                      | Mouse<br>Group                                                                      |
| Size                  | 35x35x35 mm                                                                       | 2x2x0.5 + 6x4x3 cm                                                                 | 1 cm <sup>3</sup>                                                                   |
| Weight                | 22 g                                                                              | 7 g + 40 g                                                                         | 1 g                                                                                 |
| Battery life          | 1.5 h                                                                             | 3 h                                                                                | continuous (20mW)                                                                   |
| Transmitter frequency | 2.4 GHz                                                                           | 2.4 GHz                                                                            | 915 MHz                                                                             |
| Transmission range    | 10 m                                                                              | -                                                                                  | 1 m                                                                                 |
| <b>EEG</b>            | ✓                                                                                 | ✓                                                                                  | ✓                                                                                   |
| # of channels         | 16                                                                                | 16                                                                                 | 3                                                                                   |
| Bandwidth             | 4 Hz - 3 kHz                                                                      | 1 Hz - 10 kHz                                                                      | 1 Hz - 10 kHz                                                                       |
| Sample rate           | 20kHz                                                                             | 10.4 kHz                                                                           | 20kHz                                                                               |
| Data rate             | 2560 kbps                                                                         | 120kbps                                                                            | 320 kbps                                                                            |
| <b>DBS</b>            | ✗                                                                                 | ✓                                                                                  | ✗                                                                                   |
| # of channels         | -                                                                                 | 1                                                                                  | -                                                                                   |
| <b>Optogenetics</b>   | ✗                                                                                 | ✗                                                                                  | ✓                                                                                   |
| # of channels         | -                                                                                 | -                                                                                  | 6                                                                                   |
| Colour                | -                                                                                 | -                                                                                  | Blue, Green and Red                                                                 |

\* converged from baud rate

\*\* converged from S/sec

\*\*\*assumption> ChR2 mice

\*\*\*\*based on figure, not used for stimulation

\*\*\*\*\* Bagheri2012

\*\*\*\*\* website ZigBee

The main advantage of our wireless project will be the continuous closed loop functionalities without the use of batteries. Other projects either achieved closed loop interactions, or they managed to create small enough wearables to monitor the animals natural behaviour. The new project moves one step closer to the integration of both features by adding a link from the researchers towards the mice. Thus closer to a small wearable solution that provides optogenetic stimulation based upon the brain signals.

# 3

## Communication and Modulation

The downlink that will be proposed, tested and discussed in this report is a communication link. This chapter introduces the basic principles of communication. Next chapters will use this knowledge to, for example, elaborate on and distinguish the proposed concepts. First, the function of the three essential parts of a communication system, the transmitter, the channel, and the receiver, are discussed. The basic transmission scheme is shown in Figure 3.1.

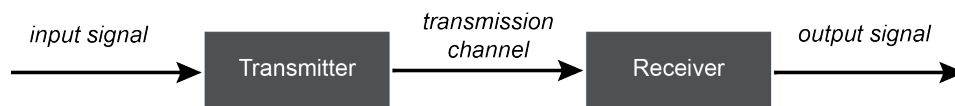


Figure 3.1: Basic transmission scheme

### Transmitter

The transmitter transforms an input signal into a suitable form for transmission through the channel. For an optical communication link the transmitter will transform the electrical input signal into an optical transmission signal. The matching of the signal to the channel is called modulation or coding and is described in more detail in Section 3.1 [5] [52].

### Transmission channel

The transmission channel covers the distance between the transmitter and the receiver. Examples of media that can guide the transmission signal are wires, coaxial cables, optic fibers, but also water or air might form the channel that transmits the signal. In wireless systems the medium is usually the ether also known as free space [5] [52].

### Receiver

At the end of the transmission channel a receiver will pick up the signal. The receiver extracts an output signal from the transmission signal, which is known as demodulation or decoding. Looking at the optical communication example again, the receiver will transform the optical signal back into the electric domain [5] [52].

### 3.1. Modulation

Modulation is a form of signal processing required for transmission of, in this case, the control signal for the modification of the stimulation paradigm. During the transmission, the information is stored on a carrier wave which is usually sinusoidal. The sinusoidal carrier can be written as:

$$u = \hat{u}_c \cdot \sin(2\pi \cdot f_c \cdot t + \varphi_c) \quad (3.1)$$

Based on the properties of a sinusoidal wave there are three different options for modulation of the carrier:

- Amplitude Modulation (AM) where  $\hat{u}_c = f\{s(t)\}$
- Frequency Modulation (FM) where  $f_c = f\{s(t)\}$
- Phase Modulation (PM) where  $\varphi_c = f\{s(t)\}$

These three modulation options are elaborated on in Subsections 3.1.1 , 3.1.2 and 3.1.3.

#### 3.1.1. Amplitude Modulation

Amplitude modulation is the oldest of the three modulation methods and originates from radio communication. Figure 3.2a shows amplitude modulation in the time domain. The carrier wave ('draaggolf' in dutch) is multiplied with data signal ( $S(t)$ ) to get the AM signal. The dotted line that covers the outline of the AM signal is called the envelope and it indicates the amplitude of the data signal. In the frequency domain the bandwidth of the AM signal is twice the bandwidth of the data signal mirrored around the carrier frequency, as can be seen in Figure 3.2b.

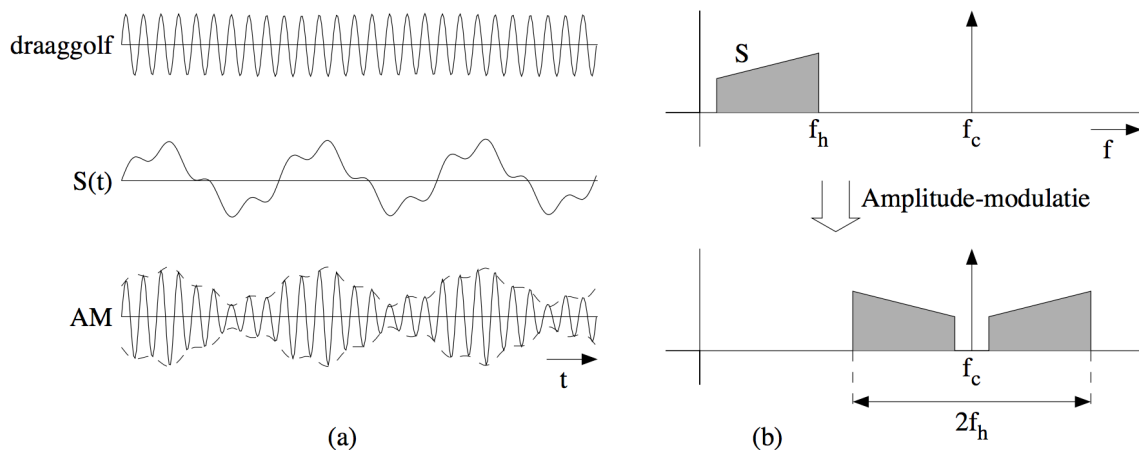


Figure 3.2: Amplitude modulation, depicted in the time domain (a) and in the frequency domain (b). Courtesy of [87]

#### 3.1.2. Frequency Modulation

Another class of modulation is angular modulation. In this case, not the gain but the argument of the sine of Equation 3.1 is modified. The angular class includes frequency modulation, FM. In FM the frequency of the carrier signal is changed by the data signal, as can be seen in Figure 3.3a. FM is harder to implement and more challenging to analyse than AM is. Another difference between AM and the angular modulation method can be found in the frequency domain. Comparing Figure 3.2b with 3.3b shows that FM has a bandwidth-expansion property. The new bandwidth is still mirrored, only this time not around a signal frequency but a bandwidth of  $f_c - f_z$  and  $f_c + f_z$ .

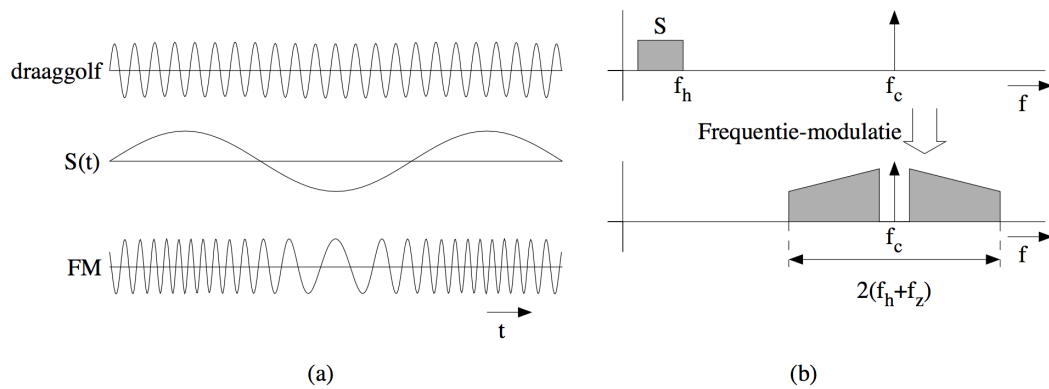


Figure 3.3: Frequency modulation, depicted in the time domain (a) and in the frequency domain (b). Courtesy of [87]

### 3.1.3. Phase Modulation

Another form of angular modulation is phase modulation. Again the argument is modified, but now the phase of the signal is changed instead of the frequency in the previous example. The two methods are similar in their properties. In PM the phase of the carrier signal is modified based on the alternations of the data signal. In Figure 3.4a a square wave is chosen since it is a clear example to show the phase changes. Figure 3.4b is similar to Figure 3.3. However, PM might also be applied in combination with other data shapes such as sinusoids.

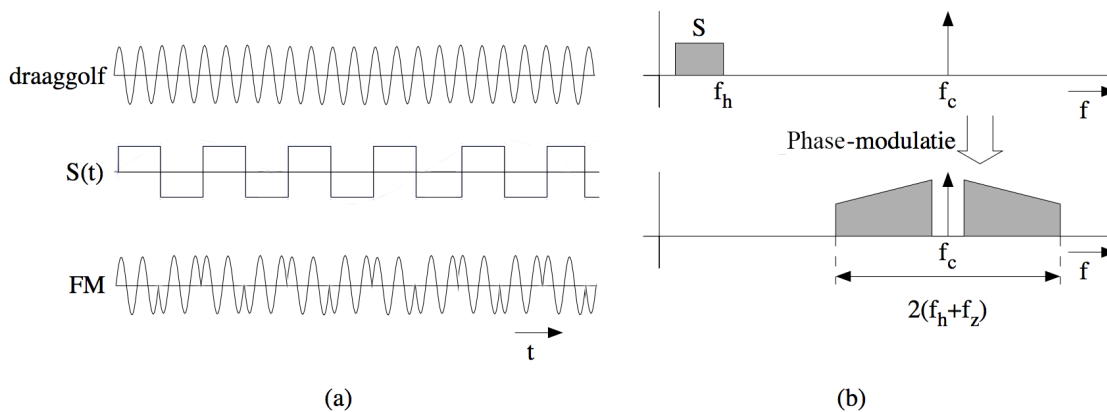


Figure 3.4: Phase modulation, depicted in the time domain (a) and in the frequency domain (b). Adapted from [87]

## 3.2. Multiple access

The communication link should be able to address four mice simultaneously. Thus next to the type of modulation of the carrier wave to encode the information on a single-channel, a multiple access technique should also be chosen to send data to multiple receivers. The four major methods are discussed. All of them divide the fixed available spectrum differently to allow for multiple access. The main principle of each method can be retrieved from the names. However, the next subsections will discuss what is behind the names and whether they apply to the Neuromate project [71][17].

Figure 3.5 represents the power division over frequency and time of the four main multiple access methods. Thereby a fundamental difference between the methods is visualised. CDMA and SDMA are both options that do not divide the power in time slots or frequency bands. Their difference is clarified in subsections 3.2.3 and 3.2.4.

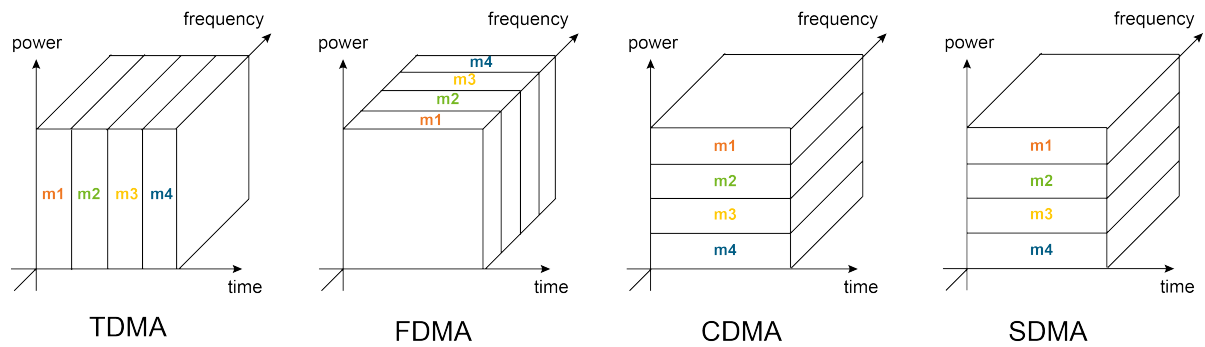


Figure 3.5: The power division over frequency and time of the four main multiple access methods

### 3.2.1. Time division multiple access (TDMA)

TDMA divides the available bandwidth into multiple time slots. One mouse a time could be addressed, as is illustrated by Figure 3.6. Depending on the type of experiment a maximum allowable delay between the control of the different mice can be determined. Some require simultaneous stimulation where others might allow less strict synchronisation. For example, if it is acceptable that all mice get their stimulation pattern updated within one second then four slots should fit within one second, resulting in a maximum of 250ms per time slot.



Figure 3.6: Time division multiple access

### 3.2.2. Frequency division multiple access (FDMA)

The bandwidth can also be separated in the frequency domain. The available spectrum is divided in multiple narrower channels. Each user is assigned with a unique frequency band. These frequency bands are separated by guard bands to prevent interference between the bands. Filters can be used at the side of the transmitter and receiver to create the distinct frequency bands; this means the hardware is different for each mouse. Differences in hardware will complicate the usage of the Neuromate, since it then becomes necessary to keep track of which mouse received which headmodule. The software could be reprogrammed in the case of doubt, but hardware can not be changed later and should indicate any difference with markings. The Neuromate already includes an FDMA application for the multiple access of the uplink, as can be seen in Figure 3.7. However, the different subcarrier frequencies are not created with hardware but can be reprogrammed [93].

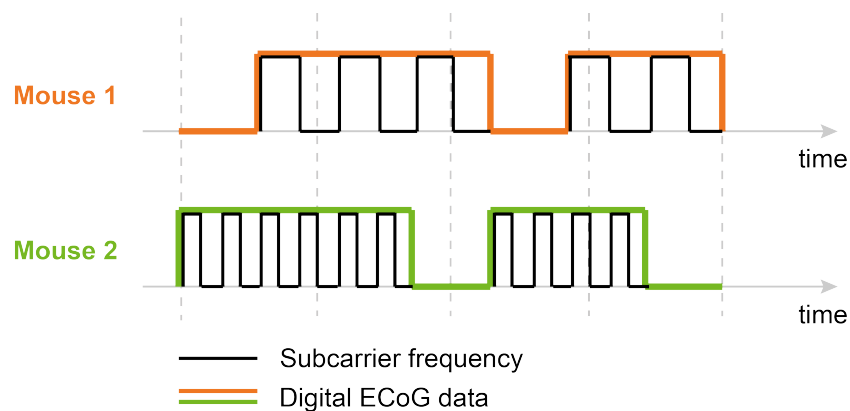


Figure 3.7: An example of FDMA in the uplink of the Neuromate, modified from [93]

### 3.2.3. Code division multiple access (CDMA)

The bandwidth can be shared without division in time or frequency domain by assigning a code, sometimes called spreading code, to the receivers. The data is processed with the code for each user and multiplied to one combined signal that is transmitted. Each receiver can decode their data from the combined signal by using their assigned code. Correct decoding at all receivers can be assured by using orthogonal codes. An example of four orthogonal codes is given in Figure 3.8. When all pairwise cross correlations are zero, a property of orthogonal signals, the data of other users will not appear in the decoding.

In appendix 3.2.3 an example of the data encoding of two bits with CDMA for four mice including their orthogonal codes is given.

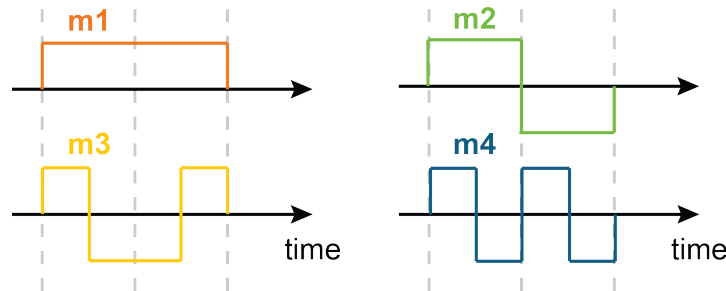


Figure 3.8: Four orthogonal spreading codes that can be used for code division multiple access

### 3.2.4. Space division multiple access (SDMA)

Space division multiple access uses the different locations of the receivers to separate the transmission signals, shown in Figure 3.9. There are two possible configurations: either the receivers are fixed at their locations or the receivers move around but do not reach the same location at any moment. The second case requires information about the current receiver locations and a steerable transmitter. SDMA will not be taken into account for the downlink since all the mice should be addressable in every corner of the cage and they should be able to interact with each other and thus be close to each other. Creating multiple narrow beams means that a mouse can walk into an area of another mouse. Future versions of the Neuromate will probably contain location information. However, SDMA is still not a suitable method because extremely high accuracies will be needed when mice are near each other resulting in a more complex solution compared to the three previously discussed multiple access methods. Therefore, in chapter 4 SDMA will not be taken into account when evaluating the possibilities of the three concepts.

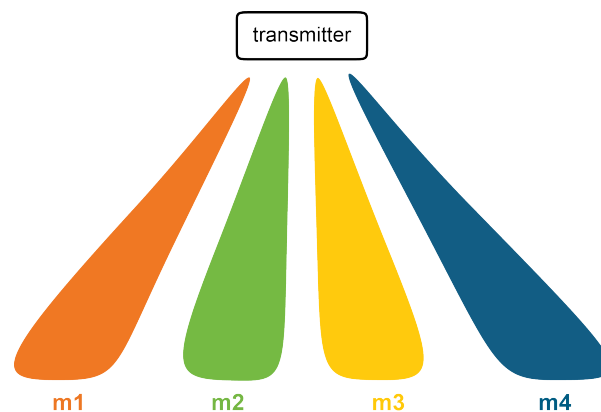


Figure 3.9: Space division multiple access

In the sections 4.1, 4.2 and 4.3 three concepts are discussed based on the carrier wave. The suitable modulation methods and multiple access techniques are discussed.



# 4

## Concepts

The main goal of this chapter is to find the best way to realise a wireless closed loop system. It should allow the neuroscientist to modify the stimulation paradigm by interacting with the module on the head of the mouse. Currently, in the wireless project mentioned in Chapter 1, communication is only possible in one direction (headmodule to researcher). This chapter considers techniques that could be added to the setup to facilitate the downlink by adding communication in the other direction (researcher to headmodule).

In the sections 4.1,4.2 and 4.3 three concepts are discussed based on the carrier wave. The suitable modulation methods and multiple access techniques are discussed.

Some carriers options are discarded for various reasons and thus not discussed here. For example, it might be discarded because it is not safe for mice or researchers e.g. near infrared radiation and x-ray. Another reason to drop a technique is the perceivability by the mice e.g. sound waves. Or it might not reach high enough data rates e.g. temperature. Alternatively, it can interfere with the two other wireless technologies e.g. magnetic switch or RF close to 915MHz [93]. The next paragraphs elucidate the three most promising carrier techniques, power source keying, optical wireless transmission (Li-Fi), and terahertz torching.

### 4.1. Power Source Keying

#### 4.1.1. Carrier

The first investigated technique was the modulation of the inductive power link. Modulating one of the previously used techniques, either from the powerlink or from the uplink both explained in Section 2.1, minimises the interference. When the power arrives at the head module on the mouse, the switching magnetic field creates an alternating current in the coil [58][53]. This alternating sine shape of the current is a potential source of information. Thus sending data together with the power over this link is feasible [76].

#### 4.1.2. Modulation

AM

Figure 4.1 shows an overview of digital modulation techniques. Since on-off keying requires periods without any transfer, and the most important function of the link is the transfer of a maximum amount of power to the head module, this is not ideal. The strength of the magnetic field is not uniformly distributed through the cage, in the corners the field is weaker. Thus the difference in amplitude should be large to also be functional in the entire cage. Amplitude modulation is the most simple option but for this carrier not the most efficient method due to the reduced amount of harvested power.



## FM

Frequency modulation is another possible modulation technique that is frequently used in RF applications as it is considered a promising tool for wireless networks [30]. Nevertheless, for the application of a combined power and communication link FM might not be the best option either. A joined resonance establishes the connection between the two coils, which in our case is not a wideband inductive link. This makes the frequency an important variable that should not be changed for applications other than setting the resonance [53] [38] [11] [13]. Thus frequency modulation is not preferred.

## PM

Phase modulation does not change the resonance frequency or the amplitude of the signal, it only switches the phase of the signal. PM is expected to be affected by the amount of harvested power the least and is thus the most promising of the three options.

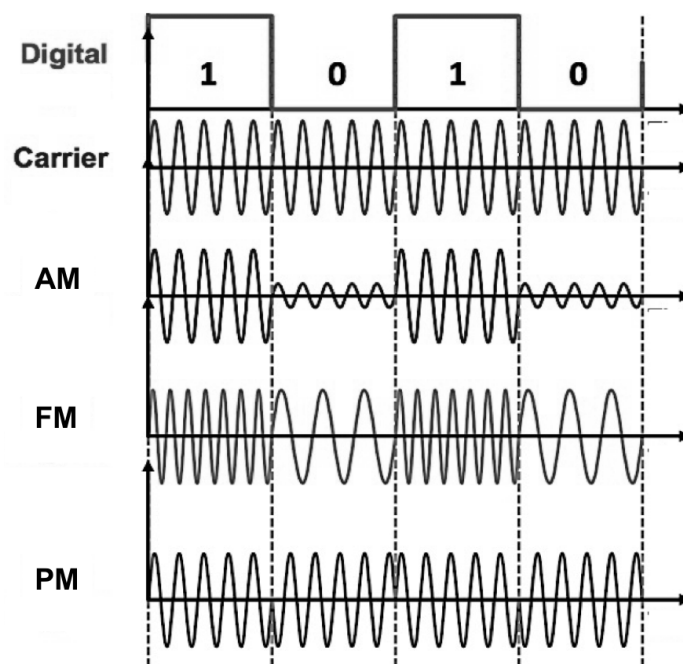


Figure 4.1: Different digital modulation methods. Adapted from Yarman et al. 2010 [80]

### 4.1.3. Multiple access

Another challenge of reusing the power link is the ability to support multi-channel communication towards the mice. Since the magnetic field is the same for all of them, there is only one power link possible within the cage [86]. When choosing for PM each mouse would be assigned a different phase shift. Comparing the assigned phase shift and the occurring phase shift enables the demodulation of the signals. This comparison can be done with differential-phase-shift-keyed (DPSK) receivers to overcome the unknown reference phase [31] [10] [75]. However, it will lead to more complex and thus larger receiver designs [16] [105] [97]. Instead multiple access methods can be used to address the right message to the intended mouse. TDMA and CDMA are both applicable since they can both be combined with a single link. In contrast to FDMA and SDMA who require four available frequencies, that are not available as was discussed above, or require four separate spacial links respectively.

When multiple mice stay in the same cage, they will all receive the same information of the phase changes via the power link [86]. By assigning a specific phase shift to every mouse, the signals are accurately distinguished. Figure 4.2 depicts these different phase changes which have to be identified and processed on the mice.

### 4.1.4. Drawbacks

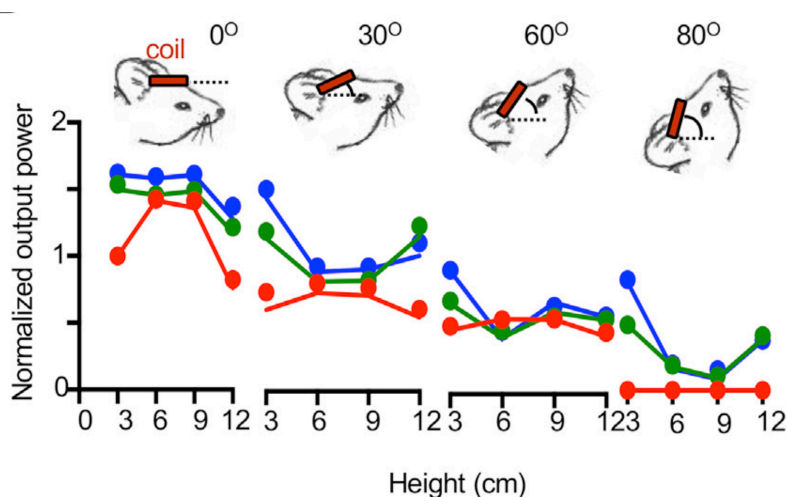


Figure 4.2: Reduction in harvested power due to misalignment in similar power harvesting for wireless rodent set up. Different colours indicate different locations in the cage. Various heights in the cage and various tilted positions of the head are compared. Courtesy of [89]

Non-continuous harvesting of the power can result in the loss of the connection. The power supply can still function well by adding a backup circuit including a capacitor. However, the communication link will suffer from interrupted harvesting. For example, when the direction of the coil on the head of the mouse is positioned orthogonal to the orientation of the magnetic field through the cage, it may lead to a considerable decrease in the harvested power and thus loss of communication as can be seen in Figure 4.2 [66] [89].

Hence, it is to be expected that the power keying is an unreliable option because it decreases the total amount of harvested power. Therefore the search for other possible non-interfering techniques was continued.

## 4.2. Visual Light Communication

### 4.2.1. Carrier

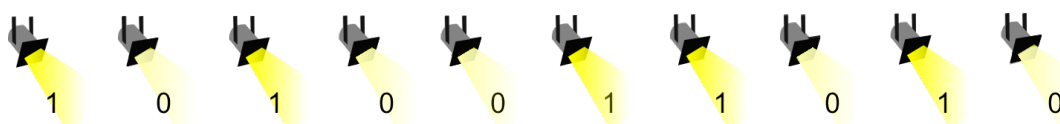


Figure 4.3: Schematic and simplified representation of VLC communication

Using the visible light spectrum for communication is known as visible light communication (VLC). By changing the intensity of the light data can be sent, as shown in Figure 4.3 The first concern of this technology is whether the mice can perceive the signals and be possibly influenced by these signals.

Some advantages of visual light communication over radio communication are the low probability of detection, interruption, jamming and 'spoofing', it will not cause interference with radio frequencies and no licence is required for using optical communication.

### 4.2.2. Modulation

#### AM

VCL also includes intensity modulation (IM) [60]. This technique recently became popular and is sometimes called Li-Fi, short for Light Fidelity. Li-Fi could complement the radio frequency spectrum that is widely used for wireless applications without interference [34]. Internet-Of-Things applications are the main target of Li-Fi. It is a technique that allows for data transmission via a widely available network of lightning bulbs. Changing the intensity of the transmitted light from a LED within a range that is not perceivable for humans will send the data. Nevertheless, rod photoreceptors in mice are packed more than twice as densely compared to the ratio in human [98]. And since the physical size of mouse rods and primate rods are similar, which is an indication of the sensitivity, it might be the case that mice can perceive much smaller differences in light intensity than humans do [46] [28] [49]. This should be further investigated.

While studying the behaviour of the mice, it is of particular importance to obtain information about their activity during the night since they are most active in the dark. When the lights are switched off, there is no data transmission. Hence, this interesting period can not be studied.

#### FM

The colour vision of mice is dichromatic, unlike that of primates who have trichromatic colour vision [46], and therefore mice can differentiate less colour grades [45] [28]. Nonetheless, the difference between the bands will be detectable with both di- and trichromatic colour vision within four generated colour bands. The signal should be undetectable for mice, and thus the use of LEDs/lasers with different colours of light is discarded unless the intensity of the total amount of light is unperceivable.

Thus, FM faces the same issues as AM faces of perceivability and light intensity variations especially during the night.

#### PM

Phase modulation is a more complex method as was discussed in Section 4.1. PM can be of value when the simpler AM and FM methods are not applicable. In this case unnecessary complexity would be added. The receiver should be kept as simple as possible to enable a light-weight and small-scale design.

### 4.2.3. Multiple access

When using Li-Fi, one way of addressing the different mice would be by using FDMA, also known as Colour Shift Keying (CSK) [34] [69]. Assigning a specific colour to each mouse will prevent multi-user system problems such as inter-user interference (IUI) [88]. At first, the use of different colours of light was discarded because the mice could react based on their visual perceptions instead of to the real stimulation. However, when the intensity variations can be proven to be undetectable by the mice, FDMA can be useful. Even as the other multiple access techniques TDMA, CDMA and SDMA. Although SDMA would require converging sources, since regular divergent light distribution will cause interference. All four methods can potentially be implemented in combination with VLC.

### 4.2.4. Drawbacks

Another important drawback of using light in the visible spectrum is the risk of shadowing and blocking by the other mice in the cage. For example, when they are sleeping mice like to crawl next to each other and the head modules may not be reachable by the light. Figure 4.4 presents the optical properties of the skin of mice. The four lines indicate skin of males and females from both albino and pigmented mice (C57BL/6 and BALB/c) [84]. The absorbing chromophores like blood, water, melanin, and fat, will block signals within the visible and infrared spectrum [47] [100] [85]. The chance of optimal line-of-sight (LoS) propagation, which is necessary for successful transmission via visible light is, reduces tremendously when the light is absorbed.

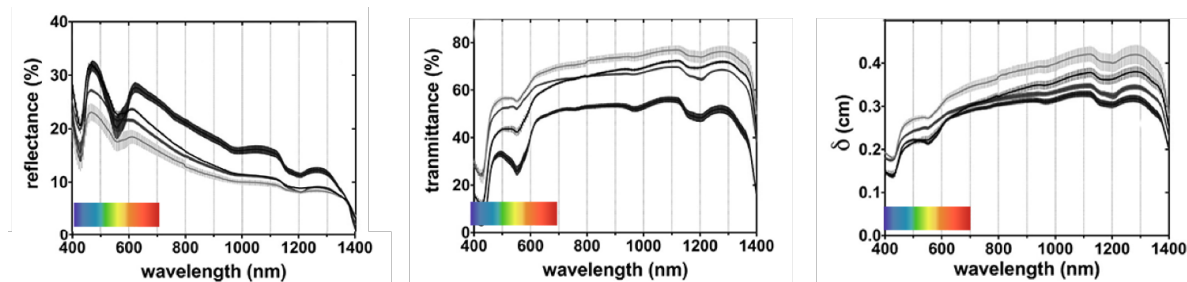


Figure 4.4: The optical properties of the skin of mice. Courtesy of [84]

Although this technique itself may not be optimal for the application, mainly due to the perceivability and the blocking effects, it did lead to the next idea of using a THz Torch since these frequencies are outside of the perceivable spectrum of mice [28] and, in principle, is less sensible to blocking.

## 4.3. Terahertz Torching

### 4.3.1. Carrier

The terahertz (THz) band covers the sub-millimeter wavelengths as is depicted in figure 4.5. The frequency band between radio waves and microwaves on one side, and the infrared spectrum followed by the visible light spectrum on the other hand. The terahertz spectrum is mainly used for astronomic and atmospheric sensing [67] and was introduced for airport security around ten years ago [23]. Recently a new application of the terahertz band is proposed by Hu et al. (2013), depicted in figure 4.6. Their goal was to create a short-link wireless communication technique [61]. Similar to our objective but executed towards a slightly different application. The borders of the terahertz band are limited in various ways, most often 0.1 up to 10 terahertz is meant when researchers use the name Terahertz. The THz Torch of professor Lucyszyn operates at the higher thermal part of the terahertz band, as he calls it: "Over the terahertz Horizon". In this report the name terahertz is used for frequencies between 0.1 and 100 THz.

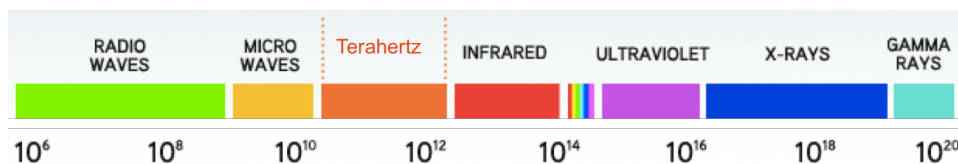


Figure 4.5: Schematic representation of terahertz band. Courtesy of [73]

The radiation in the near infrared (NIR) bands can pass through the human cornea and potentially cause damage to the retina [41]. The mid-infrared (MIR) and far infrared (FIR) bands do not induce possible eye damage [41]. The terahertz band is regarded to impose no health risk for people since it is non-ionizing radiation [23].

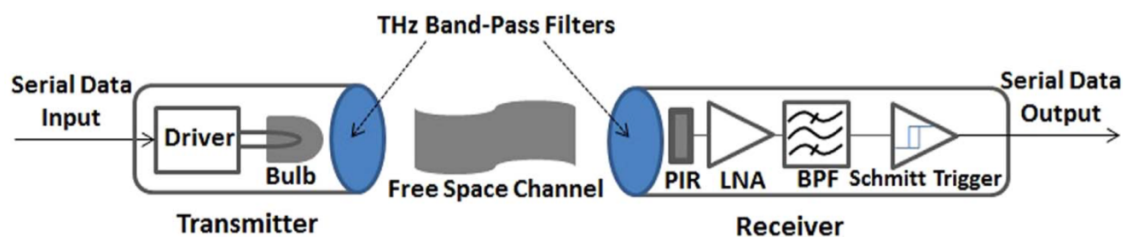


Figure 4.6: Schematic representation of Thz torch. Courtesy of [61]

The terahertz torch system consists of two parts: a transmitter and a receiver. The transmitter transforms the incoming data stream into electromagnetic waves in the terahertz spectrum. The transmitter generates a primary terahertz source, the heated tungsten filament within the bulb, and a secondary source, the increased temperature of its glass envelope [42] [18]. The terahertz band-pass filter can be used to guarantee an emission in a specific band especially functional during multi-channel communication (figure 4.7). A terahertz bandpass filter also covers the receiver. A pyroelectric infrared sensor (PIR) detects the signal and provides an output voltage when a terahertz signal is received. This voltage passes through a low-noise amplifier (LNA) and a band-pass filter (BPF), and finally, a Schmitt Trigger determines whether there was a sequence of data sent towards the receiver [40][41][42][44][43].

### 4.3.2. Modulation

#### AM

Similar to visual light communication intensity can be changed. However in this case simple on-off keying (OOK) can be used since the terahertz spectrum is not perceivable by mice. And thus a larger intensity difference can be used to modulate the signal.

#### FM

FM can be achieved by a source that can quickly switch between different frequency bands. The availability of multiple frequency bands might be more useful to create multiple access technique instead of using it for modulation, where AM is the preferred method due to its simplicity.

#### PM

Fast switching between the phase will be challenging and not beneficial over the more simple OOK scheme. As was mentioned for the two previous concepts it is difficult to detect the changing phase and demodulate the signal at the detector side.

### 4.3.3. Multiple access

Hu et al. (2014) introduced two multiple access methods based on the general FDMA, namely frequency division multiplexing (FDM) and frequency-hopping spread-spectrum (FHSS). His intention was not to enable multi-user access but to gain higher data rates. Four different frequency bands were created with the following four filters of Northumbria Optical Coating Ltd.

- SLWP-8506-000240 (0-34 THz)
- SWPB-6177-000111 (42-57 THz)
- SWPB-4596-000070 (60-72 THz)
- SWPB-3685-000091 (75-89 THz)

The setup with multiple targets created by these filters is schematically visualised in Figure 4.7.

Next to the proven application of FDMA, other multiple access methods could also be combined with the terahertz technique. TDMA and CDMA can be integrated since both do not require adaptations of the modulation or setup. SDMA is not applicable for the Neuromate application but could potentially be achieved with THz torching.

### 4.3.4. Drawbacks

The current terahertz torch example of Hu et al. 2014 is not yet applicable to the wireless mouse project mainly because of the size of the receiver [61]. Also the convergence of the beam should be addressed. Nevertheless it is possible to minimise the receiver size by choosing separate components that could be added to the head module.

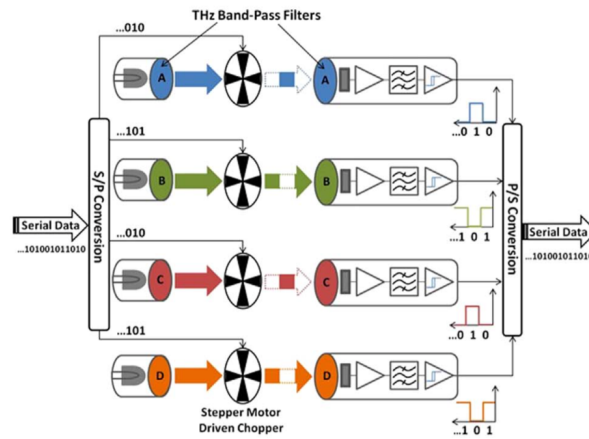


Figure 4.7: Overview of THz torching for multiple targets. Courtesy of [61]

### 4.4. Multi-criteria analysis

In order to make a choice between the described concepts a multi-criteria analysis is performed in table 4.1. The five most essential requirements, are chosen as selection criteria. A weighting value is assigned to all of them. The three options are evaluated on the chosen requirements with a scale of 1 to 5, where 1 is the lowest score and 5 the highest score. In the end, all the scores are added up to a total score for the options.

Table 4.1: Weighted criteria selection

| Requirement       | Weight | Power Keying (PK)  | Li-Fi (VCL)         | THz Torching (THz)  |
|-------------------|--------|--------------------|---------------------|---------------------|
| Size & Weight     | 3      | 3                  | 1                   | 1                   |
| Multiple mice     | 3      | 4                  | 4                   | 5                   |
| Interference      | 2      | 3                  | 5                   | 5                   |
| Power consumption | 1      | 2                  | 3                   | 4                   |
| Reliability       | 1      | 1                  | 1                   | 3                   |
| <b>Total</b>      |        | 30<br>(9+12+6+2+1) | 29<br>(3+12+10+3+1) | 35<br>(3+15+10+4+3) |

The criteria and their weights and scores are explained in more detail in Appendix 8.3.

The three most promising techniques for downlink communication that were found during this literature research have been discussed. All of them are viable options since they do fit with criteria such as safety of mouse and researcher, not perceivable by the mice, not introducing a time delay, and not interfering with the other two links. However, all three options do have their limitations.

The Power Source Phase Shifting is an attractive option because it does not add a new technique to the system by using an existing link. By doing so, it reduces the chance of interference with the other two wireless signals considerably. However, the most important function of the powerlink is to harvest as much power as possible. Using the link for other purposes will decrease the harvested amount of power, this can also be seen as a form of interference. A different phase shift could be assigned to each mouse to enable a multiple channel link. However, the powerlink is not a continuous connection, and thus data might be lost.

Visual Light Communication is an increasingly popular technique for wireless communication, mainly focused on Internet-of-Things. Fluctuating the intensity of visible light from a regular LED bulb will send a data signal without being perceivable by humans. With some modifications, this technique could fit the field observable by mice. However, shadowing and blocking are the main challenges when applying this method to the wireless mice project.

Terahertz torching is a relatively new application of the high terahertz frequency band. Signals within

the terahertz band can penetrate through tissue and are thus expected to face less blockage. And since a different band is used, the interference with the radio frequencies is limited. However, the technique is developed recently and not widely used. Therefore, the total system is not yet miniaturised, and the current terahertz torch receivers do not fit on the head of a mouse.

Based on the elaboration of the main limitations of the three most promising options and from the multiple criteria analysis terahertz torching appeared to be the most promising technique. This option mainly has practical challenges, and fundamentally provides the opportunity to form a non-interfering reliable wireless link. By creating a prototype, the feasibility of terahertz torching for the Neuromate application should be proven. However, the primary function of the powerlink is to harvest as much power as possible.

# 5

## Components

Producing and capturing terahertz waves can be done in different ways. Each technique introduces unique advantages and drawback. Based on the application, the most suitable combination of techniques should be chosen. Building a communication link, the application of the Neuromate, requires both a source and a detector, which is in contrast to observation tools in astronomy that investigate the available sources from the atmosphere and thus only require detectors. In the last 50 years, many new terahertz techniques have been developed. Below one or two examples are given to illustrate each type of source and detector, together these examples form an overview of widely used techniques in the (thermal) terahertz band. [12] [14] [21] [62]:

### terahertz Sources

- Thermal sources
  - Black bodies
  - Metamaterials
- Electrical sources
  - Backward wave oscillator (BWO)
- Optical/Photonic sources
  - Quantum cascade lasers (QCLs)
  - Photomixing

### THz Detectors

- Thermal Detectors
  - Bolometer
  - Pyroelectric device
- Photoconductive Detectors
  - Gallium Arsenide Detectors
- Heterodyne Detection
  - Schottky Diode Mixer

### 5.1. THz Sources

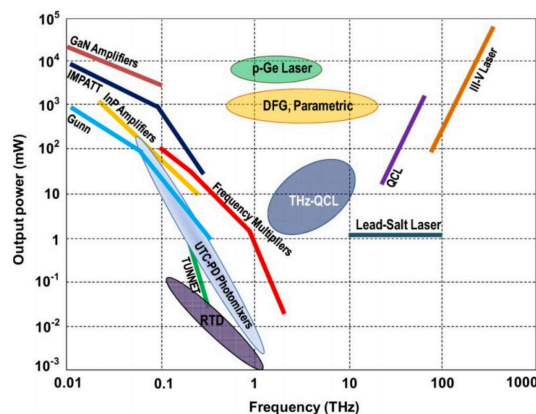


Figure 5.1: Overview of electrical (left) and optical (right) THz sources

In Figure 5.1 the output power of different Thz sources and IR sources is plotted against their operating



frequency. Not all of these sources will be discussed in this chapter. Nevertheless, it does visualise the terahertz gap clearly. The THz sources at the left loose power once the frequency goes up. And the IR sources, at the right, loose power when the frequency goes down. The region in between, around 1-10 THz, is called the THz gap.

### 5.1.1. Thermal sources

#### Black bodies

A black body is an object that behaves according to Planck's law 5.1. The absorbed and received energy are equal and solely determined by the temperature of the object. In reality, the emitted radiation also depends on the absorption of the material. Thus the concept of a black body is an idealisation. However, some objects such as the Sun behave in a comparable way to ideal black bodies. The spectrum of the Sun is very close to that of a 5778 K black body [1].

$$I(\lambda, T) = \frac{2hc^2}{\lambda^5} \frac{1}{e^{(hc)/(\lambda kT)} - 1} \quad [W/m^2/sr/m] \quad (5.1)$$

The radiated power ( $I$ ) per unit area of the emitting surface per unit solid angle per unit wavelength at absolute temperature  $T$ .  $\lambda$  is the free space wavelength;  $h$  is the Planck constant;  $c$  is the speed of light in a vacuum;  $kB$  is the Boltzmann constant.

The source that was used for the original "THz Torch" project was a black body. A tungsten filament lamp, which is a widely used source of light in homes due to its cost effectiveness and longevity.

#### Metamaterials

Blackbodies are objects that exists in nature. Metamaterials are man-made materials that are similar to blackbodies but include optimized properties. One property that scientist try to address is emission spectrum of a material. For example by creating selective emitter with a narrower thermal radiation compared to a blackbody at the same temperature [62]. Based on Kirchhoff's radiation law it is expected that material can emit exactly the same thermal emission spectrum as it has absorbed. Thus the absorption characteristics are also addressed by material scientist [6].

### 5.1.2. Electrical sources

#### Backward wave oscillator (BWO)

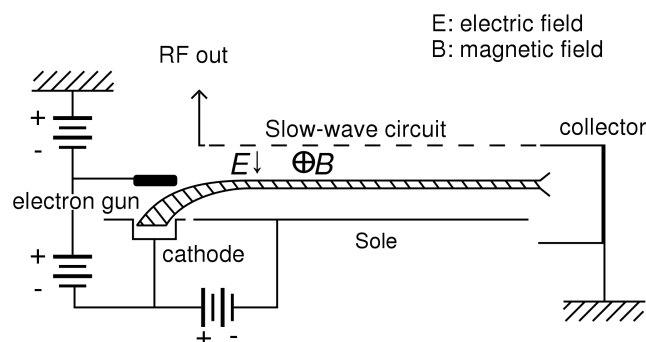


Figure 5.2: Schematic overview of an BWO. Picture from Wikimedia Commons

Backward wave oscillators also known as carcinotrons, are vacuum tubes that create terahertz frequency by shooting an electron beam through a strong magnetic field [25] [14]. BWOs are commonly used in laboratory environments but they are bulky and require high operational voltage.

### 5.1.3. Optical sources

#### Quantum cascade lasers (QCLs)

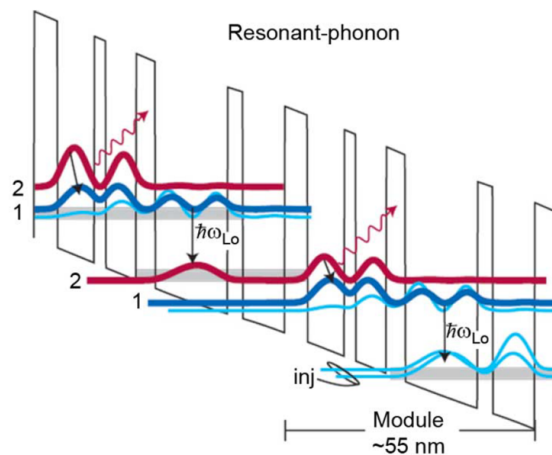


Figure 5.3: Energy levels in a quantum cascade laser. Courtesy of [14]

Quantum cascade lasers (QCLs) use the intersubband transitions between the quantum wells. Those wells are layers of gallium arsenide (GaAs) in between barriers of Aluminium gallium arsenide (Al-GaAs). The QCL exists of repeating active regions, where the electron is transitioned to a lower energy level while emitting photons, and injectors, that couples the electrons to a higher energy level before it reaches the next active region [25]. Figure 5.3 schematically represents the energy band of a QCL and the energy levels [14]. The band gap of the material determines the emission wavelength of the laser. A QCL can achieve high output power for the terahertz frequencies. However, the systems cannot operate at room temperature since it requires cooling which also increases the size.

#### Photomixing

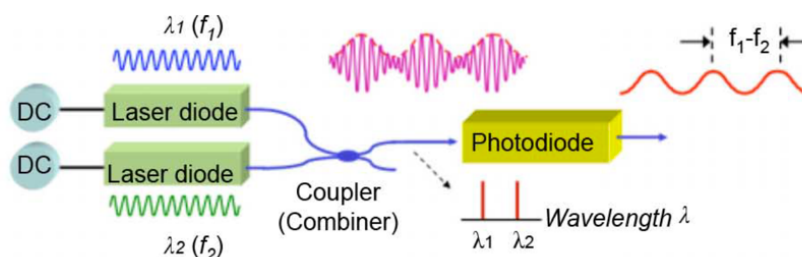


Figure 5.4: THz continuous wave generation with photomixing courtesy of [14]

Terahertz signals can also be generated by the down conversion of an optical signal. Two lasers with different output wavelengths are mixed together. The difference between their frequencies should lie within the terahertz region as shown in Figure 5.4. By combining two inexpensive lasers with commercial off-the-shelf (COTS) components a cost-effective telecommunication setup can be realised [41]. The poor frequency stability and phase noise performance are drawbacks of photomixing [14].

## 5.2. THz Detectors

### 5.2.1. Thermal Detectors

#### Bolometer

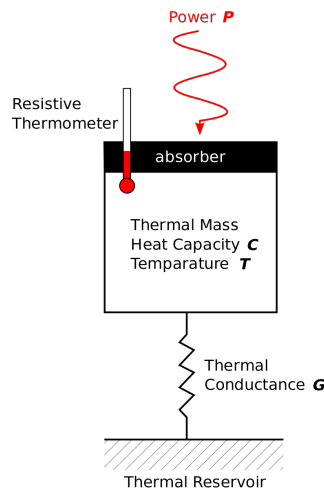


Figure 5.5: Schematic illustration of a bolometer. Picture from Wikimedia Commons

A bolometer consists of a thermometer that is connected to an absorber material and a supporting substrate. The radiation will fall onto the absorber and is conducted via the supporting substrate, which has a large thermal conductivity [81]. Bolometers have been used for almost 40 years, and they are still used and optimised. For example, superconductor bolometers were created based on the change of state of niobium [25].

#### Pyroelectric device

A pyroelectric detector converts thermal energy into electrical energy by the generation of an electric charge in response to a heat change. The equivalent circuit of an pyroelectric detector is shown in Figure 5.6. The sensor capacitance ( $C$ ) will be of importance again in Section 8.3.

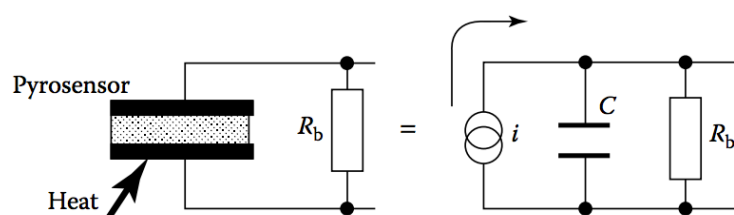


Figure 5.6: (a) Pyroelectric detector (b) equivalent electric circuit diagram; figure courtesy of [26]

A pyroelectric detector can operate at room temperature, is relatively cheap and robust, and can achieve response times up to less than a nanosecond [12].

### 5.2.2. Photoconductive Detectors

#### Gallium Arsenide Detectors

Gallium Arsenide (GaAs) is a photoconductive material. Based on the effective mass ratio of electrons in GaAs it was expected that the material could be used in the terahertz spectrum. However, GaAs

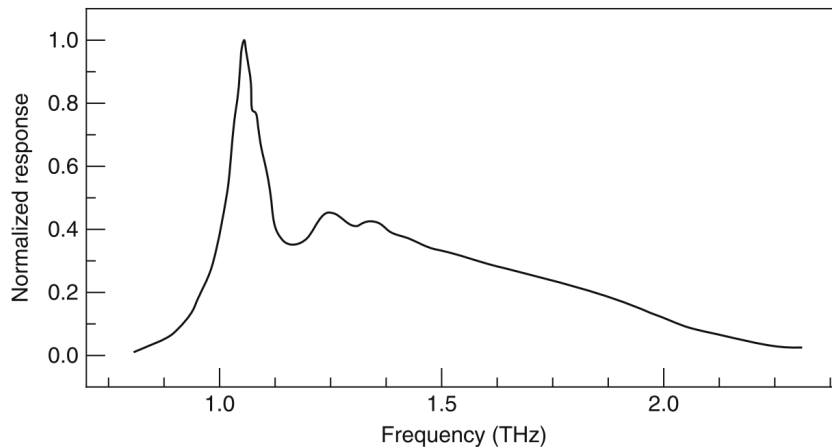


Figure 5.7: Photoconductivity of GaAs detector material. Courtesy of [12]

detectors have a high resistance, in the GOhm range, thus achieving both high speed and good detectivity can be challenging in practice. A peak response around the frequency of 1.06THz has been observed as can be seen in Figure 5.7[12].

### 5.2.3. Heterodyne Detection

#### Schottky Diode Mixer

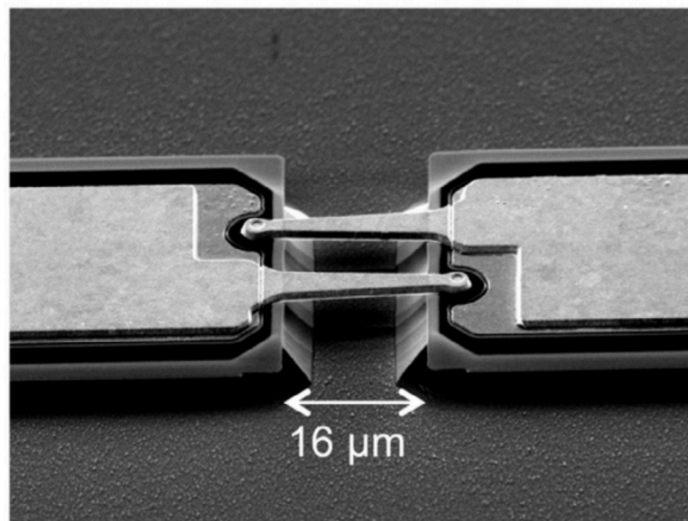


Figure 5.8: Image of an anti-parallel pair of airbridged Schottky diodes. Courtesy of [20]

Schottky diode devices, as shown in Figure 5.8, are currently the most widely used terahertz detectors. They are applied in test equipment, scientific instrumentation and transmit elements in radars and communication systems [20]. A schottky diode mixer converts the signal power to an output power by comparing the incoming signal with the frequency of a local oscillator. Schottky diode devices do not have to be cooled and can be made small-scale and low-weight [90].

### **5.3. Component Selection**

An overview of the available types of sources and detectors is given. For the Neuromate the most suitable combination of components is chosen to be the thermal link. Thus a thermal source combined with a thermal detector to make sure the operating spectrum of the source fits with the sensitivity of the detector.

The most important arguments for the selection of the thermal components are the compliance with requirement II.i about the assembly of the prototype. Which should not be too complex due to the time limitation for this thesis project of 6 months. And the compliance with requirement III.vii about the experiment location. The small-scale and low-cost thermal sources are most suitable for the Neuromate application.

# 6

## Experiment

To determine whether the proposed concept is a suitable solution for the Neuromate project a proof of principle was built. The signal quality was evaluated for different conditions. The prototype can be used in combination with the other prototypes (of the powerlink and uplink) when it can transfer bits over at least 50cm, with 40° misalignment, and with a data rate of 30bps. Thus the influence of these three parameters: distance, misalignment, and data rate, were changed and tested independently. In this chapter, the experiments and the setup will be explained in more detail. Information about the prior conducted infrared pilot experiments can be found in Appendix 8.3. And the next chapter will discuss the results and elaborate on the relation between the signal quality and the three parameters.

Figure 6.1 shows a schematic overview of the experimental setup, the basic communication scheme that was introduced in Chapter 3 can be recognised in the setup since the prototype is a communication link.

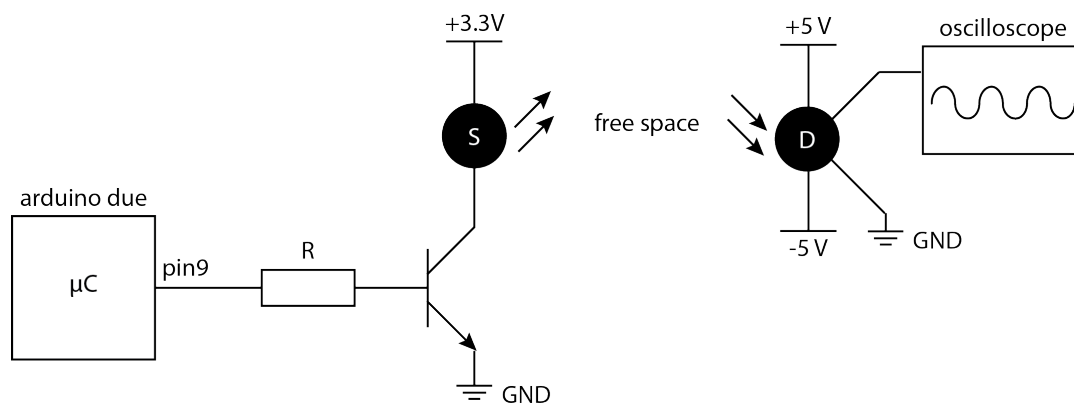


Figure 6.1: Schematic representation of the experimental setup, where S, the source, is the transmitter and D, the detector, is the receiver. The default transmission channel for the prototype is free space.

## 6.1. Materials

Next to the chosen source and detector, the experimental setup included more components. The entire setup is shown in Figure 6.2. The functional blocks are schematically represented in Figure 6.1. The transistor used was a BC550C low noise NPN transistor. The base resistor,  $R$ , was chosen to be 620 Ohm to enable a collector current (through the source) of 64 mA, the typical operational current retrieved from the data sheet of the source. The signal was generated by programming the arduino due, for the code used see the Appendix 8.3. A signal which included all possible bit transitions was generated and repeated. When those transitions are plotted on top of each other an eye diagram appears. The signal quality is determined based on those eye diagrams, in Section 6.3.1 this analysis method is explained. The power supply devices are not further discussed.

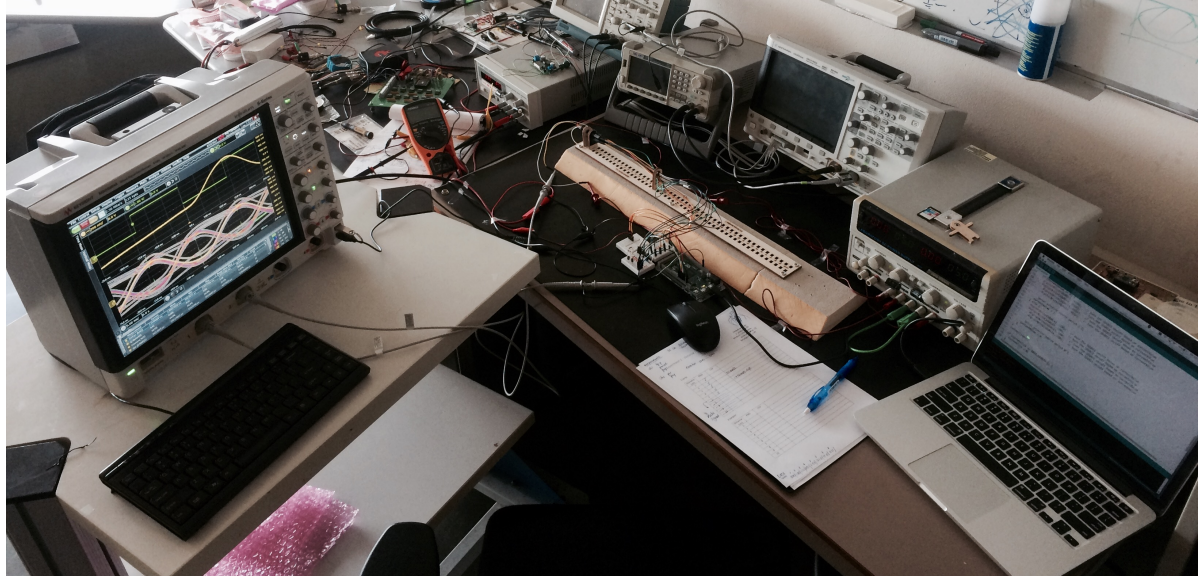


Figure 6.2: Overview of the entire experiment setup

The two most important components of the tested prototype are the source and the detector.

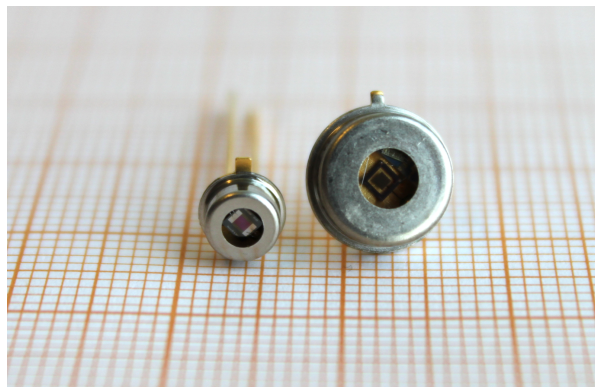


Figure 6.3: Image of the chosen source and detector on millimetre paper

### 6.1.1. Source

The chosen source is the infrared radiation source JSIR350-5-BL-C-D2.55-0-0 from Micro-Hybrid. Due to its small size, indicated in Figure 6.3, the radiation element is able to heat and cool down fast. A beneficial property when higher data rates are required.

### 6.1.2. Detector

The chosen detector is the one channel pyroelectric low noise detector PS1x1C2-A-S3.7-open from Micro-Hybrid. The PS1 is a current mode pyroelectric detector. The active area of the detector is  $0.8 \times 0.8\text{mm}^2$  and made of nanoamorphous carbon (NAC) which has a wide range of infrared transparency ( $1\text{-}14\ \mu\text{m}$ ) and a conductivity that can reach  $10^3\ \text{S/cm}$  resulting in a high detectivity ( $D^*$ ) of  $2.8 \times 10^8 \frac{\text{cm}\sqrt{\text{Hz}}}{\text{W}}$ . [datasheet Microhybrid].

#### Filter

Without an optical filter the detector was completely saturated when connected. The output value was always high and could only be influenced by blocking the detector. The nanoamorphous carbon (NAC) material appeared to be sensitive to background sources of radiation, such as sunlight and human heat. By mounting an optic filter in front of the detector only specific signals were captured. The filter was removed from a IRA-S210ST01 PIR detector that was used during the pilot. In the datasheet of the PIR the graph, shown in Figure 6.4, was presented. From the graph it becomes clear that the filter transmits all signals with a longer wavelength than  $5\mu\text{m}$ . However, even in the higher region the transmission was decrease by the filter to a level of 80-90%.

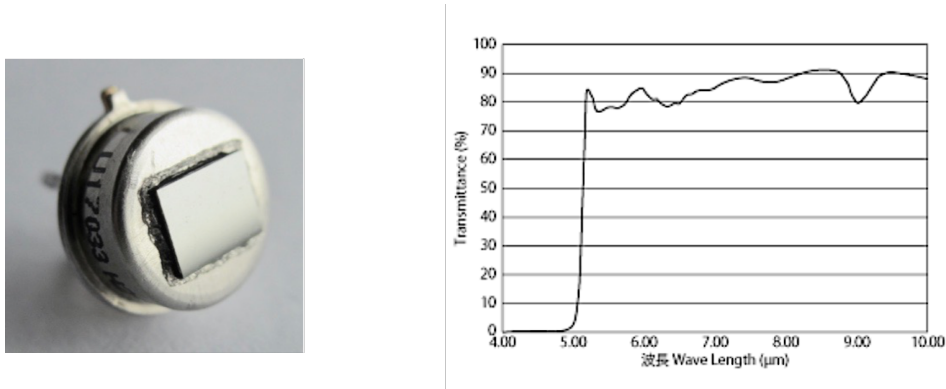


Figure 6.4: Spectral transmittance for the  $5\mu\text{m}$  long-pass filter [41]

### 6.1.3. Cases and Baseplate

The source and the detector both had their own lasercutted wooden cases. They were designed to align the active elements of both components. The feet at the bottom of the cases fit into the holes of the base-plates. These holes were designed to locate the cases at an exact distance or at the intended misalignment. An example of the baseplate and the cases is shown in Figure 6.5 and 6.6 respectively.

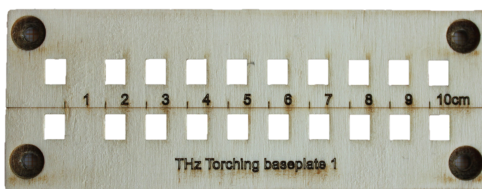


Figure 6.5: First version of the first baseplate (top)



Figure 6.6: Cases source and detector (back)

The design was created in illustrator and produced with a lasercutting machine from Lionlasers at the PMB in the faculty of Industrial Design Engineering. To systematically vary the distance and the



misalignment two baseplates were produced: 1. Distance varying from 1cm increased with steps of 1cm up to 50cm. 2. Misalignment options form  $0^\circ$  up to  $90^\circ$ . Wood is a product of nature thus accuracy can vary between prototypes. The 'feet' of the cases were produced too large on purpose to make a tight connection with the baseplate. After sandpapering and with pressure the cases were fixated to the baseplate.

#### 6.1.4. Oscilloscope

The signal quality was measured with the MSOS804A oscilloscope from Keysight, which was generously lent by the Microelectronics group that share their floor and measurement rooms with the Bioelectronics group. This oscilloscope has many features including the creation, display and automatic measurement of an eye diagram, due to embedded clock recovery. An eye diagram provides a visual of the signal quality and includes parameters such as the jitter and the Q-level. This analysis method will be explained in 6.3.1.

## 6.2. Measurement Method

The source and the detector were secured in their wooden case by means of damping folded tissue bands, glue and duck-tape. The the wires of the sources and the detector were all thickened with solder tin to create a tight connection with the regular female jump-wire connectors. In front of the detector an IR filter was placed and secured with glue. The first conducted experiment was the data rate experiment which determined the default setting for all other experiments.

### 6.2.1. Experiment 1 - Data rate

Table 6.1: The default settings for the data rate experiment

|                 |                  |
|-----------------|------------------|
| # sources       | 4                |
| <b>interval</b> | <b>5 - 17 ms</b> |
| distance        | 2 cm             |
| misalignment    | $0^\circ$        |
| power supply    | 3.3 V            |
| medium          | free space       |

From the data sheet of the detector a minimum data rate of 30bps was expected, since the time constant was typically 17 ms. The graph in Figure 6.7 illustrates controlling the source on a minimum speed versus a maximum speed. Minimum control drives the source up to a point of 63% of the power and back to the baseline, which requires twice the minimum of 17ms delay. The maximum achievable data rate depends on the smallest value of  $\Delta T$ . However, due to the overlaying low-pass and high-pass filters from the internal circuit of the components a single optimum data rate was expected to lay around 35Hz, as shown in Figure 8.5. A series of tests with a data rate varying between 29.4Hz and 100Hz was conducted to determine the most optimal data rate experimentally.

Since the interval [ms] between the on and off state of the source determined the data rate [Hz] both units are used, Table 6.7 shows their relation.

| Interval | Data rate |
|----------|-----------|
| 17 ms    | 29.41 Hz  |
| 16 ms    | 31.25 Hz  |
| 15 ms    | 33.33 Hz  |
| 14 ms    | 35.71 Hz  |
| 13 ms    | 38.46 Hz  |
| 12 ms    | 41.66 Hz  |
| 11 ms    | 45.45 Hz  |
| 10 ms    | 50.00 Hz  |
| 9 ms     | 55.56 Hz  |
| 8 ms     | 62.50 Hz  |
| 7 ms     | 71.43 Hz  |
| 6 ms     | 83.33 Hz  |
| 5 ms     | 100.00 Hz |

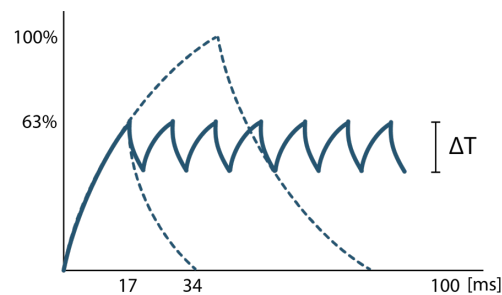


Figure 6.7: Table: Data rate relation to interval. Fig: Influence of timedelay source on data rate

### 6.2.2. Experiment 2 - Distance

Table 6.2: The default settings for the distance experiment

|                 |                  |
|-----------------|------------------|
| # sources       | 4                |
| interval        | 14 ms            |
| <b>distance</b> | <b>1 - 10 cm</b> |
| misalignment    | 0°               |
| power supply    | 3.3 V            |
| medium          | free space       |

The parameter varied was the distance between the source and the detector. Starting from a distance of 1cm and increased with steps of 1cm up to a maximum of 50cm misalignment (which was not reached during the experiments). The experiment was conducted four times in a row, first with only one source operating, then two sources, followed by three sources, and finally with all four sources radiating simultaneously.

### 6.2.3. Experiment 3 - Misalignment

Table 6.3: The default settings for the misalignment experiment

|                     |                   |
|---------------------|-------------------|
| # sources           | 4                 |
| interval            | 14 ms             |
| distance            | 2 cm              |
| <b>misalignment</b> | <b>10° to 90°</b> |
| power supply        | 3.3 V             |
| medium              | free space        |

The parameter varied was the misalignment. Starting from an angle of 0° and increased with steps of 10° up to a maximum of 90° misalignment. A special baseplate was created in Indesign by Adobe, the distance between the two components was kept constant the angle from the midline was increased for each step, as shown in Figure 6.9.

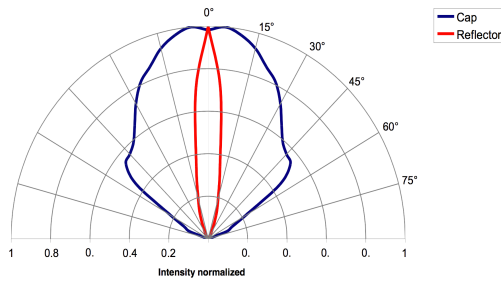


Figure 6.8: Two caps result in different radiation patterns, the reflector will form a more focused and powerful beam compared to the cap option that was used during the experiments

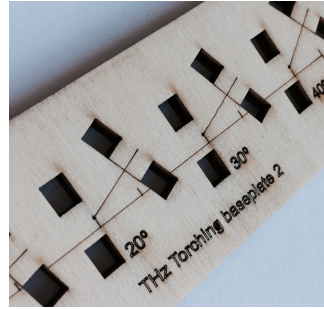


Figure 6.9: First version of the second baseplate, distance was 1cm in the image but the final version included 2cm distance between source and detector

### 6.2.4. Experiment 4 - Power

Table 6.4: The default settings for the power experiment

|                     |                                    |
|---------------------|------------------------------------|
| # sources           | 4                                  |
| interval            | 14 ms                              |
| distance            | 2 cm                               |
| misalignment        | 0°                                 |
| <b>power supply</b> | <b>alternating vs. constant ON</b> |
| medium              | free space                         |

The current driven from the power supply by the source(s) was read for different conditions, the total current drawn with 1,2,3 or 4 sources connected and for continuous high output or during transmission of the data. The current driven by the detector was too low to be presented by the power supply. Thus was decided for this experiment to focus on other parameters. The output voltage range of the detector was measured for different amount of sources and continuous or alternating transfer of data, to present the effect of the different power levels of the source.

### 6.2.5. Experiment 5 - Medium

Table 6.5: The default settings for the medium experiment

|               |                |
|---------------|----------------|
| # sources     | 4              |
| interval      | 14 ms          |
| distance      | 5 cm           |
| misalignment  | 0°             |
| power supply  | 3.3 V          |
| <b>medium</b> | <b>varying</b> |

In this case different media were tested on their influence to the attenuation of the signal. The signal was not strong enough to penetrate through tissue of a human hand. Therefore was decided to not test with real mice tissue. A prototype with stronger source is required to test the penetration through a mouse ear, tail, claw, or total body. However, the transmission of paper, fabric, plastic and wood were tested.

## 6.3. Analysis Method

### 6.3.1. Eyediagram

An eye diagram is a visual representation of the signal quality. Often used in telecommunication to compare system quality with similar protocols. All eight possible 3 bit combinations are plotted on top

of each other together forming the shape of an eye, as is illustrated in Figure 6.10. The opening of the eye is related to the bit rate error. Namely, the larger the opening of the eye, the clearer the difference between 1 and 0 and the more easy a bit can be detected. And for a more closed eye the chance is higher that a bit gets incorrectly flipped [95][27][48].

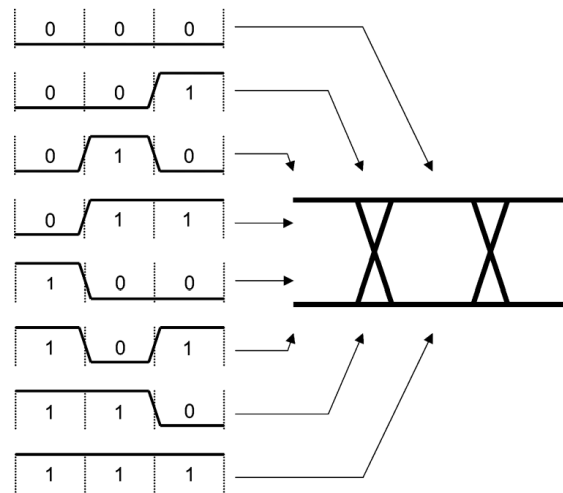


Figure 6.10: All possible bit transitions plotted on top of each other results in an eye diagram courtesy of [48]

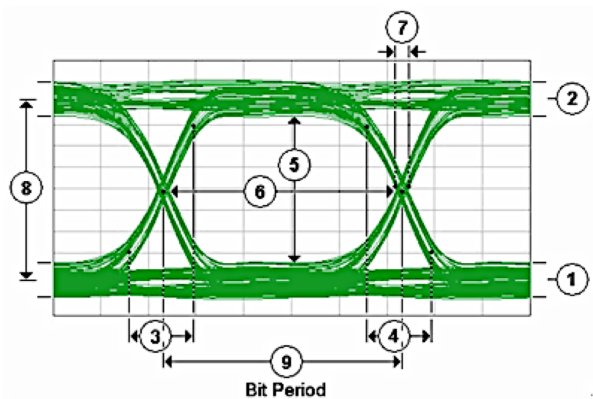


Figure 6.11: The key eye diagram definitions, source: Keysight

The most important quality measure in optical communication links is the bit error rate (BER). However, measuring the BER takes a substantial amount of time if it is small. Thus counting errors is not an ideal method to define the quality of an optical communication link [27]. Another important quality measure is the Q-factor, which is related to the BER. Both measures are used in the field of optical communication and it is possible to estimate the BER based on the Q-factor and vice versa.

Since the oscilloscope did measure the the Q-factor and not the BER the optimum BER value was estimated with the following formula, provided by Freude et al. 2012, to allow for comparison with other methods [27]:

$$BER_{op} = \frac{1}{2} \operatorname{erfc}\left(\frac{Q}{\sqrt{2}}\right) \tag{6.1}$$

All parameters that include their units and do not specifically mention otherwise were measured during the experiment.

Table 6.6: Eyediagram definitions, # link to Figure 6.11

| # | Name                         | Explanation                                                                    |
|---|------------------------------|--------------------------------------------------------------------------------|
| 1 | Eye zero level [mV]          | The mean value of the logical zero                                             |
| 2 | Eye one level [mV]           | The mean value of the logical one                                              |
| 3 | Rise Time (not measured)     | Time the upward transition from the 10% to 90% level takes                     |
| 4 | Fall Time (not measured)     | Time the downward transition from the 90% to 10% level takes                   |
| 5 | Eye height [mV]              | Vertical opening of the eye, $(onelevel - 3\sigma[1])(zerolevel + 3\sigma[0])$ |
| 6 | Eye width [ms]               | Horizontal opening of the eye                                                  |
| 7 | Eye jitter RMS [ms]          | Deviation from the ideal periodicity                                           |
| 8 | Eye Amplitude (not measured) | Difference between zero level and one level                                    |
| 9 | Bit Rate (not measured)      | Data rate, width of one bit from crossing to crossing                          |
| - | Crossing [%]                 | Crossing points amplitude relative to one and zero level                       |
| - | Q-factor [-]                 | General metric of signal quality often used to estimate BER                    |
| - | Duty Cycle [ms]              | Time difference between rising and falling edge at 50% (middle) threshold      |

# 7

## Results

### 7.1. Data rate

The data rate experiments was conducted first to determine the default data rate for the other experiments. An optimal data rate of 35Hz was expected due to the 'high-pass/low-pass misinterpretation', which will be explained in Section 8.3. From the eyediagrams that were created for data rates between 29.41 Hz and 100 Hz (between 17ms and 5ms interval). Different parameters, explained in Section 6.3.1, were measured and are displayed in the graphs in Figure 7.1. The two plots on the top are the most important since they show the BER values and Q-factors.

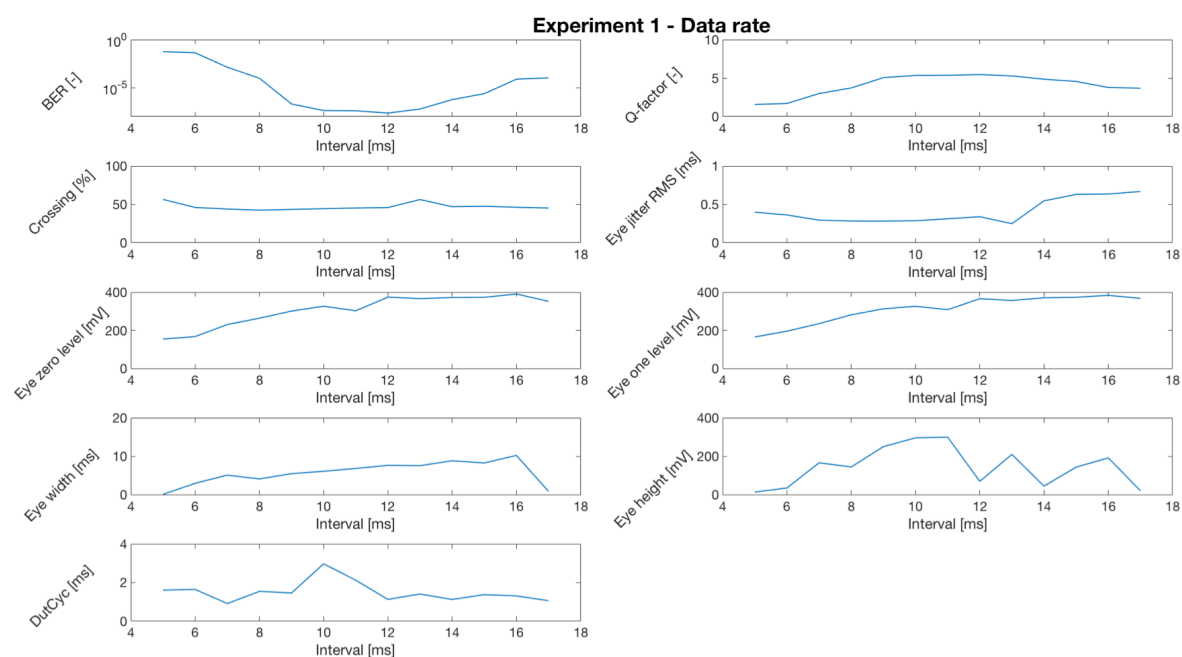


Figure 7.1: Mean parameter changes over varying data rate

There are some important notes about the results to make. The Eye zero level is given as an absolute value, thus higher the zero-level the better. The Crossing should optimally be around 50%. And the longer the sources stays on the more time it has to heat up and thus slower data rates will result in higher output power.

## 7.2. Distance

Four situations were tested for transmission over the increasing distance. The first case was with 4 sources turned on simultaneously, represented by the blue lines in Figure 7.2, in the second case three sources were powered, the red lines, two sources, yellow lines, and the setup with only one source connected is represented by the purple lines.

The distance has a major impact on the signal strength, an exponential decay can be seen output peak-to-peak voltage. The quality of the link decreases within a few centimetres to unacceptably high BER values. The importance of the power that the source can transmit is indicated by the different lines. Four times higher power, when all four sources were transmitting simultaneously, show better results for almost all parameters. Especially the BER, Q-factor, zero and one levels, and output voltage show higher quality of the link with the use of a stronger signal.

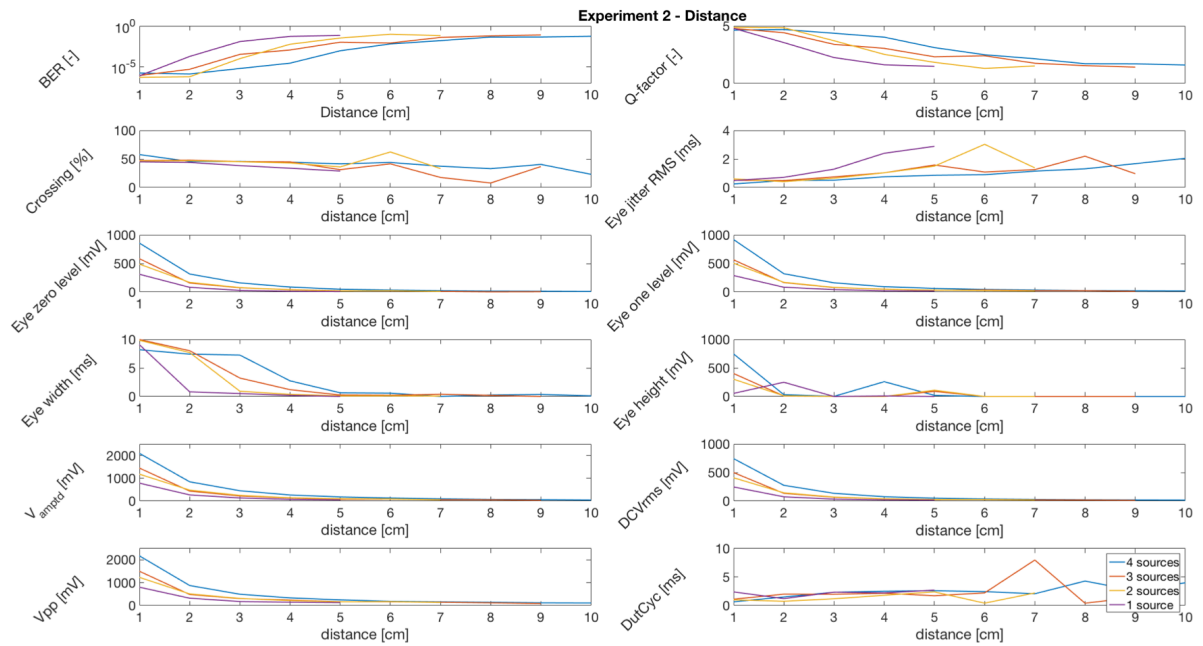


Figure 7.2: Mean parameter changes over varying distance

### 7.3. Misalignment

A beam divergence close to that of a Lambertian emission is expected based on the transmission shape shown in Figure 8.7.

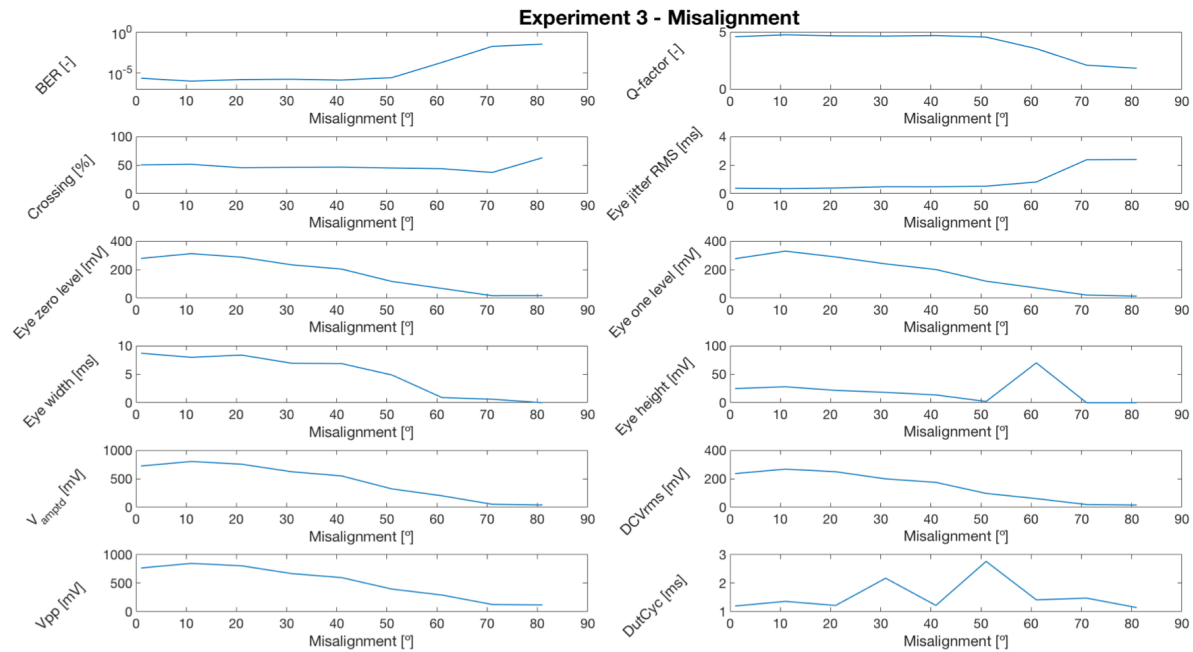


Figure 7.3: Mean parameter changes over varying misalignment

In this experiment the emission angle of the source is proven to be wide, as was expected. Between 40° and 60° the signal quality started to decay. And from Figure 7.3 it can be seen that the BER value is stable around  $< 10^{-5}$  for a misalignment up to 50°. This validates the assumption of the source having a Lambertian emission spectrum.

### 7.4. Power

Sources draw around 64mA each, thus step wise increase means the setup was a valid simulation of four times higher power compared to a single source. In the situation were data was transferred the sources was alternating. Therefore, the current drawn was not stable and more difficult to read.

Table 7.1: Source

| Source(s)   | 1 source   | 2 sources  | 3 sources   | 4 sources   |
|-------------|------------|------------|-------------|-------------|
| ON          | 64 [mA]    | 123 [mA]   | 183 [mA]    | 241 [mA]    |
| Alternating | 24-35 [mA] | 52-67 [mA] | 75-100 [mA] | 97-137 [mA] |

A pyroelectric detector is only sensitive to changes, thus constant high signal results in a low output signal. The default output value of the detector was 35mV, which was observed during all constant illumination values. The output voltage for the alternating signal did increase with the increase in signal power. Four active sources resulted in four times higher output voltages from the detector.

Table 7.2: Detector

| Detector    | 1 source | 2 sources | 3 sources | 4 sources |
|-------------|----------|-----------|-----------|-----------|
| ON          | 35 [mV]  | 36 [mV]   | 35 [mV]   | 35 [mV]   |
| Alternating | 250 [mV] | 520 [mV]  | 773 [mV]  | 1000 [mV] |



## 7.5. Medium

In Figure 7.4 the output of the detector from communication links with different media is shown. In A. the signal was transmitted through free space, the default situation. B. indicates the penetration through a human hand, which did not result in a detectable output signal because there was too much attenuation. C. shows that a signal could be send through coloured bubble wrap since it is a material mainly consisting of air, thus the attenuation is lower than for tissue. Situation D. a single sheet of paper was put in between the source and the detector and it blocked the signal, similar to the blockage of a human hand.

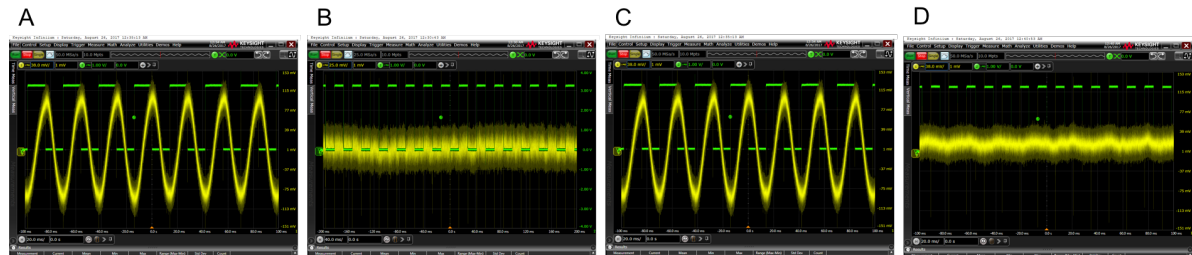
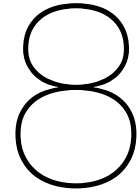


Figure 7.4: Output signal of the detector when transmitted through different media. A) free space (no obstruction), B) human hand, C) bubble wrap, D) paper A4 (thickness)

Source and detector were placed on a distance of 5cm from each other so that different material could be placed in between. The distance experiment 6.2.2 already showed a strong decay of the signal power at 5cm.

One advantage of THz over VLC was expected to be the reduced blocking of soft tissue. However, it was unknown whether the THz Torch could indeed penetrate through mouse tissue. Especially because of the high water content of the tissue and the known attenuation of THz due to water. Whether the blocking issue of a THz Torch are reduced in comparison to VLC could not be eliminated by this experiment. The tests should be repeated with a future version of the prototype including a more powerful source.



# Concluding remarks

## 8.1. Conclusion

This report describes an exploratory study to a new small-scale, low-cost, divergent, wireless communication method for multi-user biomedical applications such as the Neuromate project. The first goal was to find an optimal technique to complement the current Neuromate project with a wireless downlink to enable continuous and individual control over the stimulation patterns of the four mice. Furthermore, the new principle had to be tested with a prototype thus the second goal was to build a proof-of-principle and evaluate it in a series of experiments.

In Chapter 2 the requirements were determined and an overview of the current status of wireless projects was created. After that an introduction is given to communication and modulation in Chapter 3, including the two main components: the transmitter (source) and the receiver (detector). Amplitude and angular (frequency and phase) modulation were explained next to four multiple access methods, TDMA, FDMA, CDMA and SDMA. Chapter 4 elucidated the three most promising techniques to realise a wireless closed loop system. All of them were viable options since they do fit with criteria such as the safety of mouse and researcher, the unperceivability by the mice, not introducing a time delay, and not interfering with the other two links.

The first concept, Power Source Keying, was an interesting option because it does not add a new technique to the system by using an existing link. By doing so, it reduces the chance of interference with the other two wireless signals considerably. However the power link was not a continuous link, and thus data might be lost. The second concept, Visual Light Communication, an increasingly popular technique for wireless communication, mainly focused on Internet-Of-Things. Fluctuating the intensity of visible light from a regular bulb would send a data signal with out being perceivable by humans or in our case by mice. However, shadowing and blocking were the main foreseen challenges for the application in the Neuromate project. The third concept, Terahertz torching, was the relatively new application of the thermal Terahertz frequency band. Signals within the terahertz band can penetrate through soft tissue and thus were expected to face less blockage. However, the technique was developed recently and not widely used. Therefore, the total system was not yet miniaturised, and the current Terahertz torch receivers did not fit on the head of a mouse.

From the multiple criteria analysis Terahertz Torching appeared to be the most promising technique for our specific application. This option mainly has practical challenges, and fundamentally provides the opportunity to form a reliable non-interfering wireless link. Thus the feasibility of THz Torching was tested by creating a proof-of-principle and conducting five different experiments with it.

In Chapter 5 examples were given to illustrate different types of widely used sources and detectors in the (thermal) terahertz band. Concluding with the most suitable types for the downlink prototype. Chapter 6 started by describing the prototype in more detail and continued with the experiment design which was divided into five separate experiments. The results of these experiments were presented in Chapter 7.

During the experiments the principle of communication with a THz Torch was proven to be feasible. Experiment 3 resulted in an optimum data rate of 35.71 bps, allowing for the simultaneous stimulation of the mice. And the divergence of the source was sufficient to cover the entire cage, as in Experiment 2 an angle of  $50^\circ$  was proven to be the maximum misalignment that still allowed transfer of the data. However, the prototype did fail to reach the required distance. In experiment 2 only 8 cm could reliably be bridged. The source was not strong enough to overcome the attenuation in the air. A more powerful source will allow an increased reachable distance and makes sure the entire cage will be covered.

Figures 8.1,8.2,8.3 show the bit error rates (BER) of the first three experiments. From these quality measures it can be seen that the signal quality decreases for larger distance, larger misalignment, and for higher or lower data rates than optimal. In the middle graph the influence of the power of the source can clearly be seen. When more sources are radiating, thus the higher the power, the BER value will stay lower for further distances.

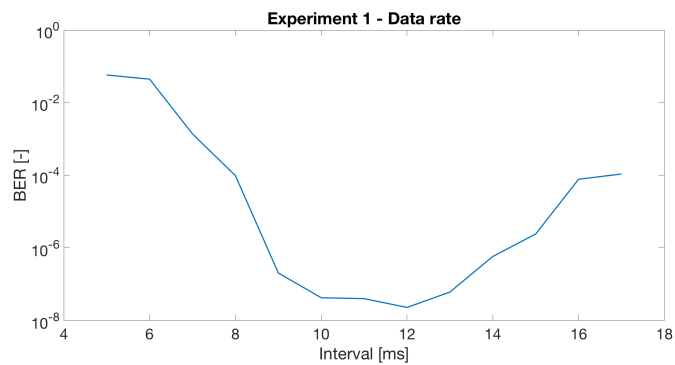


Figure 8.1: BER values of the first three experiments

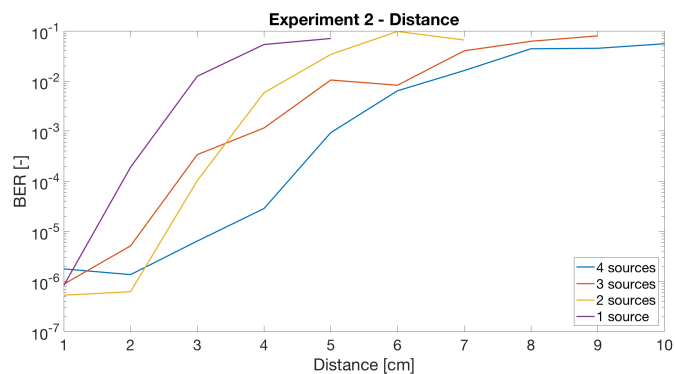


Figure 8.2: BER values of the first three experiments

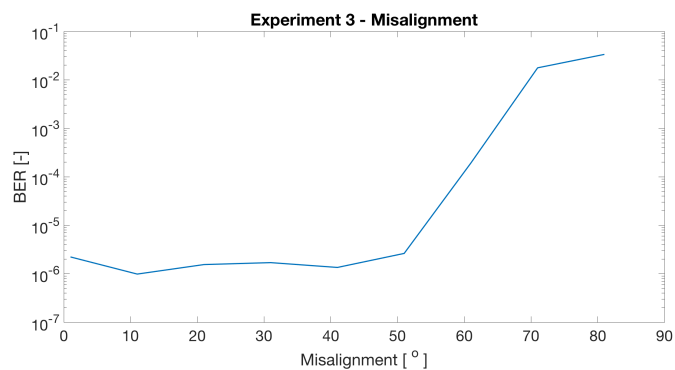


Figure 8.3: BER values of the first three experiments

## 8.2. Contribution

The contribution of this thesis to the academic field is an exploratory study to a new small-scale, low-cost, divergent, wireless communication method for multi-user biomedical applications such as the Neuromate project. In this work an innovative proof-of-concept has been realized for this project.

In Table 8.1 a comparison of this work with the work of professor Stepan Lucyszyn,[63], and his former PhD student Fangjing Hu,[41], is shown. The first publication about their "THz Torch" dates from 2011, the proof-of-concept version. They build a proof of principle of which the measured performance in terms of data rate and range at that time was described and they concluded that it was rather limited. However, it was just the very first step and their next versions rapidly improved in quality. The performance of the data rate and BER that Hu achieved and reported in his PhD thesis in 2014 are higher than those performances of this work. This work can be seen as a first proof-of-concept in a new application direction. Therefore, improvements are expected in the next versions of the prototype similar to the rapid improvements their work showed. This work is focused on the new requirements that Neuromate application brings on top of the requirements of the original THz Torch. The thermal Terahertz technology is still in its infancy and this is the first time a small-scale, divergent application of it is tested.

Table 8.1: Comparison of THz Torch proof-of-concept version, THz Torch improvement and this work

|                | <b>Stepan Lucyszyn (2011)</b>         | <b>Fangjing Hu (2014)</b>                  | <b>This work</b>                                         |
|----------------|---------------------------------------|--------------------------------------------|----------------------------------------------------------|
| Application    | ultra-low cost, short-range, security | ubiquitous, low-cost, security and defense | low-cost, small-scale, divergent, multi-user, biomedical |
| Frequency      | 20-40 & 60-100Hz                      | 20-40 & 60-100Hz                           | 20-100Hz                                                 |
| Data rate      | 5 bps (at 0.5cm)                      | >2kbps                                     | 35.71 bps                                                |
| Distance       | 2.5 cm (with <1bps)                   | >10cm                                      | 8 cm (4sources)                                          |
| Misalignment   | unknown                               | unknown                                    | functional <50°                                          |
| BER            | unknown                               | <10 <sup>-6</sup> (2.5 cm)                 | 10 <sup>-6</sup> (2 cm)                                  |
| Size prototype | unknown                               | 6 x 4 x 10 cm                              | 9 ∅ x 4 mm                                               |

## 8.3. Discussion and recommendations

### Highpass-lowpass misinterpretation

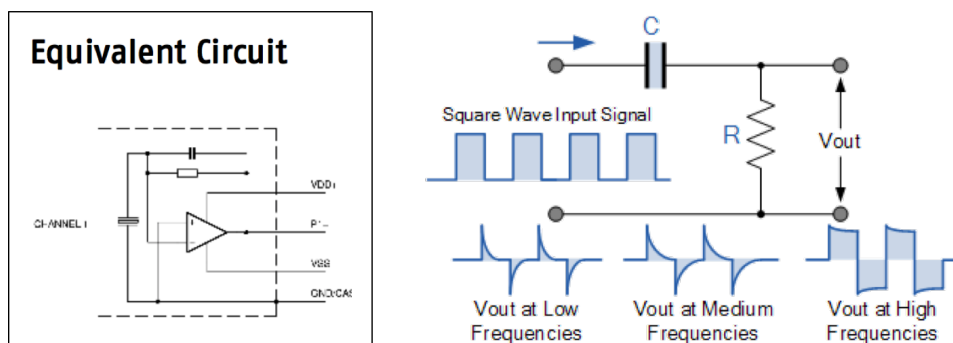


Figure 8.4: Equivalent circuit and RC circuit of passive highpass filter. Image from Electronics-tutorials

During the selection of the detector a misinterpretation occurred of the presented equivalent circuit in the given data sheet of the detector. Looking at the parallel feedback capacitance and feedback resistor the assumption was made that the value of the feedback resistor would influence the low-pass properties of the detector. However, the active element also acts as a capacitor and thus forms a high-pass filter together with the feedback resistor. Thus, instead of choosing the highest possible resistor, which would have been the most beneficial, the lowest value was chosen. Therefore, instead of a range of optimal frequencies only one optimal frequency appeared. Figure 8.5 shows the bodeplot of both filters and their crossing point at  $\approx 36$  Hz. This optimum is unfortunately located -5.5 dB lower than

the optimum of correctly matched components. Which means that at the optimum the output power of the prototype could actually be 3.5 times higher than it was in the current experiment. And thus that the results that were achieved by combining four sources should be achievable with only one (correctly matched) source and detector.

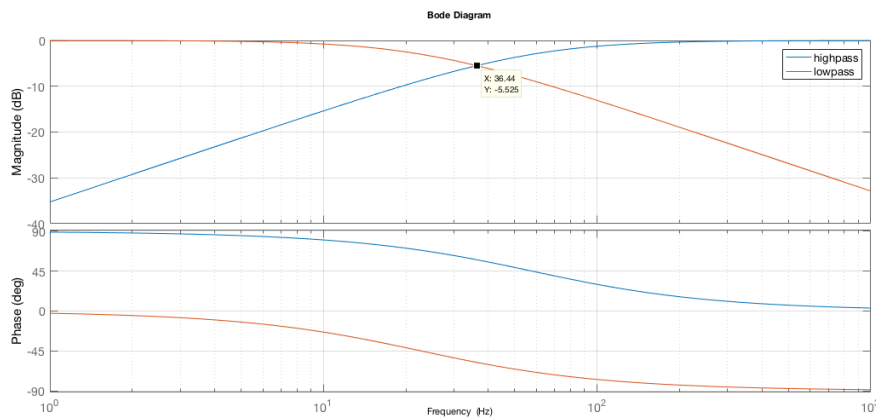


Figure 8.5: Overlap of the lowpass and highpass filters of the prototype

### Power consumption

In Chapter 2 a rough estimation of the available power was made based on the results of the work of Swager(2016) and Nassirinia(2016) [93] [72]. From this estimation a total power of 0.3mW would be available for the downlink at the side of the headmodule. The source will be located on top of the cage, thus can be powered externally and does not have such strict power requirements. From the datasheet of the detector a total operational power consumption of 0.3mW can be calculated for a supply voltage (Vdd) of 2.2V and a maximum operational current of 0.07 mA. This is a comparable result to the backscattering technique used for the uplink and thus fits with the criteria. However, the power required for the demodulation is not taken into account nor is the power consumption of the microcontroller in the powerlink project, 0.99 mW [72]. Since both projects are not optimised it is expected that the power consumption of the microcontrollers can be reduced up to the point that all three functionalities will together required < 10 mW of power consumption from the microcontroller.

### Wooden baseplate and cases

Wood is a product of nature and thus the accuracy of the prototype was less than it could have been if it was produced from other material. It might have influenced the alignment of the sources and detector. However, the soft wood allowed for secure fixation of the components and between the baseplate and the cases, due to an intended over-sizing.

### Divergence

Most Terahertz applications for communication purposes use collimated lenses [43] [70]. Those lenses converge the beam and reduce the scattering and thus gain a higher signal-to-noise ratio. For the downlink, a divergent beam is desirable to address the entire surface of the cage. In experiment 2 an angle of 50° proved to be the maximum misalignment that still allowed transfer of the data. This angle could be reduced when multiple sources are used on top of the cage.

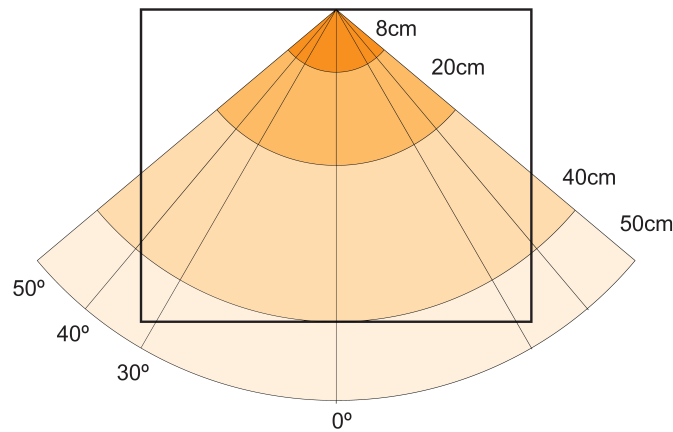


Figure 8.6: Required divergence of the terahertz beam presented in a diagonal cross-section of the cage.

### Metal reflection

The metal coil of the power link covers the entire cage and the reflector of the uplink covers the bottom in metal. This inclusion might be an advantage since metal is used to create THz mirrors because of its high reflectance. Figure 8.7 schematically shows how the coil and bottom might become a benefit.

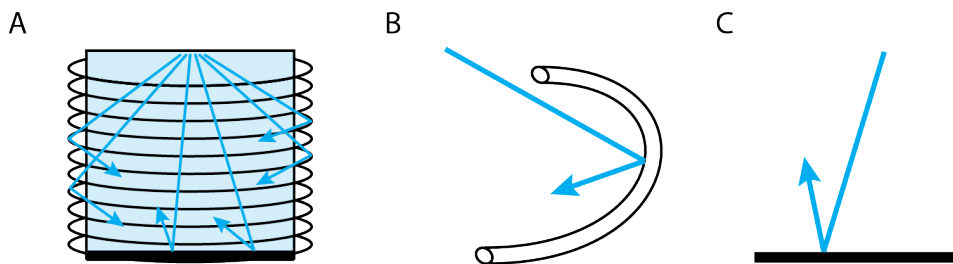


Figure 8.7: A. Possible reflectance of metal B. Reflectance of coil C. Reflectance of the metal floor, also used as reflector for uplink waves.

### Multiple access

Due to time limitations only a single-channel experiment was conducted, multi-channel experiments can in the future be performed with the same prototype to test the multiple access methods and to investigate the interference between the channels. The preferred option is currently Code Division Multiple Access (CDMA). However, both Frequency Division Multiple Access (FDMA) and Time Division Multiple Access (TDMA) are viable options and can be tested with future prototypes. For FDMA a new prototype is required which include optical filters in front of the source and detector to split the terahertz spectrum in four different bands as has been done by Hu et al. (2014) [41]. Further research should be done to make the optimal choice between the multiple access methods.

### Interference

The interference with the other two prototypes has not been tested yet because the current prototype is not powerful enough to cover the entire cage. Once by iterations a strong enough combination of transmitter and receiver is found the three separate Neuromate solutions should be tested together to ensure that none of them is influenced by the others.

### Thermal background

All objects above 0K are emitting thermal energy. Thus in the environment where the Neuromate will end up multiple thermal sources will be present. Examples of sources that will definitely be present

are the sun (through windows), the mice and the researchers. The detector is only responsive to rapid changes in temperature. Thus during the experiment the presence of the hands next to the setup did not influence the results, as was tested during the pilot studies. However, it was possible to activate the detector by quickly waving the hand in and out of the detectable field. In Figure 8.8 the difference in body heat of a mouse and a human is visualized with a thermal camera. The mouse has a lower temperature and thus radiates with lower power and lower frequencies. How much influence the fast running mice in the receptive field of the detector will have should be tested with the next generation of the prototype.

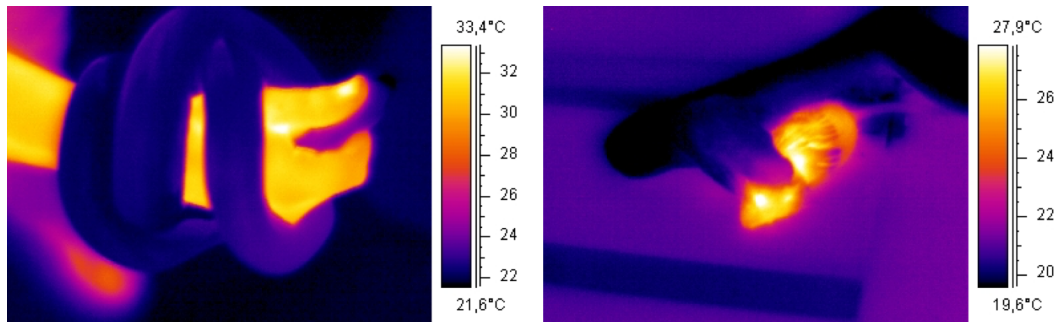


Figure 8.8: Thermal image of a snake around a human hand and a snake with a mouse. Note the difference in legend. Pictures from Wikimedia Commons

The behavioural experiments will mostly occur in the dark which will cause a better signal-to-noise ratio due to the lower amount of background energy.

### State feedback and error correction

Even with low BER values bit errors might occur during long-term experiments. The neuroscientist should always be able to rely on the link and they should be able to check and reset the current state of the control paradigm. State feedback can be send over the uplink with a small delay, which is acceptable for the control paradigm state information. For error information and correction the path via the uplink will be too slow. Therefore, other solutions like forward error correction should be implemented to correct for the incorrectly received bits without the need to report the error via the uplink. By adding extra bits to the message a redundancy is created that enables the decoder to retract the original message even when it contains errors. One example of forward error correction is the use of parity bits that indicate whether the amount of ones in the message is even or odd. It will increase the bit length of a message and thus lowers the data rate but will ensure a reliable link.

### Safety

Infrared can cause eye damage when wavelengths below 1400nm are used. The human cornea is opaque to wavelengths higher than 1400 nm and thus the risk at ocular hazard is reduced when using lower frequencies such as the thermal part of the terahertz band.

Terahertz is non-ionizing radiation thus generally considered safe for humans. However, there has been discussion on whether terahertz radiation could interfere with DNA. One study modelled the influence of a Terahertz field on double-stranded DNA and found that at high intensities nonlinear mechanisms could lead to spatial perturbations that create large localized openings (bubbles) in the DNA [2]. However, this is only shown in simulations and extremely unlikely to happen in real-life. Nevertheless, interaction of terahertz with human tissue has barely been studied and should be investigated more closely to be able to make safety statements.

### Animal studies

All experiments conducted on mice in the Erasmus MC are approved by Dutch Dierexperimenten commissie (DEC) ethics committee and are performed in accordance with Dutch animal care and use laws.

Nevertheless, reticence with the amount of animals used for studies is desirable. The Neuromate project wants to achieve natural behaviour thus automatically creating more animal-friendly environments.

The headmodules will be less disturbing to the animals since after the single surgery they can move freely and live group-housed.

### **Downlink**

The results of experiment 2 indicate that a more powerful source is required to reach the required distance. Another option is to use multiple sources simultaneously.

The size of the detector can be minimized, since SMD versions of pyroelectric detectors are available. However, the properties do not match the properties of the chosen component in the prototype. The current detector has proven to meet all the requirements of the application. To make sure it is not overqualified different smaller detectors with other properties such as lower detectivity could be tested. Thus further investigation whether SMD detectors are more interesting than the currently chosen TO packaged one is recommended.

### **NeuroMate**

In this work an innovative and promising proof-of-concept has been realized for the wireless downlink of the Neuromate project.

Currently two separate one-way communications have been proposed. However, both include innovative solutions and require more development time to reach a functional prototype. This development will take time and expertise. The alternative solution is to use a single solution that includes a two-way communication link

The time it will take to finalise the separate solutions of the Neuromate plus the time it will take to integrate the solutions depends on the availability of master students who want to do their graduation project for the Neuromate project. In the mean time current commercially available two way communication links will improve and probably increase in power efficiency up to a level that is compatible with the requirements of the Neuromate system. A commercial solution could possibly be more reliable than two innovative techniques combined. This should be examined by the Neuromate team.

However, given the above mentioned options for optimisation the proposed wireless terahertz downlink is a promising solution for the Neuromate project. And given the foreseen rapid improvements the technique could well be developed in a series of further prototypes.





# Acknowledgement

I wish to thank various people for their contribution to this project;

Wouter who is a unique, supportive, confident, and admirable professor and teacher. I am honoured by the opportunity he gave me to join the Bioelectronics group. He never judges students on their background, only on their potential. Which was a great motivation for me.

Freek who has always been encouraging, helpful, open and committed to supporting me during my internship and graduation project. His enthusiasm and knowledge stimulated fascination for the brain even more.

Alfred who was always interested and involved even from the sideline of this project. And who I will see much more often during my next challenge, a PhD position. A chance and the trust he provided for which I am grateful.

Dr. Peter H. Siegel and Dr. Jian Rong Gao, who are experts in the field of Terahertz and who were willing to provide advice.

Colleagues from the Bioelectronics group, the Hoebeek lab, and the Neuromuscular control group for their feedback and advice.

Ali whom I could go to with practical questions at any moment and who took the time to help me realise a functional setup for the experiments.

The summer crew of the PMB, Model Making and Machine Lab, at the faculty of Industrial Design Engineering. Especially, Rein, Joy, and Vianne who helped me to improve and produce my prototype.

Atef from the Microelectronics group who has generously lent me their brand-new and barely unpacked MSOS804A oscilloscope from Keysight, for the measurements of the eyediagrams.

Lily who is always willing to help, even for a last-minute English check. She boosted my abstract to a higher level.

Last but not least I would like to thank my family and friend who always were or at least pretended to be interested in the progress of my project. Their support was the base of my perseverance.



# Bibliography

- [1]
- [2] B. S. Alexandrov, V. Gelev, A. R. Bishop, A. Usheva, and K. Rasmussen. DNA breathing dynamics in the presence of a terahertz field. *Physics Letters, Section A: General, Atomic and Solid State Physics*, 374(10):1214–1217, 2010. ISSN 03759601. doi: 10.1016/j.physleta.2009.12.077.
- [3] Fatemeh Amirnavaei and Min Dong. Online Power Control Strategy for Wireless Transmission with Energy Harvesting and Storage. 1276(c):6–10, 2015. ISSN 1536-1276. doi: 10.1109/SPAWC.2015.7226989.
- [4] Gian Nicola Angotzi, Fabio Boi, Stefano Zordan, Andrea Bonfanti, and Alessandro Vato. A programmable closed-loop recording and stimulating wireless system for behaving small laboratory animals. *Scientific reports*, 4:5963, 2014. ISSN 2045-2322. doi: 10.1038/srep05963. URL <http://www.pubmedcentral.nih.gov/articlerender.fcgi?artid=4123143&tool=pmcentrez&rendertype=abstract>.
- [5] Tarmo Anttalainen. *Introduction to Telecommunications Network Engineering, Second Edition*. Artech House, 2003. ISBN 978-1580535007.
- [6] Takashi Asano, Masahiro Suemitsu, Kohei Hashimoto, Menaka De Zoysa, Tatsuya Shibahara, Tatsunori Tsutsumi, and Susumu Noda. Near-infrared – to – visible highly selective thermal emitters based on an intrinsic semiconductor. pages 1–6, 2016. ISSN 2375-2548. doi: 10.1126/sciadv.1600499.
- [7] Thermpoon Ativanichayaphong, Ji Wei He, Christopher E. Hagains, Yuan B. Peng, and J. C. Chiao. A combined wireless neural stimulating and recording system for study of pain processing. *Journal of Neuroscience Methods*, 170(1):25–34, 2008. ISSN 01650270. doi: 10.1016/j.jneumeth.2007.12.014.
- [8] Meysam Azin, Student Member, David J Guggenmos, Scott Barbay, and Randolph J Nudo. A Miniaturized System for Spike-Triggered Intracortical Microstimulation in an Ambulatory Rat. 58(9):2589–2597, 2011.
- [9] David Ball, Russell Kliese, Francois Windels, Christopher Nolan, Peter Stratton, Pankaj Sah, and Janet Wiles. Rodent scope: A user-configurable digital wireless telemetry system for freely behaving animals. *PLoS ONE*, 9(2):1–10, 2014. ISSN 19326203. doi: 10.1371/journal.pone.0089949.
- [10] I. Bar-David. Direct differential detection of phase-shift-keyed signals: a local-oscillatorless DPSK receiver. *IEE Proceedings - Optoelectronics*, 141(1):38–42, 1994. ISSN 1350-2433. doi: 10.1049/ip-opt:19949725. URL <http://digital-library.theiet.org/content/journals/10.1049/ip-opt{ }19949725>.
- [11] TeckChuan Beh, Masaki Kato, Takehiro Imura, and Yoichi Hori. Wireless power transfer system via magnetic resonant coupling at fixed resonance frequency -power transfer system based on impedance matching-. *World Electric Vehicle Journal*, 4(1):744–753, 2011. ISSN 20326653.
- [12] Erik Brundermann, Heinz-Wilhelm Hubers, and Maurice FitzGerald Kimmitt. *Terahertz Techniques*. Springer Series in Optical Sciences, 2012. ISBN 9783642025914.
- [13] B.L. Cannon, J.F. Hoberg, D.D. Stancil, and S.C. Goldstein. Magnetic Resonant Coupling As a Potential Means for Wireless Power Transfer to Multiple Small Receivers. *IEEE Transactions on Power Electronics*, 24(7):1819–1825, 2009. ISSN 0885-8993. doi: 10.1109/TPEL.2009.2017195.

- [14] Goutam Chattopadhyay. Technology, capabilities, and performance of low power terahertz sources. *IEEE Transactions on Terahertz Science and Technology*, 1(1):33–53, 2011. ISSN 2156342X. doi: 10.1109/TTHZ.2011.2159561.
- [15] Hsin Yung Chen, Jin Shang Wu, Brian Hyland, Xiao Dong Lu, and Jia Jin Jason Chen. A low noise remotely controllable wireless telemetry system for single-unit recording in rats navigating in a vertical maze. *Medical and Biological Engineering and Computing*, 46(8):833–839, 2008. ISSN 01400118. doi: 10.1007/s11517-008-0355-6.
- [16] Minghui Chen Minghui Chen and M.-C.F. Chang. A 2.2 Gb/s DQPSK Baseband Receiver in 90-nm CMOS for 60 GHz Wireless Links. *2007 IEEE Symposium on VLSI Circuits*, pages 8–9, 2007. doi: 10.1109/VLSIC.2007.4342764.
- [17] J.kameswararao T.Manikyala Rao D. Chiranjevulu. *International Journal of Engineering Research and General Science* Volume 4, Issue 2, 2016. ISBN 2091-2730.
- [18] Carlo Corsi and Fedir Sizov. *THz and Security Applications*. 2014. ISBN 978-94-017-8827-4. doi: 10.1007/978-94-017-8828-1.
- [19] K Deisseroth. Optogenetics. *Nature Methods*, 2011. ISSN 1548-7105. doi: 10.1038/nmeth.f.324.
- [20] S S Dhillon, M S Vitiello, E H Linfield, A G Davies, Matthias C Hoffmann, John Booske, Claudio Paoloni, M Gensch, P Weightman, G P Williams, E Castro-Camus, D R S Cumming, F Simoens, I Escorcia-Carranza, J Grant, Stepan Lucyszyn, Makoto Kuwata-Gonokami, Kuniaki Konishi, Martin Koch, Charles A Schmuttenmaer, Tyler L Cocker, Rupert Huber, A G Markelz, Z D Taylor, Vincent P Wallace, J Axel Zeitler, Juraj Sibik, Timothy M Korter, B Ellison, S Rea, P Goldsmith, Ken B Cooper, Roger Appleby, D Pardo, P G Huggard, V Krozer, Haymen Shams, Martyn Fice, Cyril Renaud, Alwyn Seeds, Andreas Stöhr, Mira Naftaly, Nick Ridler, Roland Clarke, John E Cunningham, and Michael B Johnston. The 2017 terahertz science and technology roadmap. *Journal of Physics D: Applied Physics*, 50(4):043001, 2017. ISSN 0022-3727. doi: 10.1088/1361-6463/50/4/043001. URL <http://stacks.iop.org/0022-3727/50/i=4/a=043001?key=crossref.f5a017d17c44cbeabd74f9646d531e1d>.
- [21] Richard Dudley and Mira Naftaly. Presentation: Introduction to Terahertz, 2009.
- [22] David Fan, Dylan Rich, Tahl Holtzman, Patrick Ruther, Jeffrey W. Dalley, Alberto Lopez, Mark A. Rossi, Joseph W. Barter, Daniel Salas-Meza, Stanislav Herwik, Tobias Holzhammer, James Morizio, and Henry H. Yin. A wireless multi-channel recording system for freely behaving mice and rats. *PLoS ONE*, 6(7), 2011. ISSN 19326203. doi: 10.1371/journal.pone.0022033.
- [23] John F Federici, Brian Schulkin, Feng Huang, Dale Gary, Robert Barat, Filipe Oliveira, and David Zimdars. THz imaging and sensing for security applications—explosives, weapons and drugs. *Semiconductor Science and Technology*, 20(7):S266–S280, 2005. ISSN 0268-1242. doi: 10.1088/0268-1242/20/7/018.
- [24] Lief Fenno, Ofer Yizhar, and Karl Deisseroth. The development and application of optogenetics. *Annual review of neuroscience*, 2011. ISSN 0147-006X. doi: 10.1146/annurev-neuro-061010-113817.
- [25] Bradley Ferguson and Xi-cheng Zhang. Materials for terahertz science and technology. 1(nature materials | [www.nature.com/naturematerials](http://www.nature.com/naturematerials)):1–8, 2002.
- [26] Jacob Fraden. 69. Human Occupancy Detectors.
- [27] W. Freude, R. Schmogrow, B. Nebendahl, M. Winter, A. Josten, D. Hillerkuss, S. Koenig, J. Meyer, M. Dreschmann, M. Huebner, C. Koos, J. Becker, and J. Leuthold. Quality metrics for optical signals: Eye diagram, q-factor, osnr, evm and ber. In *2012 14th International Conference on Transparent Optical Networks (ICTON)*, pages 1–4, July 2012. doi: 10.1109/ICTON.2012.6254380.

- [28] Yingbin Fu and King Wai Yau. Phototransduction in mouse rods and cones. *Pflugers Archiv European Journal of Physiology*, 454(5):805–819, 2007. ISSN 00316768. doi: 10.1007/s00424-006-0194-y.
- [29] G Gagnon-Turcotte, Y LeChasseur, C Bories, Y De Koninck, and B Gosselin. A Wireless Optogenetic Headstage with Multichannel Neural Signal Compression. *Biomedical Circuits and Systems Conference (BioCAS), 2015*, 2015. ISSN 1424-8220. doi: 10.3390/s150922776.
- [30] Maysam Ghovanloo and Khalil Najafi. A wideband frequency-shift keying wireless link for inductively powered biomedical implants. *IEEE Transactions on Circuits and Systems I: Regular Papers*, 51(12):2374–2383, 2004. ISSN 10577122. doi: 10.1109/TCSI.2004.838144.
- [31] A H Gnauck, Senior Member, and P J Winzer. Optical Phase-Shift-Keyed Transmission. 23(1): 115–130, 2005. doi: 10.1109/JLT.2004.840357.
- [32] Peter J. Grahn, Grant W. Mallory, Obaid U. Khurram, B. Michael Berry, Jan T. Hachmann, Allan J. Bieber, Kevin E. Bennet, Hoon Ki Min, Su Youne Chang, Kendall H. Lee, and J. L. Lujan. A neurochemical closed-loop controller for deep brain stimulation: Toward individualized smart neuromodulation therapies. *Frontiers in Neuroscience*, 8(8 JUN):1–11, 2014. ISSN 1662453X. doi: 10.3389/fnins.2014.00169.
- [33] Logan Grosenick, James H Marshel, and Karl Deisseroth. Closed-Loop and Activity-Guided Optogenetic Control. *Neuron*, 86(1):106–139, 2015. ISSN 0896-6273. doi: 10.1016/j.neuron.2015.03.034. URL <http://dx.doi.org/10.1016/j.neuron.2015.03.034>.
- [34] Harald Haas, Liang Yin, Yunlu Wang, and Cheng Chen. What is LiFi? *Journal of Lightwave Technology ( Volume: 34, Issue: 6, March 15, 15 2016 )*, 34(6):1533–1544, 2016. doi: 10.1109/JLT.2015.2510021.
- [35] Ria De Haas, Rolf Struikmans, Geoffrey Van Der Plasse, Linda Van Kerkhof, Jan H Brakkee, Martien J H Kas, and Herman G M Westenberg. Wireless implantable micro-stimulation device for high frequency bilateral deep brain stimulation in freely moving mice. *Journal of Neuroscience Methods*, 209(1):113–119, 2012. ISSN 0165-0270. doi: 10.1016/j.jneumeth.2012.05.028. URL <http://dx.doi.org/10.1016/j.jneumeth.2012.05.028>.
- [36] Robert E. Hampson, Vernell Collins, and Sam A. Deadwyler. A wireless recording system that utilizes Bluetooth technology to transmit neural activity in freely moving animals. *Journal of Neuroscience Methods*, 182(2):195–204, 2009. ISSN 01650270. doi: 10.1016/j.jneumeth.2009.06.007.
- [37] Emerson S. Hawley, Eric L. Hargreaves, John L. Kubie, Bruno Rivard, and Robert U. Muller. Telemetry system for reliable recording of action potentials from freely moving rats. *Hippocampus*, 12(4):505–513, 2002. ISSN 10509631. doi: 10.1002/hipo.10040.
- [38] By John S Ho, Sanghoek Kim, and A.S.Y Poon. Midfield Wireless Powering for Implantable Systems. *IEEE*, (1):1–10, 2013. doi: 10.1109/JPROC.2013.2251851.
- [39] John S. Ho, Yuji Tanabe, Shrivats Mohan Iyer, Amelia J. Christensen, Logan Grosenick, Karl Deisseroth, Scott L. Delp, and Ada S Y Poon. Self-tracking energy transfer for neural stimulation in untethered mice. *Physical Review Applied*, 4(2):1–6, 2015. ISSN 23317019. doi: 10.1103/PhysRevApplied.4.024001.
- [40] Fangjing Hu and Stepan Lucyszyn. Improved 'THz Torch' technology for short-range wireless data transfer. *2013 IEEE International Wireless Symposium, IWS 2013*, 2013. doi: 10.1109/IEEE-IWS.2013.6616775.
- [41] Fangjing Hu and Stepan Lucyszyn. Noise Analysis for Multi-channel 'THz Torch' Thermal Infrared Wireless Communications Systems. *Asia-Pacific Microwave Conference Proceedings, APMC*, pages 5–7, 2014.

- [42] Fangjing Hu and Stepan Lucyszyn. Modelling Miniature Incandescent Light Bulbs for Thermal Infrared 'THz Torch' Applications. *Journal of Infrared, Millimeter, and Terahertz Waves*, 36(4): 350–367, 2015. ISSN 18666906. doi: 10.1007/s10762-014-0130-8.
- [43] Fangjing Hu and Stepan Lucyszyn. Advances in Front-end Enabling Technologies for Thermal Infrared THz Torch Wireless Communications. *Journal of Infrared, Millimeter, and Terahertz Waves*, 37(9):881–893, 2016. ISSN 18666906. doi: 10.1007/s10762-016-0279-4. URL <http://dx.doi.org/10.1007/s10762-016-0279-4>.
- [44] Fangjing Hu, Jingye Sun, Helen E. Brindley, Xiaoxin Liang, and Stepan Lucyszyn. Systems Analysis for Thermal Infrared 'THz Torch' Applications. *Journal of Infrared, Millimeter, and Terahertz Waves*, 36(5):474–495, 2015. ISSN 1866-6892. doi: 10.1007/s10762-014-0136-2. URL <http://link.springer.com/10.1007/s10762-014-0136-2>.
- [45] Gerald H. Jacobs. In *Visual Transduction and Non-Visual Light Perception - Cone Pigments and Vision in the Mouse*. Humana Press, 2008. doi: 10.1007/978-1-59745-374-5.
- [46] Gerald H. Jacobs, Gary A. Williams, Hugh Cahill, and Jeremy Nathans. Emergence of Novel Color Vision in Mice Engineered to Express a Human Cone Photopigment. *Science*, 315(March): 1723–25, 2007. ISSN 0036-8075. doi: 10.1126/science.1138838.
- [47] Steven L Jacques. Corrigendum: Optical properties of biological tissues: a review. *Physics in Medicine and Biology*, 58(14):5007–5008, 2013. ISSN 0031-9155. doi: 10.1088/0031-9155/58/14/5007. URL <http://iopscience.iop.org/article/10.1088/0031-9155/58/11/R37%5Cnhttp://stacks.iop.org/0031-9155/58/i=14/a=5007?key=crossref.c531ac37cfa1f77bbc0d33a8e92de8c9>.
- [48] Jeffrey A Jargon, Senior Member, C M Jack Wang, Paul D Hale, and Senior Member. A Robust Algorithm for Eye-Diagram Analysis. 26(21):3592–3600, 2008. doi: 10.1109/JLT.2008.917313.
- [49] C J Jeon, E Strettoi, and R H Masland. The major cell populations of the mouse retina. *J Neurosci*, 18(21):8936–8946, 1998. ISSN 0270-6474. URL <http://www.ncbi.nlm.nih.gov/pubmed/9786999>.
- [50] Jae-woong Jeong, Jordan G Mccall, Gunchul Shin, Yonggang Huang, Michael R Bruchas, John A Rogers, Jae-woong Jeong, Jordan G Mccall, Gunchul Shin, Yihui Zhang, Ream Al-hasani, Minku Kim, and Shuo Li. Wireless Optofluidic Systems for Programmable In Vivo Pharmacology and Optogenetics. *Cell*, 162(3):662–674, 2015. ISSN 0092-8674. doi: 10.1016/j.cell.2015.06.058. URL <http://dx.doi.org/10.1016/j.cell.2015.06.058>.
- [51] Yaoyao Jia, Zheyuan Wang, S. Abdollah Mirbozorgi, and Maysam Ghovanloo. Live demonstration: A smart homepage system with behavior analysis and closed-loop optogenetic stimulation capabilities. *IEEE Biomedical Circuits and Systems Conference: Engineering for Healthy Minds and Able Bodies, BioCAS 2015 - Proceedings*, page 1408318, 2015. doi: 10.1109/BioCAS.2015.7348331.
- [52] Masoud Salehi John G. Proakis. *Fundamentals of communication systems*. Pearson Education, 2005. ISBN 9780131471351.
- [53] Olutola Jonah, Student Member, Stavros V Georgakopoulos, and Senior Member. Wireless Power Transfer in Concrete via Strongly Coupled Magnetic Resonance. *IEEE Transactions on Antennas and Propagation*, 61(3):1378–1384, 2013. ISSN 0018-926X. doi: 10.1109/TAP.2012.2227924.
- [54] Hossein Kassiri, Aditi Chemparathy, M Tariqus Salam, Richard Boyce, Antoine Adamantidis, Roman Genov, and Senior Member. Electronic Sleep Stage Classifiers : A Survey and VLSI Design Methodology. pages 1–12, 2016. doi: 10.1109/TBCAS.2016.2540438.
- [55] Lieke Kros, Oscar H J Eelkman Rooda, Chris I. De Zeeuw, and Freek E. Hoebeek. Controlling Cerebellar Output to Treat Refractory Epilepsy. *Trends in Neurosciences*, 38(12):789–799, 2015. ISSN 1878108X. doi: 10.1016/j.tins.2015.10.002.

- [56] Lieke Kros, Oscar H. J. Eelkman Rooda, Jochen K. Spanke, Parimala Alva, Marijn N. van Dongen, Athanasios Karapatis, Else a. Tolner, Christos Strydis, Neil Davey, Beerend H. J. Winkelman, Mario Negrello, Wouter a. Serdijn, Volker Steuber, Arn M. J. M. van den Maagdenberg, Chris I. De Zeeuw, and Freek E. Hoebeek. *Cerebellar output controls generalized spike-and-wave discharge occurrence.*, volume 77. 2015. ISBN 0364-5134. doi: 10.1002/ana.24399. URL <http://doi.wiley.com/10.1002/ana.24399>{%}5Cn<http://www.ncbi.nlm.nih.gov/pubmed/25762286>.
- [57] Levin Kuhlmann, David B Grayden, Fabrice Wendling, and Steven J Schiff. Role of multiple-scale modeling of epilepsy in seizure forecasting. *Journal of clinical neurophysiology : official publication of the American Electroencephalographic Society*, 32(3):220–6, 2015. ISSN 1537-1603. doi: 10.1097/WNP.000000000000149. URL <http://www.ncbi.nlm.nih.gov/pubmed/26035674>{%}5Cn<http://www.pubmedcentral.nih.gov/articlerender.fcgi?artid=PMC4455036>.
- [58] André Kurs, Aristeidis Karalis, Robert Moffatt, J D Joannopoulos, Peter Fisher, and Marin Soljac. Wireless Power Transfer via Strongly. *SCIENCE VOL 317 6 JULY 2007*, (July):83–87, 2007.
- [59] Damien Lapray, J??rgen Bergeler, Erwan Dupont, Oliver Thews, and Heiko J. Luhmann. A novel miniature telemetric system for recording EEG activity in freely moving rats. *Journal of Neuroscience Methods*, 168(1):119–126, 2008. ISSN 01650270. doi: 10.1016/j.jneumeth.2007.09.029.
- [60] Shuai Li, Ashish Pandharipande, and Frans M J Willems. Unidirectional visible light communication and illumination with LEDs. 6778(c), 2016. ISSN 1530-437X. doi: 10.1109/JSEN.2016.2614968.
- [61] Xiaoxin Liang, Fangjing Hu, Yuepeng Yan, and Stepan Lucyszyn. Secure thermal infrared communications using engineered blackbody radiation. *2014 31th URSI General Assembly and Scientific Symposium, URSI GASS 2014*, pages 1–7, 2014. ISSN 2045-2322. doi: 10.1109/URSIGASS.2014.6929214.
- [62] Xianliang Liu, Talmage Tyler, Tatiana Starr, Anthony F. Starr, Nan Marie Jokerst, and Willie J. Padilla. Taming the blackbody with infrared metamaterials as selective thermal emitters. *Physical Review Letters*, 107(4):4–7, 2011. ISSN 00319007. doi: 10.1103/PhysRevLett.107.045901.
- [63] Stepan Lucyszyn, Hanchao Lu, and Fangjing Hu. Ultra-low cost THz short-range wireless link. *2011 IEEE MTT-S International Microwave Workshop Series on Millimeter Wave Integration Technologies, IMWS 2011*, pages 49–52, 2011. doi: 10.1109/IMWS3.2011.6061884.
- [64] BB McShane, RJ Galante, and Michael Biber. Assessing REM sleep in mice using video data. *Sleep*, 35(3):433–42, 2012. ISSN 1550-9109. doi: 10.5665/sleep.1712. URL <http://www.pubmedcentral.nih.gov/articlerender.fcgi?artid=3274345>{&}tool=pmcentrez{&}rendertype=abstract{%}5Cn<http://www.ncbi.nlm.nih.gov/pmc/articles/PMC3274345/>.
- [65] John D. Medaglia, Perry Zurn, Walter Sinnott-Armstrong, and Danielle S. Bassett. Mind Control: Frontiers in Guiding the Mind. 2016. URL <http://arxiv.org/abs/1610.04134>.
- [66] S. Abdollah Mirbozorgi, Hadi Bahrami, Mohamad Sawan, and Benoit Gosselin. A Smart Cage With Uniform Wireless Power Distribution in 3D for Enabling Long-Term Experiments With Freely Moving Animals. *IEEE Transactions on Biomedical Circuits and Systems*, 10(2):424–434, 2016. ISSN 19324545. doi: 10.1109/TBCAS.2015.2414276.
- [67] Daniel Mittleman. In *Sensing with terahertz radiation*. Springer, 2003. ISBN 3540456015, 9783540456018.
- [68] Kate L Montgomery, Alexander J Yeh, John S Ho, Vivien Tsao, Shrivats Mohan Iyer, Logan Grosenick, Emily A Ferenczi, Yuji Tanabe, Karl Deisseroth, Scott L Delp, and Ada S Y Poon. Wirelessly powered, fully internal optogenetics for brain, spinal and peripheral circuits in mice. *Nature Methods*, 12(10):969–974, 2015. ISSN 1548-7091. doi: 10.1038/nmeth.3536. URL <http://dx.doi.org/10.1038/nmeth.3536>.



- [69] Mrinmoyee Mukherjee. Wireless Communication-Moving from RF to Optical. pages 788–795, 2016.
- [70] Tadao Nagatsuma, Guillaume Ducournau, and Cyril C. Renaud. Advances in terahertz communications accelerated by photonics. *Nature Photonics*, 10(6):371–379, 2016. ISSN 1749-4885. doi: 10.1038/nphoton.2016.65. URL <http://www.nature.com/doi/finder/10.1038/nphoton.2016.65>.
- [71] Abdulkarim A. Oloyode Adeseko A. Ayeni Nasir Faruk, Mohammed I. Gumel. International Journal of Communications, Network and System Sciences, Vol.6 No.1,, January 29, 2013. ISBN [http://www.iitg.ernet.in/scifac/qip/public\\_html/cd\\_cell/chapters/amitra\\_mobile\\_communication/chapter8.pdf](http://www.iitg.ernet.in/scifac/qip/public_html/cd_cell/chapters/amitra_mobile_communication/chapter8.pdf).
- [72] Farnaz Nassirinia. Wireless Power Transfer and Optogenetic Stimulation of Freely Moving Rodents. *Master Thesis TU Delft, Bioelectronics*, 2016.
- [73] May Alelin Pagal. In *Online article: The market for terahertz products will reach \$570 million by 2021 (retrieved in November 2016)*. PreScouter, Inc., December 2nd, 2014.
- [74] Miguel Pais-Vieira, Miguel Pais-Vieira, Amol P. Yadav, Derek Moreira, David Guggenmos, Amílcar Santos, Mikhail Lebedev, and Miguel A. L. Nicolelis. A Closed Loop Brain-machine Interface for Epilepsy Control Using Dorsal Column Electrical Stimulation. *Scientific Reports*, 6(April):1–9, 2016. ISSN 2045-2322. doi: <http://dx.doi.org/10.1038/srep32814>. URL <http://dx.doi.org/10.1038/srep32814>.
- [75] Pere Pala-Schonwalder, Jordi Bonet-Dalmau, F. Xavier Moncunill-Geniz, Francisco Del Aguila-Lopez, and Rosa Giralt-Mas. A superregenerative QPSK receiver. *IEEE Transactions on Circuits and Systems I: Regular Papers*, 61(1):258–265, 2014. ISSN 15498328. doi: 10.1109/TCSI.2013.2268313.
- [76] Terry J Parks and David S Register. inductively coupling power and data, patent number: 5,455,466, date of patent: Oct. 3, 1995, 1995.
- [77] R C Pinnell, J Dempster, and J Pratt. Miniature wireless recording and stimulation system for rodent behavioural testing. *Journal of neural engineering*, 12(6):066015, 2015. ISSN 1741-2552. doi: 10.1088/1741-2560/12/6/066015. URL <http://iopscience.iop.org/article/10.1088/1741-2560/12/6/066015>.
- [78] Richard C. Pinnell, Rand K. Almajidy, Robert D. Kirch, Jean C. Cassel, and Ulrich G. Hofmann. A wireless EEG recording method for rat use inside the water maze. *PLoS ONE*, 11(2):1–15, 2016. ISSN 19326203. doi: 10.1371/journal.pone.0147730.
- [79] Ada S Y Poon. A new kind of Wireless mouse. 26 | DEC 2016 | NORTH AMERICAN | SPECTRUM.IEEE.ORG, dec, 2016.
- [80] Dr Binboga Siddik Yarman Professor. In *Design of Ultra Wideband Power Transfer Networks*. John Wiley and Sons, Ltd, 2010. doi: 10.1002/9780470688922.
- [81] P. L. Richards. Bolometers for infrared and millimeter waves. *Journal of Applied Physics*, 76(1):1–24, 1994. ISSN 00218979. doi: 10.1063/1.357128.
- [82] Mark A Rossi, Vinson Go, Tracy Murphy, Quanghai Fu, James Morizio, and Henry H Yin. A wirelessly controlled implantable LED system for deep brain optogenetic stimulation. *Frontiers in Integrative Neuroscience*, 9(February):8, 2015. ISSN 1662-5145. doi: 10.3389/fnint.2015.00008. URL <http://www.pubmedcentral.nih.gov/articlerender.fcgi?artid=4322607&tool=pmcentrez&rendertype=abstract%5Cnhttp://journal.frontiersin.org/Article/10.3389/fnint.2015.00008/abstract>.
- [83] David M Russell, Daniel McCormick, Andrew J Taberner, Simon C Malpas, and David M Budgett. A High Bandwidth Fully Implantable Mouse Telemetry System for Chronic ECG Measurement. pages 7666–7669, 2011.

- [84] Caetano P. Sabino, Alessandro M. Deana, Tania M. Yoshimura, Daniela F.T. da Silva, Cristiane M. França, Michael R. Hamblin, and Martha S. Ribeiro. The optical properties of mouse skin in the visible and near infrared spectral regions. *Journal of Photochemistry and Photobiology B: Biology*, 160:72–78, 2016. ISSN 10111344. doi: 10.1016/j.jphotobiol.2016.03.047. URL <http://linkinghub.elsevier.com/retrieve/pii/S1011134415300117>.
- [85] Julia L. Sandell and Timothy C. Zhu. A review of in-vivo optical properties of human tissues and its impact on PDT. *Journal of Biophotonics*, 4(11-12):773–787, 2011. ISSN 1864063X. doi: 10.1002/jbio.201100062.
- [86] Seong-Min Kim, Jung-Ick Moon, In-Kui Cho, Jae-Hoon Yoon, and Woo-Jin Byun. 130W power transmitter for wireless power charging using magnetic resonance. *2014 IEEE 36th International Telecommunications Energy Conference (INTELEC)*, pages 1–5, 2014. doi: 10.1109/INTLEC.2014.6972203. URL <http://ieeexplore.ieee.org/lpdocs/epic03/wrapper.htm?arnumber=6972203>.
- [87] Wouter A. Serdijn. *Reader Electronics ET3604LR*. Delft University of Technology, Faculty of Information Technology and Systems, Electronics Research Laboratory, September 5, 2005. ISBN 9780131471351.
- [88] Hong Shen, Yuqin Deng, and W E I Xu. Rate Maximization for Downlink Multiuser Visible Light Communications. 4:6567–6573, 2016. doi: 10.1109/ACCESS.2016.2614598.
- [89] Gunchul Shin, Adrian M Gomez, Ream Al-hasani, Jeong Sook Ha, Michael R Bruchas, and John A Rogers. Flexible Near-Field Wireless Optoelectronics as Subdermal Implants for Broad Applications in NeuroResource Flexible Near-Field Wireless Optoelectronics as Subdermal Implants for Broad Applications in Optogenetics. pages 509–521, 2017. doi: 10.1016/j.neuron.2016.12.031.
- [90] Peter Sobis. *Advanced Schottky Diode Receiver Front-Ends for Terahertz Applications*. Terahertz and Millimetre Wave Laboratory Department of Microtechnology and Nanoscience - MC2 CHALMERS UNIVERSITY OF TECHNOLOGY Göteborg, Sweden 2011, 2011. ISBN 9789173855440.
- [91] William C Stacey and Brian Litt. Technology insight: neuroengineering and epilepsy-designing devices for seizure control. *Nature clinical practice. Neurology*, 4(4):190–201, 2008. ISSN 1745-834X. doi: 10.1038/ncpneuro0750.
- [92] Felice T Sun, Martha J Morrell, Robert E Wharen, Sun F.T., Morrell M.J., and Wharen Jr. R.E. Responsive Cortical Stimulation for the Treatment of Epilepsy. *Neurotherapeutics*, 5(1):68–74, 2008. ISSN 1933-7213. doi: 10.1016/j.nurt.2007.10.069. URL <http://ovidsp.ovid.com/ovidweb.cgi?T=JS{&}PAGE=reference{&}D=emed8{&}NEWS=N{&}AN=2007620738{&}5Cnhttp://www.sciencedirect.com/science/article/pii/S1933721307002577>.
- [93] Ide Simon Swager. Passive wireless multi-subject ECoG monitoring. *Master Thesis TU Delft, Bioelectronics*, 2016.
- [94] A. Ulate-Campos, F. Coughlin, M. Gaínza-Lein, I. Sánchez Fernández, P. L. Pearl, and T. Loddenkemper. Automated seizure detection systems and their effectiveness for each type of seizure. *Seizure*, 40:88–101, 2016. ISSN 15322688. doi: 10.1016/j.seizure.2016.06.008.
- [95] unknown author. Anritsu Company, 2010.
- [96] M. N. Van Dongen, A. Karapatis, L. Kros, O. H J Eelkman Rooda, R. M. Seepers, C. Strydis, C. I. De Zeeuw, F. E. Hoebeek, and W. A. Serdijn. An implementation of a wavelet-based seizure detection filter suitable for realtime closed-loop epileptic seizure suppression. *IEEE 2014 Biomedical Circuits and Systems Conference, BioCAS 2014 - Proceedings*, 1:504–507, 2014. doi: 10.1109/BioCAS.2014.6981773.
- [97] Philippe Velha, Stefano Faralli, and Giampiero Contestabile. A compact silicon photonic DQPSK receiver based on microring filters. *IEEE Journal on Selected Topics in Quantum Electronics*, 22(6), 2016. ISSN 1077260X. doi: 10.1109/JSTQE.2016.2551939.

- [98] Stefanie Volland, Julian Esteve-Rudd, Juyea Hoo, Claudine Yee, and David S. Williams. A comparison of some organizational characteristics of the mouse central retina and the human macula. *PLoS ONE*, 10(4):1–13, 2015. ISSN 19326203. doi: 10.1371/journal.pone.0125631.
- [99] Junsong Wang, Ernst Niebur, Jinyu Hu, and Xiaoli Li. Suppressing epileptic activity in a neural mass model using a closed-loop proportional-integral controller. *Scientific Reports*, 6(October 2015):27344, 2016. ISSN 2045-2322. doi: 10.1038/srep27344. URL <http://www.nature.com/articles/srep27344>.
- [100] Kevin Welsher, Sarah P Sherlock, and Hongjie Dai. Deep-tissue anatomical imaging of mice using carbon nanotube fluorophores in the second near-infrared window. *Proceedings of the National Academy of Sciences of the United States of America*, 108(22):8943–8948, 2011. ISSN 0027-8424. doi: 10.1073/pnas.1014501108.
- [101] Christian T Wentz, Jacob G Bernstein, Patrick Monahan, Alexander Guerra, Alex Rodriguez, and Edward S Boyden. A wirelessly powered and controlled device for optical neural control of freely-behaving animals. *Journal of neural engineering*, 8(4):046021, 2011. ISSN 1741-2560. doi: 10.1088/1741-2560/8/4/046021.
- [102] Shaohua Xu, Sanjiv K. Talwar, Emerson S. Hawley, Lei Li, and John K. Chapin. A multi-channel telemetry system for brain microstimulation in freely roaming animals. *Journal of Neuroscience Methods*, 133(1-2):57–63, 2004. ISSN 01650270. doi: 10.1016/j.jneumeth.2003.09.012.
- [103] Xuesong Ye, Peng Wang, Jun Liu, Shaomin Zhang, Jun Jiang, Qingbo Wang, Weidong Chen, and Xiaoxiang Zheng. A portable telemetry system for brain stimulation and neuronal activity recording in freely behaving small animals. *Journal of Neuroscience Methods*, 174(2):186–193, 2008. ISSN 01650270. doi: 10.1016/j.jneumeth.2008.07.002.
- [104] Ofer Yizhar, Lief E. Fenno, Thomas J. Davidson, Murtaza Mogri, and Karl Deisseroth. Optogenetics in Neural Systems, 2011. ISSN 08966273.
- [105] Mehmet Rasit Yuce and Wentai Liu. A low-power multirate differential PSK receiver for space applications. *IEEE Transactions on Vehicular Technology*, 54(6):2074–2084, 2005. ISSN 00189545. doi: 10.1109/TVT.2005.858196.
- [106] Andrew Zayachivsky, Mark J Lehmkuhle, and F Edward Dudek. Long-term Continuous EEG Monitoring in Small Rodent Models of Human Disease Using the Epoch Wireless Transmitter System. (July): 1–12, 2015. doi: 10.3791/52554.
- [107] Mingrui Zhao, Rose Alleva, Hongtao Ma, Andy G.S. Daniel, and Theodore H. Schwartz. Optogenetic tools for modulating and probing the epileptic network. *Epilepsy Research*, 116:15–26, 2015. ISSN 09201211. doi: 10.1016/j.eplesyres.2015.06.010. URL <http://linkinghub.elsevier.com/retrieve/pii/S0920121115300152>.
- [108] Chao Zuo, Xiaofei Yang, Yang Wang, Christopher E Hagains, Ai-Ling Li, Yuan B Peng, and J-C Chiao. A digital wireless system for closed-loop inhibition of nociceptive signals. *Journal of Neural Engineering*, 9(5):056010, 2012. ISSN 1741-2560. doi: 10.1088/1741-2560/9/5/056010.

# Appendices



# A - Multiple Criteria Analysis

## **Size & Weight** (VI.i.a & VI.i.b )

This is critical for the success of the total project, a mouse should be able to carry the device. Therefore the highest weight of 3 is assigned to this requirement. PK does not require additional receiving components. However, the decoding does require a more complex receiver design. Thus a little size and weight is added, and the PK score is higher but not perfect. Both VCL and THz require added sensors that use space and bring extra weight. The lowest score is therefore assigned to both.

## **Multiple mice** (VI.iv)

The success of the prototype relies on the allowance of communication with multiple mice at once. This unique feature adds value to the solution and differentiates from currently available wireless setups. Therefore the highest weight of 3 is assigned to this requirement. PK and VCL provide the possibility for multiple access. However, both require modulation techniques and thus demodulation at the receiver side. THz easily provides different bands through filters and does not require demodulation techniques after detection.

## **Interference** (VI.v)

Is less demanding compared to the previous two, the product can still exist and be innovative. However, the functionality will decrease with too much interference. Thus has a lower weight than the first two requirements. Due to the productivity dependence, a value of 2 is assigned. PK uses one of the two existing links and thus does not provide an extra source of interference. However, the powerlink did previously show to cause some interference with the uplink and thus a score of 3 is given. Both VCL and THz are expected not to cause any interference since their in a range of the electromagnetic spectrum.

## **Power Consumption** (VI.ii.a )

Achieving a functional end product is still possible, but the demand for harvested power increases if the consumption of the downlink increases. Therefore the lowest weight of 1 is assigned to this requirement. PK is using the power link which will reduce in effectiveness. This decrease in effectiveness might be minimised by using the phase information. However, the demodulation of the phase differences will require more power. VCL and THz both do not affect the power link and use passive sensors. However, VCL does require more complex demodulation, due to the passive filters of THz. All of the options do require some power, and therefore none of them scores 5 points.

## **Reliability** (VI.ii.b )

It does not affect the functionality of the product either. However, the usefulness of the device decreases when the communication link fails too often. Hence, the lowest weight of 1 is selected for this requirement. PK will encounter misalignment issues as described in Chapter 3.1. When the receiving coil is placed orthogonal to the magnetic field the signal might get lost. VCL will probably also encounter reliability issues due to blocking. When the sensor is covered no signal can be transferred. THz does not get blocked by soft matter. However, there is still a chance that the water in the mice tissue cause attenuation or that the mirroring properties of metal will induce problems. Thus THz did not score all the 5 points.



# B - Pilot

## Materials

The source and detector had to be produced by hand and thus involved a very long delivery time. In the mean time different pilot studies were conducted to gain experience with the setup. These pilot studies could be divided in NIR-pilot and a MIR-pilot. The components were controlled with via an Arduino.

### Pilot - Near Infrared Transmitter - IR LEDs

- I 5mm HE3-290AC
- II Solid State Lamp GaAs 5mm L-53F3C
- III TSAL6200 GaAlAs IR Zennodiode

### Receiver - IR Diodes

- I TSOP31240
- II TSOP1838 VIS

### Pilot - Mid Infrared

#### Transmitter - Miniature light bulbs

- I Gloeilampje E10 3.5V 0.3A
- II Kogellampje Barthelme 00810650
- III Miniatuurlamp 4.5V 0.06A 30cm
- IV Bipin-LP T1 5V 60mA

#### Receiver - PIR movementsensor

- I Panasonic AMN31112 (digital) and AMN21112 (analog)
- II Velleman VMA314

## Single-channel

During the pilots only single-channel setups were build. The intention was to gather data to later on compare to the THz Torch data. However due to practical limitations described in the next section there was no useful data gained from the pilot studies. The experience did help in building the final setup but are not suitable for comparison.

**Distance** 1cm, 10cm, 40cm (height of the cage), 1m

**Misalignment** an angle of 15°, 30°, 60°, 90°

**Data rate** 30bps, 60bps, 300 bps, 1kbps.

**Power** 1. Determine the power consumption of the source and the detector at 40cm, 0°, 30bps, 10-3 BER (value to be determined 10-3 from  $I_{de}$ ).

## Struggles

IR LEDs and diodes only work at a modulation frequency of 38kHz or 40 kHz since the discrete receiving components already include a decomposition circuit. Regular IR communication between devices like



TV remote controls all work on this modulation frequencies to reduce the influence of background radiation. The modulation method of each brand slightly differs from how the uptime and downtime are used to encode the bits. Therefore not all remote controls work on all IR controlled devices. But the modulation frequency is similar for all, around 40kHz.

PIR movement sensors include two sensitive elements. Only a difference between the two elements result in a high output signal. By moving the sources in front of the receivers a signal could be detected. However by simply switching them on and off no difference was generated and thus no output signal.

# C - CDMA

## CDMA example

| Mouse | Data | Code | X-OR      |
|-------|------|------|-----------|
| 1     | 10   | 0101 | 1010 0101 |
| 2     | 01   | 0011 | 0011 1100 |
| 3     | 11   | 0000 | 1111 1111 |
| 4     | 00   | 0110 | 0110 0110 |

**Modulate the combined signal**

0 = 1V

1 = -1V

|       |           |             |             |
|-------|-----------|-------------|-------------|
| X-OR1 | 1010 0101 | -1 1 -1 1   | 1 -1 1 -1   |
| X-OR2 | 0011 1100 | 1 1 -1 -1   | -1 -1 1 1   |
| X-OR3 | 1111 1111 | -1 -1 -1 -1 | -1 -1 -1 -1 |
| X-OR4 | 0110 0110 | 1 -1 -1 1   | 1 -1 -1 1   |
| Combi |           | 0 0 -4 0    | 0 -4 0 0    |

**Demodulate the combined signal**

## Mouse 1

|          |               |             |    |
|----------|---------------|-------------|----|
| Code     | 1 -1 1 -1     | 1 -1 1 -1   |    |
| Combi    | 0 0 -4 0      | 0 -4 0 0    |    |
| Multiply | 0 0 -4 0      | 0 4 0 0     |    |
|          | -4/4 = -1 → 1 | 4/4 = 1 → 0 | 10 |

## Mouse 2 : 0011

|          |             |               |    |
|----------|-------------|---------------|----|
| Code     | 1 1 -1 -1   | 1 1 -1 -1     |    |
| Combi    | 0 0 -4 0    | 0 -4 0 0      |    |
| Multiply | 0 0 4 0     | 0 -4 0 0      |    |
|          | 4/4 = 1 → 0 | -4/4 = -1 → 1 | 01 |

## Mouse 3

|          |               |               |    |
|----------|---------------|---------------|----|
| Code     | 1 1 1 1       | 1 1 1 1       |    |
| Combi    | 0 0 -4 0      | 0 -4 0 0      |    |
| Multiply | 0 0 -4 0      | 0 -4 0 0      |    |
|          | -4/4 = -1 → 1 | -4/4 = -1 → 1 | 11 |

## Mouse 4 0110

|          |             |             |    |
|----------|-------------|-------------|----|
| Code     | 1 -1 -1 1   | 1 -1 -1 1   |    |
| Combi    | 0 0 -4 0    | 0 -4 0 0    |    |
| Multiply | 0 0 4 0     | 0 4 0 0     |    |
|          | 4/4 = 1 → 0 | 4/4 = 1 → 0 | 00 |

Figure 9: Example of CDMA with 4 users. Each user is assigned with a orthogonal code that enables decodation after receiving the combined signal.

# D - Arduino

```
/*
 * Experiments - Modulate data and send
 *
 * written by Jinne Geelen
 * August 22, 2017
 *
 */
#include "Timer.h"
Timer t;

const int TEST          = 7;
const int SOURCE1       = 8;
const int SOURCE2       = 9;
const int INTERVAL      = 17; //ms
const int INT_C         = 2.5;

const int DATA_LENGTH = 25;
int currentTick = 0;
int currentValue = 0;
int currentTable[DATA_LENGTH];

//001011100 110000111

//char data[DATA_LENGTH] = {1, 1, 1, 0, 1, 0, 1, 1, 0,
0, 1, 1, 0, 1, 0, 1, 0, 0, 1, 0, 1, 0, 0, 0};
char data[DATA_LENGTH] = {1, 0, 1, 0, 1, 0, 1, 0, 1,
0, 1, 0, 1, 0, 1, 0, 1, 0, 1, 0, 1, 0, 1, 0, 1, 0};

void setup() {
  Serial.begin(9600);
  pinMode(SOURCE1, OUTPUT);
  pinMode(SOURCE2, OUTPUT);
  pinMode(TEST, OUTPUT);

  t.oscillate(TEST, INT_C, HIGH);
```

```
t.every(INTERVAL, doTick, (void*)0); //int
tickEvent =
}

void loop() {
  t.update();
}

void doTick(void* context) {

  int check = data[currentTick];

  if (check != currentValue) {
    if (currentValue == 0) {
      digitalWrite(SOURCE1, HIGH); // turn the
SOURCE on/off based on currentValue
      digitalWrite(SOURCE2, HIGH); // turn the
SOURCE on/off based on currentValue
//      Serial.println("source switch 1");
      currentValue = 1;
    } else {
      digitalWrite(SOURCE1, LOW); // turn the SOURCE
on/off based on currentValue
      digitalWrite(SOURCE2, LOW); // turn the SOURCE
on/off based on currentValue
//      Serial.println("source switch 0");
      currentValue = 0;
    }
  }
  currentTick++;

  if (currentTick == DATA_LENGTH-1) {
    currentTick = 0;
  }
}
```

Figure 10: Arduino code for creating the transmitted data signal



# E - Matlab



```

%% Analysis THz Torching prototype experiments

clear all; close all; clc
format long

files = dir('*.csv');
% filescomb = zeros(13*length(files),5);

% Create new matrices with row: conditions (var), col: mean, min, max, range, std (5)
DutCyc = zeros(length(files),5);
Q_factor = zeros(length(files),5);
Crossing = zeros(length(files),5);
Eye_jit_RMS = zeros(length(files),5);
Eye_zero_level = zeros(length(files),5);
Eye_one_level = zeros(length(files),5);
Eye_width = zeros(length(files),5);
Eye_height = zeros(length(files),5);
V_amptd = zeros(length(files),5);
DCVrms = zeros(length(files),5);
Vpp = zeros(length(files),5);

for i=1:length(files)
    eval(['load ' files(i).name ' -ascii'])
end

filescomb = [ X10d_normalized(1:11,:);
              X20d_normalized(1:11,:);
              X30d_normalized(1:11,:);
              X40d_normalized(1:11,:);
              X50d_normalized(1:11,:);
              X60d_normalized(1:11,:);
              X70d_normalized(1:11,:);
              X80d_normalized(1:11,:);
              X90d_normalized(1:11,:)];

for i=1:length(files)
    index = 1;
    DutCyc(i,:) = filescomb(1+(11*(i-1)),:);
    Q_factor(i,:) = filescomb(2+(11*(i-1)),:);
    Crossing(i,:) = filescomb(3+(11*(i-1)),:);
    Eye_jit_RMS(i,:) = filescomb(4+(11*(i-1)),:);
    Eye_zero_level(i,:) = filescomb(5+(11*(i-1)),:);
    Eye_one_level(i,:) = filescomb(6+(11*(i-1)),:);
    Eye_width(i,:) = filescomb(7+(11*(i-1)),:);
    Eye_height(i,:) = filescomb(8+(11*(i-1)),:);
    V_amptd(i,:) = filescomb(9+(11*(i-1)),:);
    DCVrms(i,:) = filescomb(10+(11*(i-1)),:);
    Vpp(i,:) = filescomb(11+(11*(i-1)),:);
end

%%
Q = Q_factor;
BER = 0.5*erfc(Q/sqrt(2));

%% Create plots (from here other .m file)

clear all; close all; clc

load('data2.mat')

%%
d = 1:10:10*length(DutCyc(:,1));

figure()
    semiLogy(d, BER(:,1),'Linewidth', 2)
    xlabel('Misalignment [°]')
    ylabel('BER [-]')
    ax = gca; % current axes
    ax.FontSize = 25;

    axes;
    h = title('Experiment 3 - Misalignment');
    set(gca,'Visible','off');
    set(h,'Visible','on');
    set(gca,'fontsize',25);

%% Plot datarate
d = 1:10:10*length(DutCyc(:,1));
pos = [-14 1 0];

for i=1:length(DutCyc(1,:))
    figure(i)

    subplot(6,2,1)
    semiLogy(d, BER(:,i),'Linewidth', 2)
    xlabel('Misalignment [°]')
    ylabel('BER [-]')
    ylim([10^-7 10^0]);
    ax = gca; % current axes
    ax.FontSize = 25;
    set(get(gca,'YLabel'),'Rotation',45);
    set(get(gca,'YLabel'),'Position',[-15 0.00001 0])

    subplot(6,2,2)
    plot(d, Q_factor(:,i),'Linewidth', 2)
    xlabel('Misalignment [°]')
    ylabel('Q-factor [-]')
    ax = gca; % current axes
    ax.FontSize = 25;
    set(get(gca,'YLabel'),'Rotation',45);
    set(get(gca,'YLabel'),'Position',pos)

    subplot(6,2,3)
    plot(d, Crossing(:,i),'Linewidth', 2)
    xlabel('Misalignment [°]')
    ylabel('Crossing [%]');
    ylim([0 100]);
    ax = gca; % current axes

```

```

ax.FontSize = 25;
set(get(gca,'YLabel'),'Rotation',45);
set(get(gca,'YLabel'),'Position',pos)

subplot(6,2,4)
plot(d, Eye_jit_RMS(:,i),'Linewidth', 2)
xlabel('Misalignment [?]')
ylabel('Eye jitter RMS [ms]')
ax = gca; % current axes
ax.FontSize = 25;
set(get(gca,'YLabel'),'Rotation',45);
set(get(gca,'YLabel'),'Position',pos)

subplot(6,2,5)
plot(d, Eye_zero_level(:,i),'Linewidth', 2);
xlabel('Misalignment [?]')
ylabel('Eye zero level [mV]')
ax = gca; % current axes
ax.FontSize = 25;
set(get(gca,'YLabel'),'Rotation',45);
set(get(gca,'YLabel'),'Position',pos)

subplot(6,2,6)
plot(d, Eye_one_level(:,i),'Linewidth', 2);
xlabel('Misalignment [?]')
ylabel('Eye one level [mV]')
ax = gca; % current axes
ax.FontSize = 25;
set(get(gca,'YLabel'),'Rotation',45);
set(get(gca,'YLabel'),'Position',pos)

subplot(6,2,7)
plot(d, Eye_width(:,i),'Linewidth', 2)
xlabel('Misalignment [?]')
ylabel('Eye width [ms]');
ax = gca; % current axes
ax.FontSize = 25;
set(get(gca,'YLabel'),'Rotation',45);
set(get(gca,'YLabel'),'Position',pos)

subplot(6,2,8)
plot(d, Eye_height(:,i),'Linewidth', 2)
xlabel('Misalignment [?]')
ylabel('Eye height [mV]');
ax = gca; % current axes
ax.FontSize = 25;
set(get(gca,'YLabel'),'Rotation',45);
set(get(gca,'YLabel'),'Position',pos)

subplot(6,2,9)
plot(d, V_ampd(:,i),'Linewidth', 2)
xlabel('Misalignment [?]')
ylabel('V_{ampd} [mV]')
ax = gca; % current axes
ax.FontSize = 25;
set(get(gca,'YLabel'),'Rotation',45);
set(get(gca,'YLabel'),'Position',pos)

subplot(6,2,10)
plot(d, DCVrms(:,i),'Linewidth', 2)
xlabel('Misalignment [?]')
ylabel('DCVrms [mV]')
ax = gca; % current axes
ax.FontSize = 25;
set(get(gca,'YLabel'),'Rotation',45);
set(get(gca,'YLabel'),'Position',pos)

subplot(6,2,11)
plot(d, Vpp(:,i),'Linewidth', 2)
xlabel('Misalignment [?]')
ylabel('Vpp [mV]')
ax = gca; % current axes
ax.FontSize = 25;
set(get(gca,'YLabel'),'Rotation',45);
set(get(gca,'YLabel'),'Position',pos)

subplot(6,2,12)
plot(d,DutCyc(:,i),'Linewidth', 2);
xlabel('Misalignment [?]')
ylabel('DutCyc [ms]')
ax = gca; % current axes
ax.FontSize = 25;
% ax.XTickLabelRotation = -45;
set(get(gca,'YLabel'),'Rotation',45);
set(get(gca,'YLabel'),'Position',pos)

axes;
h = title('Experiment 3 - Misalignment');
set(gca,'Visible','off');
set(h,'Visible','on');
set(gca,'fontSize',35);

end

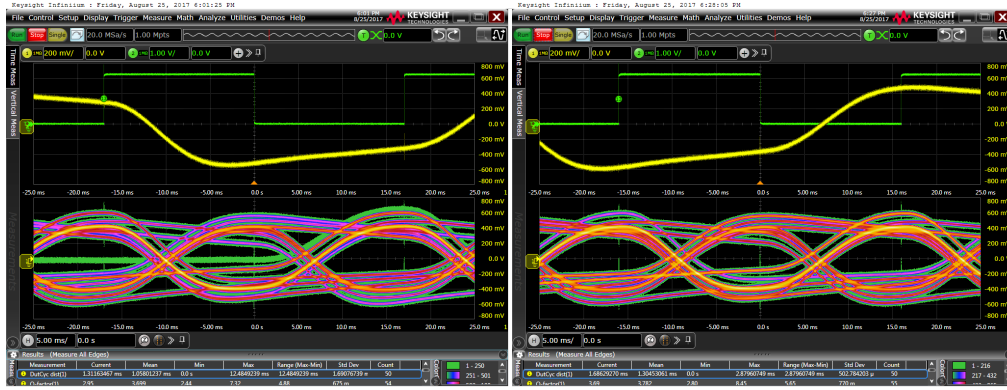
```

Figure 11: Matlab code



# F - Eyediagrams

# Experiment 1 - Data rate



17 ms

16 ms



15 ms

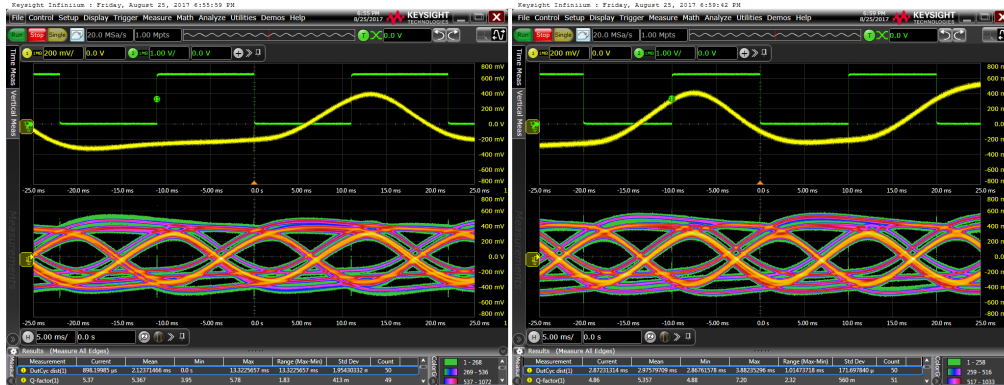
14 ms



13 ms

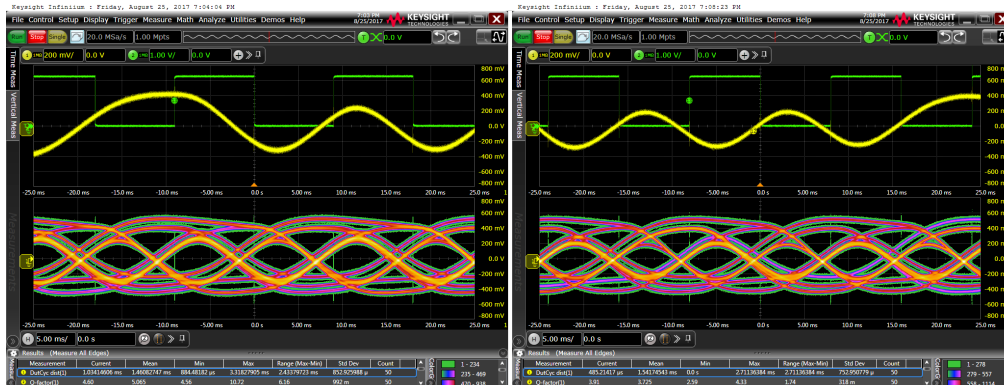
12 ms

# Experiment 1 - Data rate



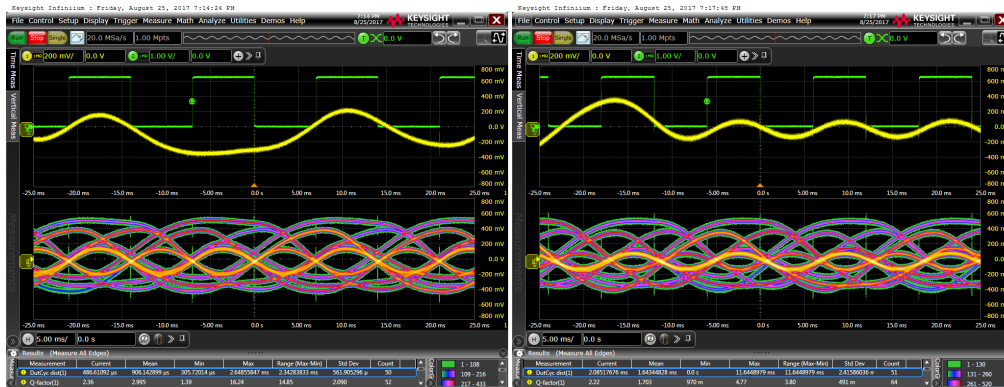
11 ms

10 ms



9 ms

8 ms



7 ms

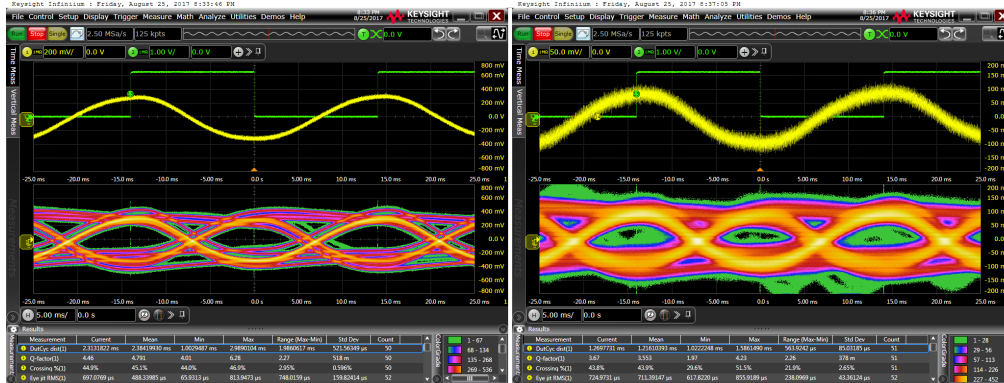
6 ms

## Experiment 1 - Data rate



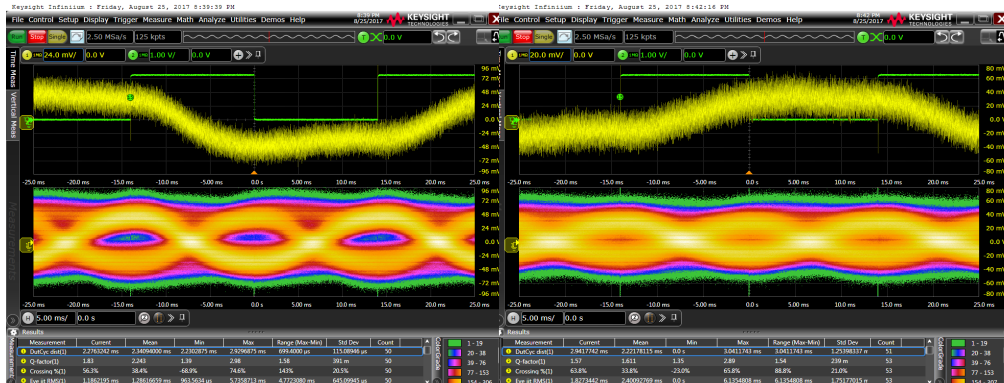
5 ms

# Experiment 2 - Distance (1 source)



1 cm

2 cm



3 cm

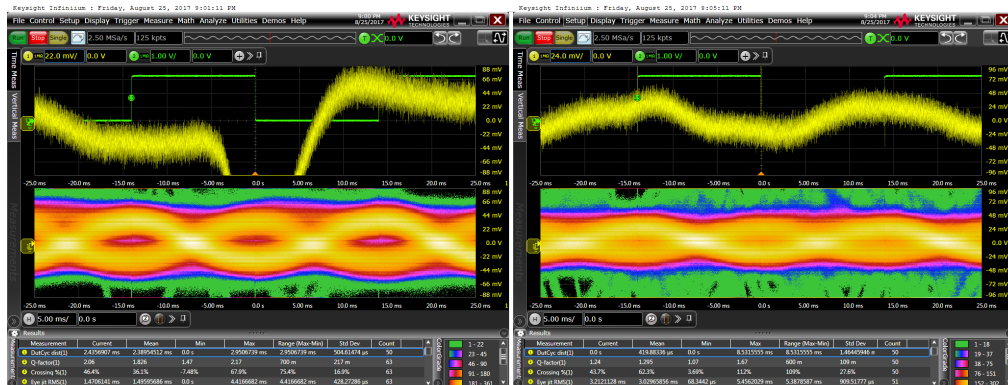
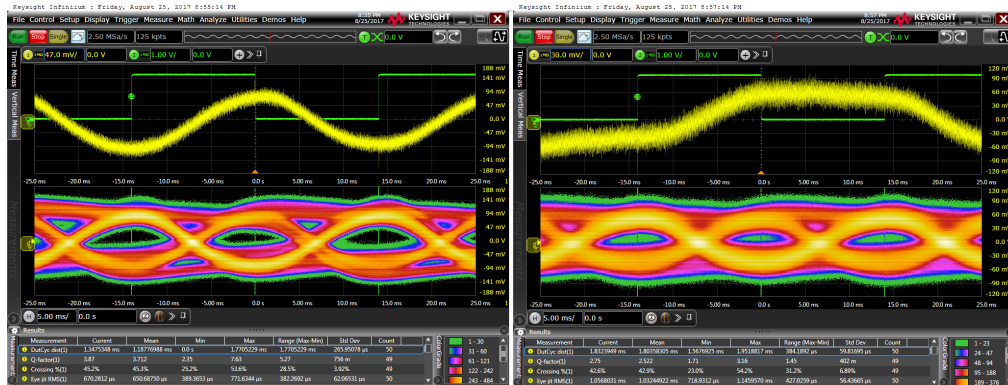
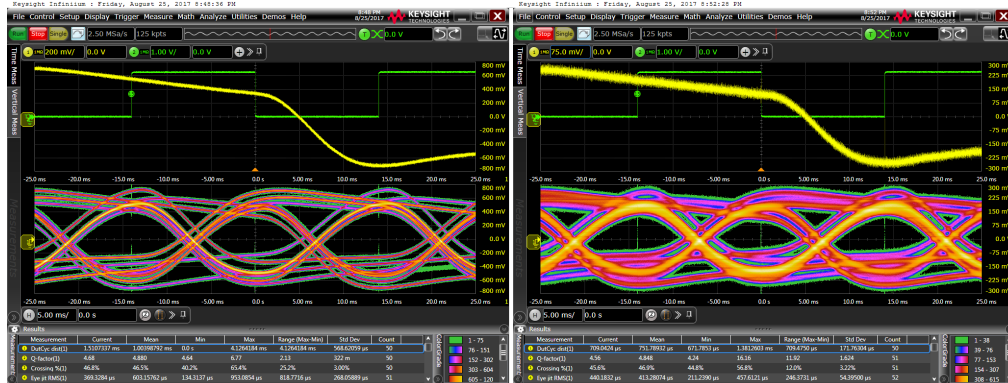
4 cm



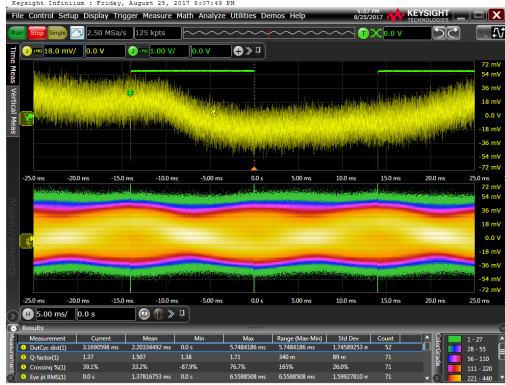
5 cm



# Experiment 2 - Distance (2 sources)

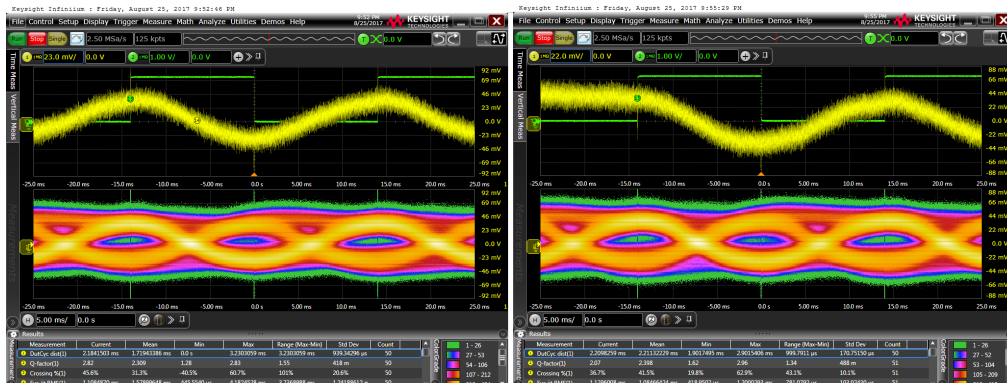
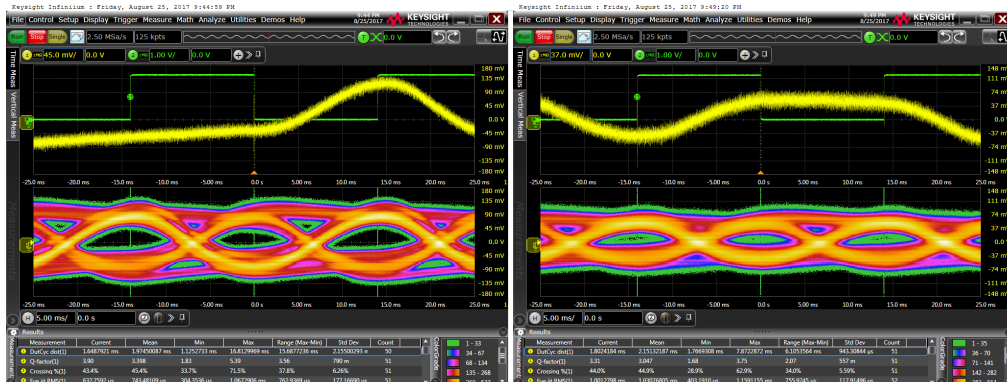
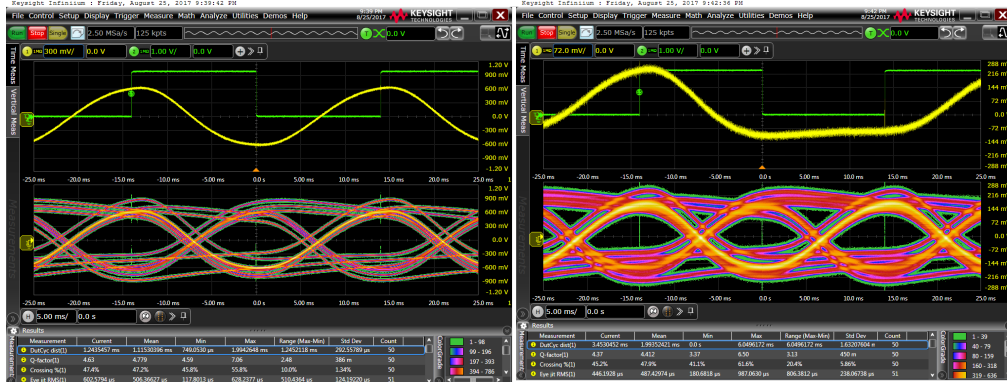


## Experiment 2 - Distance (2 sources)

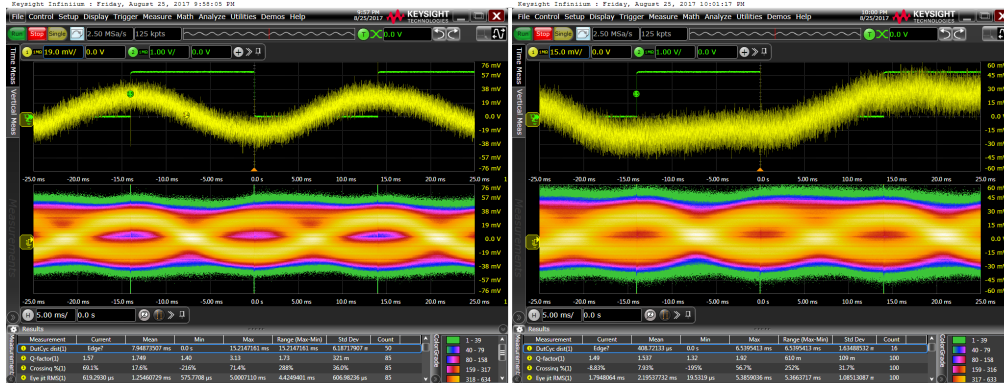


7 cm

# Experiment 2 - Distance (3 sources)

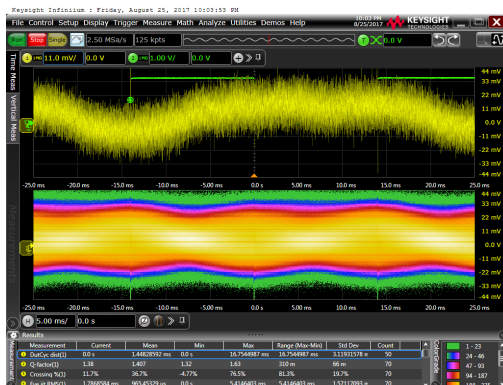


# Experiment 2 - Distance (3 sources)



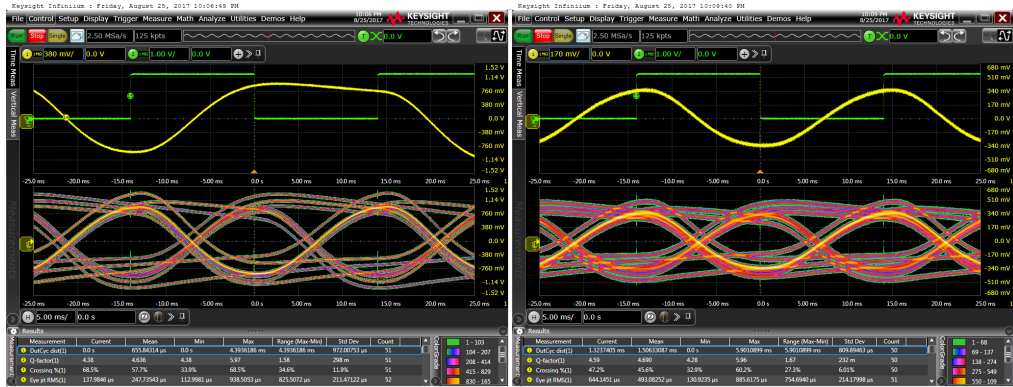
7 cm

8 cm



9 cm

# Experiment 2 - Distance (4 sources)



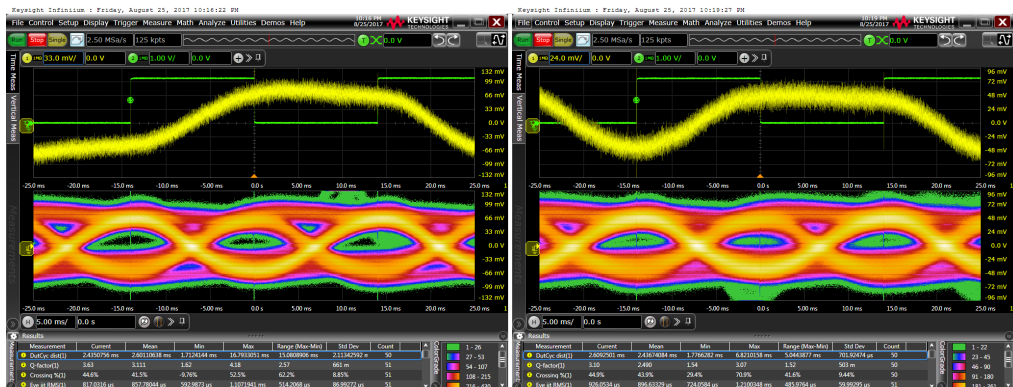
1 cm

2 cm



3 cm

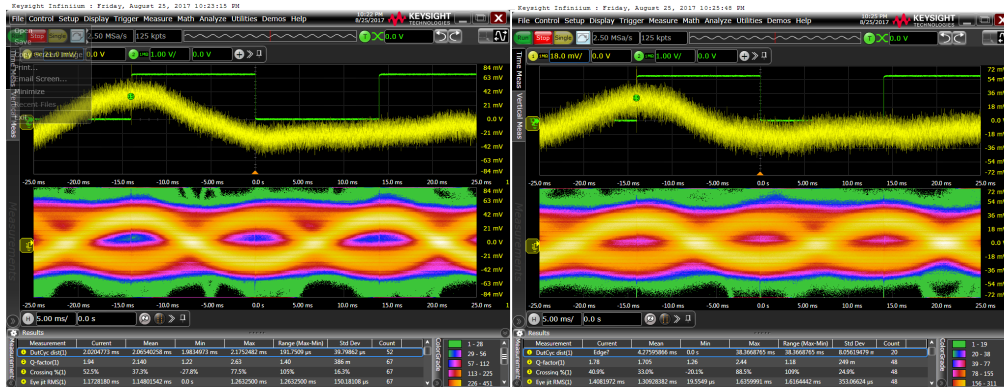
4 cm



5 cm

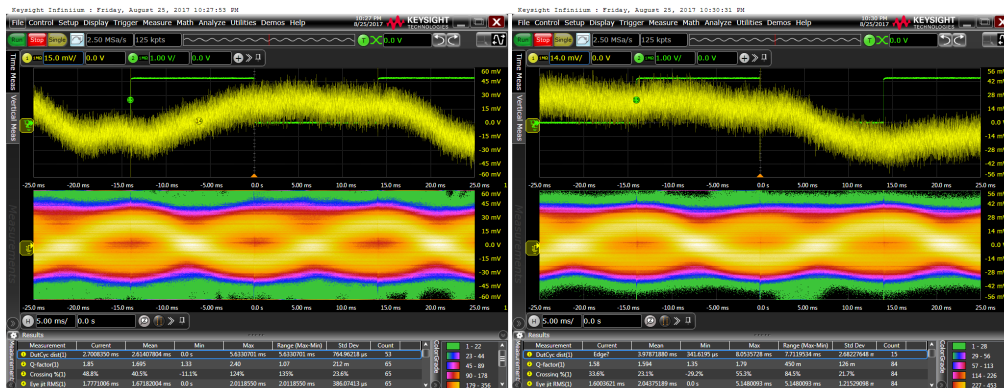
6 cm

# Experiment 2 - Distance (4 sources)



7 cm

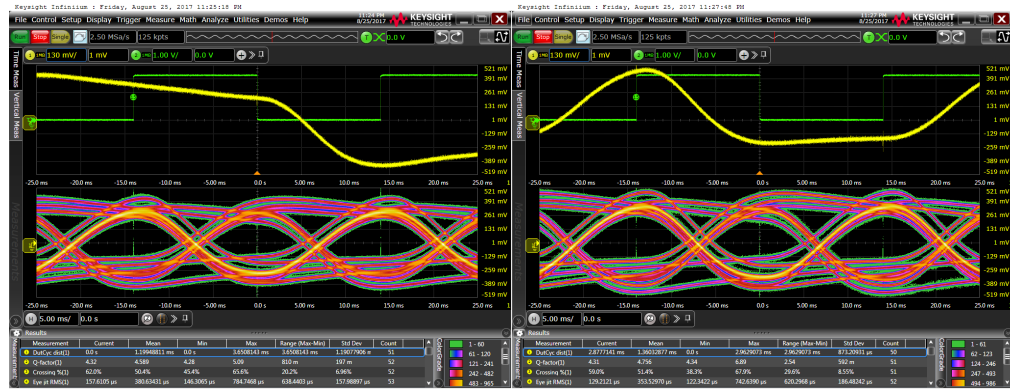
8 cm



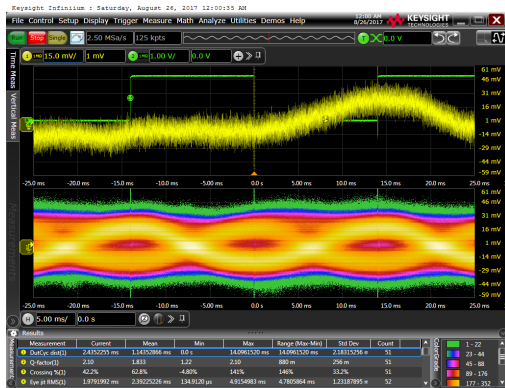
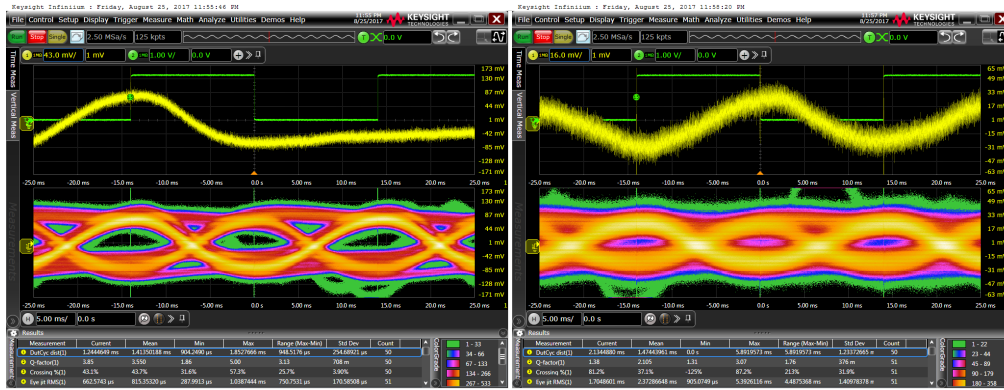
9 cm

10 cm

# Experiment 3 - Misalignment

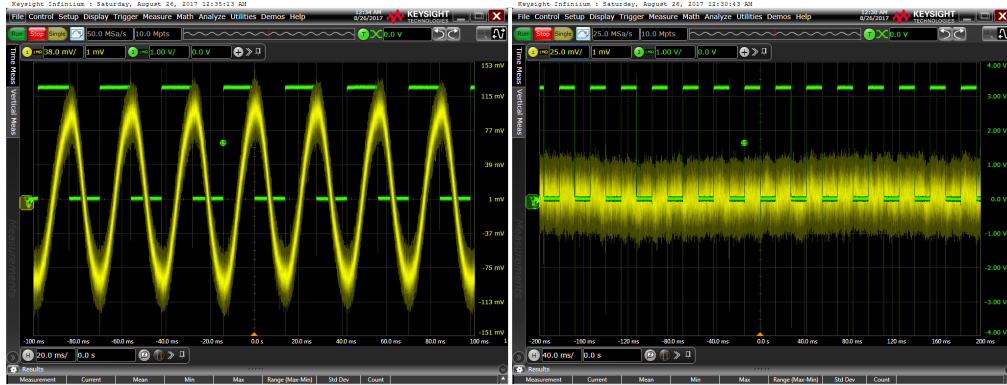


# Experiment 3 - Misalignment



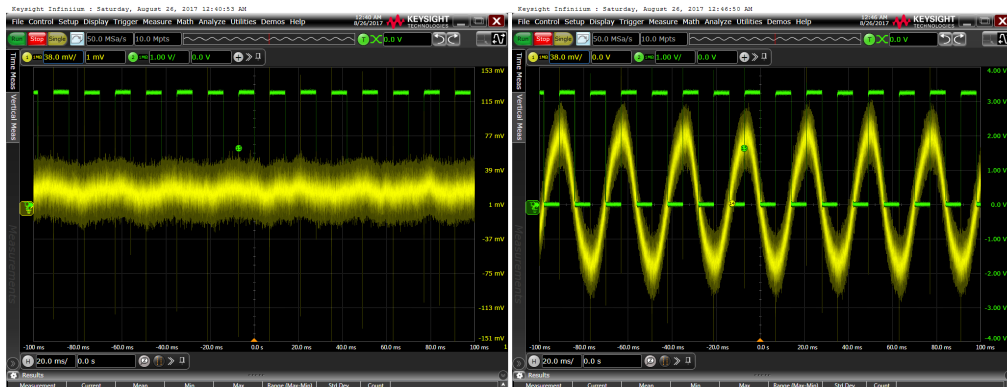


# Experiment 5 - Medium



free space (no obstruction)

hand



paper (1 A4)

bubble wrap



plastic ruler (transparent)

fabric (shawl, cotton blend)

# G - Lunteren



Contact: jinnegeelen@gmail.com

## Terahertz Torching: towards closed-loop wireless neurostimulation of group-housed rodents

Jinne E. Geelen<sup>1,2</sup> Freek E. Hoebeek<sup>1</sup> Wouter A. Serdijn<sup>2</sup>



<sup>1</sup> Department of Neuroscience, Erasmus MC, Rotterdam  
<sup>2</sup> Section Bioelectronics, Delft University of Technology

### NeuroMate

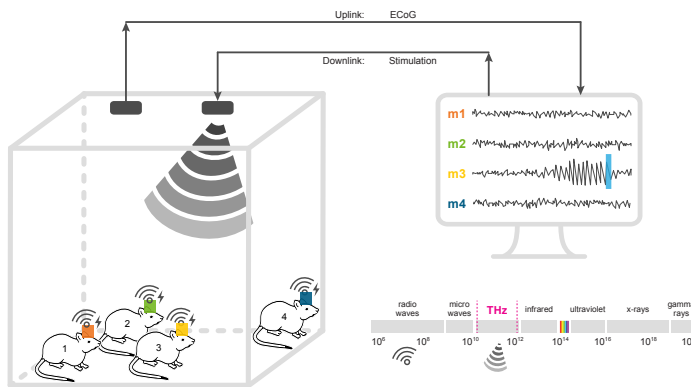
A project that originates from the multidisciplinary consortium NeuroDelta

### Challenges

- Individual monitoring
- Wireless & freely moving
- Multiple mice simultaneously
- Control individual stimulation

### Goal

Our goal is to build a setup for long-term studies of group-housed mice, that enables continuous monitoring and interaction with each animal.



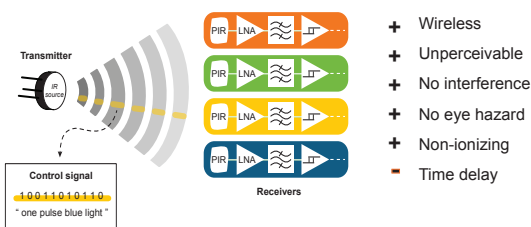
### Concepts

Elaboration of three data transmission concepts for the downlink

Table 1 - Multi-criteria analysis: three data transmission concepts are weighed and added

| Criterion         | Weight | PSK       | VLC       | TT        |
|-------------------|--------|-----------|-----------|-----------|
| Size and weight   | 3x     | 3         | 1         | 1         |
| Multiple mice     | 3x     | 4         | 4         | 5         |
| Interference      | 2x     | 3         | 5         | 5         |
| Power consumption | 1x     | 2         | 3         | 4         |
| Reliability       | 1x     | 1         | 1         | 4         |
| <b>Total</b>      |        | <b>30</b> | <b>29</b> | <b>36</b> |

- Power Shifting Keying (PSK) modulation of the inductive magnetic field
- Visual Light Communication (VLC) modulation of visible light carrier
- Terahertz Torching (TT) electro-magnetic wave modulation in the THz band



### Terahertz Torching

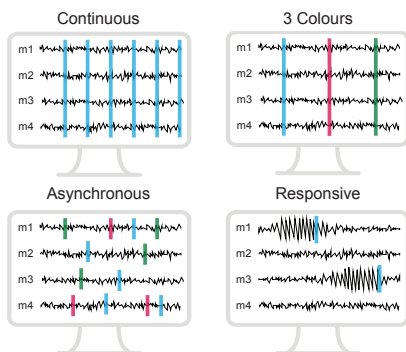
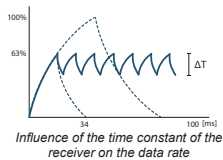
- + Wireless
- + Unperceivable
- + No interference
- + No eye hazard
- + Non-ionizing
- Time delay

### Applications

MicroLED optogenetic stimulation

Data rate at least 30 bps

24 stimulation paradigms per mouse (e.g. 3 colours x 8 frequencies)



### Conclusion

THz Torching is a new one-way communication method that is suitable for long-term wireless monitoring and stimulation of group-housed freely moving rodents

### Future Work

- Determine time delay
- Test penetration THz through tissue
- Miniaturize headmodule → implantable
- Add electrical stimulation



Dutch Neuroscience Meeting | Lunteren | 15 June 2017



Figure 12: Poster Lunteren